

MICROFACIES ANALYSIS OF THE LOWER PALEOCENE BEDA FORMATION IN
WESTERN CONCESSION 59 AND BLOCK 59F,
SIRTE BASIN, LIBYA

by

ISMAIL A. AMR

A thesis presented to the Department of Geological Sciences

Brock University

in partial fulfillment of the requirements for the degree of
Master of Science in Geology

© Ismail A. Amr, 1992

Dr. J. Terasmae
Dr. U. Brand

Supervisors

ABSTRACT

The rock sequence of the Tertiary Beda Formation of S. W. concession 59 and 59F block in Sirte Basin of Libya has been subdivided into twelve platformal carbonate microfacies. These microfacies are dominated by muddy carbonates, such as skeletal mudstones, wackestones, and packstones with dolomites and anhydrite. Rock textures, faunal assemblages and sedimentary structures suggest shallow, clear, warm waters and low to moderate energy conditions within the depositional shelf environment. The Beda Formation represents a shallowing-upward sequence typical of lagoonal and tidal flat environments marked at the top by sabkha and brackish-water sediments. Microfossils include benthonic foraminifera, such as miliolids, *Nummulites*, *Periculina* and other smaller benthonics, in addition to dasycladacean algae, ostracods, molluscs, echinoderms, bryozoans and charophytes. Fecal pellets and pelloids, along with the biotic allochems, contributed greatly to the composition of the various microfacies. Dolomite, where present, is finely crystalline and an early replacement product. Anhydrite occurs as nodular, chickenwire and massive textures indicating supratidal sabkha deposition.

Compaction, micritization, dolomitization, recrystallization, cementation, and dissolution resulted in alteration and obliteration of primary sedimentary structures of the Beda Formation microfacies.

The study area is located in the Gerad Trough which developed as a NE-SW trending extensional graben. The Gerad

trough was characterized by deep-shallow water conditions throughout the deposition of the Beda Formation sediments. The study area is marked by several horsts and grabens; as a result of extensional tectonism. The area was tectonically active throughout the Tertiary period.

Primary porosity is intergranular and intragranular, and secondary processes are characterized by dissolution, intercrystalline, fracture and fenestral features. Diagenesis, through solution leaching and dolomitization, contributed greatly to porosity development. Reservoir traps of the Beda Formation are characterized by normal fault blocks and the general reservoir characteristics/properties appear to be facies controlled.

ACKNOWLEDGEMENTS

I would like to express my gratitude to Dr. Jaan Terasmae, Dr. Uwe Brand and Dr. Francine McCarthy for their guidance, understanding and support throughout the course of this thesis.

I would like to take this opportunity to thank the academic and technical staff of the Department of Geological Sciences of Brock University for providing their endless support and technical expertise throughout the production of this thesis. Special thanks are due to Mr. Mike Lozon for drafting the figures of my thesis and Miss. Candace Kramer for thin section preparation.

My gratitude is also extended to the Charophyte specialists, Dr. Monique Feist, Laboratory of Paleobotany, University of Montpellier II, France, and Dr. Janine Riveline, Department of Stratigraphy of Sedimentary Basins, University of Pierre and Marie Curie, France, for their identification of the discovered charophytes of the Beda Formation of the Study Area.

I would like to express my appreciation to Waha Oil Company of Libya for their financial support; a special thanks goes to Mr. Ramadan M. Aburawi and his staff of the Exploration Department of Waha Oil Company for assisting in the acquisition of the required data.

Above all, I wish to express my sincere thanks to my wife for her support and understanding during the past three years I spent at Brock University.

TABLE OF CONTENTS

	<u>Page No.</u>
ABSTRACT	2
ACKNOWLEDGEMENTS	4
TABLE OF CONTENTS	5
LIST OF TABLES	8
LIST OF FIGURES	9
LIST OF APPENDICES	10
CHAPTER ONE: INTRODUCTION	11
Introduction	11
Purpose of Study	12
Location	12
Methods of Study	15
CHAPTER TWO: GEOLOGY OF SIRTE BASIN	18
Introduction	18
Geologic Setting	18
Tectonic Evolution	19
CHAPTER THREE: GENERAL STRATIGRAPHY	24
Introduction	24
Stratigraphic Sequences	24
CHAPTER FOUR: MICROPALAEONTOLOGY	37
Introduction	37
Charophytes	38
Introduction	38
Occurences: Living Charophytes	40
Fossil Charophytes	40
Charophytes Assemblage of the Sirte Basin in the Formation of the Study Area	41
Benthonic Foraminifera	46
Introduction	46
Benthonic Foraminiferal Assemblages of Beda Formation	47
Ecology of Living Benthonic Foraminifera	50
Paleobiogeography	50
Systematic Paleontology	51

CHAPTER FIVE: MICROFACIES DESCRIPTIONS	55
Introduction	55
Foraminiferal Mudstone Microfacies (MF12) . .	63
Dasyclad-Pelletal Wackestone (MF11)	63
Pelloidal Packstone Microfacies (MF10)	64
Skeletal Wackestone-Mudstone Microfacies (MF9)	65
Pellet-Dasyclad-Foraminiferal Packstone	
Microfacies (MF8)	65
Foraminiferal Wackestone Mudstone Microfacies	
(MF7)	66
Foraminiferal Packstone Microfacies (MF6) . .	67
Ostracoda-foraminiferal Wackestone Microfacies	
(MF5)	67
Dasyclad-foraminiferal Packstone Microfacies	
(MF4)	69
Skeletal Mudstone Microfacies (MF3)	70
Foraminiferal Dolomitic Packstone Microfacies	
(MF2)	72
The Terminal Microfacies Complex (TMFC1) . . .	73
CHAPTER SIX: INTERPRETATION OF DEPOSITIONAL	
ENVIRONMENTS	78
Introduction	78
Microfossils as Indicators of the	
Paleoenvironments	78
Foraminiferal Mudstone Microfacies (MF12) . .	83
Dasyclad-Pelletal Wackestone Microfacies (MF11)	83
Pelloidal Packstone Microfacies (MF10)	84
Skeletal Wackestone-mudstone Microfacies (MF9)	84
Pellet-Dasyclad-Foraminiferal Packstone	
Microfacies (MF8)	84
Foraminiferal Wackestone-Mudstone Microfacies	
(MF7)	85
Foraminiferal Packstone Microfacies (MF6) . .	85
Ostracoda-foraminiferal Wackestone Microfacies	
(MF5)	86
Dasyclad-foraminiferal Packstone Microfacies	
(MF4)	87
Skeletal Mudstone Microfacies (MF3)	88
Foraminiferal-Dolomitic Packstone Microfacies	
(MF2)	90
Terminal Microfacies Complex (TMFC1)	91
Summary of Enviromental Conditions During	
Deposition of Beda Sediments and	
Allochems	92
CHAPTER SEVEN: GENERAL PALEOGEOGRAPHY	96
Sirte Basin	96
Paleogeography of the Study Area	97
The General Model of Deposition	101
The Major Controls of Beda Formation	
Sedimentation	101

CHAPTER EIGHT: PETROLEUM GEOLOGY	106
Petroleum Exploration History in the Study Area	106
Porosity and Permeability	110
Source and Seal Rocks	112
CONCLUSIONS	114
RECOMMENDATIONS	117
REFERENCES	118
APPENDICES	132
APPENDIX I	133
APPENDIX II	168

LIST OF TABLES

		<u>Page No.</u>
1	- Summary of Microfacies Descriptions . . .	56
2	- Ecological Conditions and Environments of Major Groups of Calcareous algae . . .	81
3	- Ecological Conditions and Environments of Benthonic Foraminifera, Ostracods, Molluscs, Bryozoans and Echinoderms . . .	82
4	- Summary of Petroleum Geology of the Study Area	107

LIST OF FIGURES

		<u>Page No.</u>
1	- Location of Study Area and Major Tectonic Regions of Libya	13
2	- Major Tectonic Elements and Oil Fields of Sirte Basin	14
3	- Regional Structural Cross-sections: . . .	21
	a) Northern Sirte Basin	21
	b) Central Sirte Basin	22
	c) Southern Sirte Basin	23
4	- Correlation Chart of the Late Cretaceous and Tertiary of Northern Libya	
5	- Columnar Section showing the General Lithology of the Study Area Encountered in A1-59F Well	26
6	- Structural Cross-section of the Study Area	
7	- Isopach Map of the Lower Beda Member . .	27
8	- Stratigraphic Cross-sections:	
	a) Southwest - Northeast	
	b) Northwest - Southeast	
9	- The Vertical Sequences of the Beda Formation Microfacies	62
10	- Standard Microfacies and their Depositional Environments	79
11	- Summary Diagram of Environmental Conditions During Deposition of Beda Sediments and Allochthems	94
12	- a) A Sketch of Tectonic Elements of Sirte Basin	98
	b) A Profile of the Tectonic Elements	98
	c) General Stratigraphy of the Beda Formation	98
13	- Reconstruction of the Paleogeography of the Study Area	105
14	- Structure Map on Top of Lower Beda Member	

LIST OF APPENDICES

	<u>Page No.</u>
I Plates	133
Plate A: Charophytes	134
Plate B: Benthonic Foraminifera	135
Plate C: Microfacies	137
II Sample Descriptions of Beda Formation, well	
Y3-59	168

CHAPTER ONE: INTRODUCTION

Introduction

Sirte Basin is one of the most prolific hydrocarbon producing basins in Libya and contains most of the discovered hydrocarbon reserves. Carbonates of the Beda Formation are widespread throughout the study area and other parts of the Sirte Basin. It is a potential reservoir in several oil fields, and is a primary hydrocarbon exploration target in many areas of the basin. Beda Formation sediments vary greatly in thickness, lithology and reservoir properties from one area to another.

This study represents a detailed microfacies analysis and paleoenvironmental reconstruction of the Beda Formation sediments in Western Concession 59 and 59F Block. The formation represents one of the thickest sedimentary units in the western Sirte Basin. The study area is characterized by several structural features as a result of extensional tectonics. The faults are basement controlled and trend NNW-SSE. These features are responsible for the oil entrapment wherever adequate reservoirs are available. Recent seismic structural maps show several structural closures at the Beda level. The structural closures coincide with thick sections of Beda Formation carbonates, with relatively good reservoir qualities. The Beda Formation reservoir rocks are capped by anhydrite beds near the top and by the conformably overlying Khalifa Shale. Oil has been tested in previously drilled Y1, Y3, 6A1 and CC1-59 wells. The reservoir potential varies from one location to another depending on paleogeography and diagenetic processes.

Purpose of Study

The purpose of this study is to interpret the textures and constituents of the original sediments comprising the Beda Formation in the study area and to interpret their depositional environments.

The Beda Formation is of great economic importance for hydrocarbon exploration and production in southwestern Sirte Basin. This study is also an attempt to delineate the major factors that control and influence the oil accumulation in the formation. These factors may include porosity, permeability, facies and structural changes. The results of this study will outline reservoir intervals with good porosity and permeability for development and completion of the oil fields at the production stage. In addition, these results will assist future exploration planning to determine the most favourable structures for hydrocarbon exploration drilling.

Location

The study area is located within western Concession 59 and 59F Block at the southwestern portion of the Sirte Basin in Libya. It is approximately 260 km south of the Mediterranean Sea, between co-ordinates 28° to $28^{\circ} 15'$ N latitude and $18^{\circ} 30'$ to $18^{\circ} 45'$ E longitude (Fig. 1).

The study area lies in a tectonically complicated southwestern portion of the Sirte Basin, where several tectonic features intersect. These features are the Beda Platform, Gerad Trough, Dahra-Hofra Platform and Zella Trough (Fig. 2).

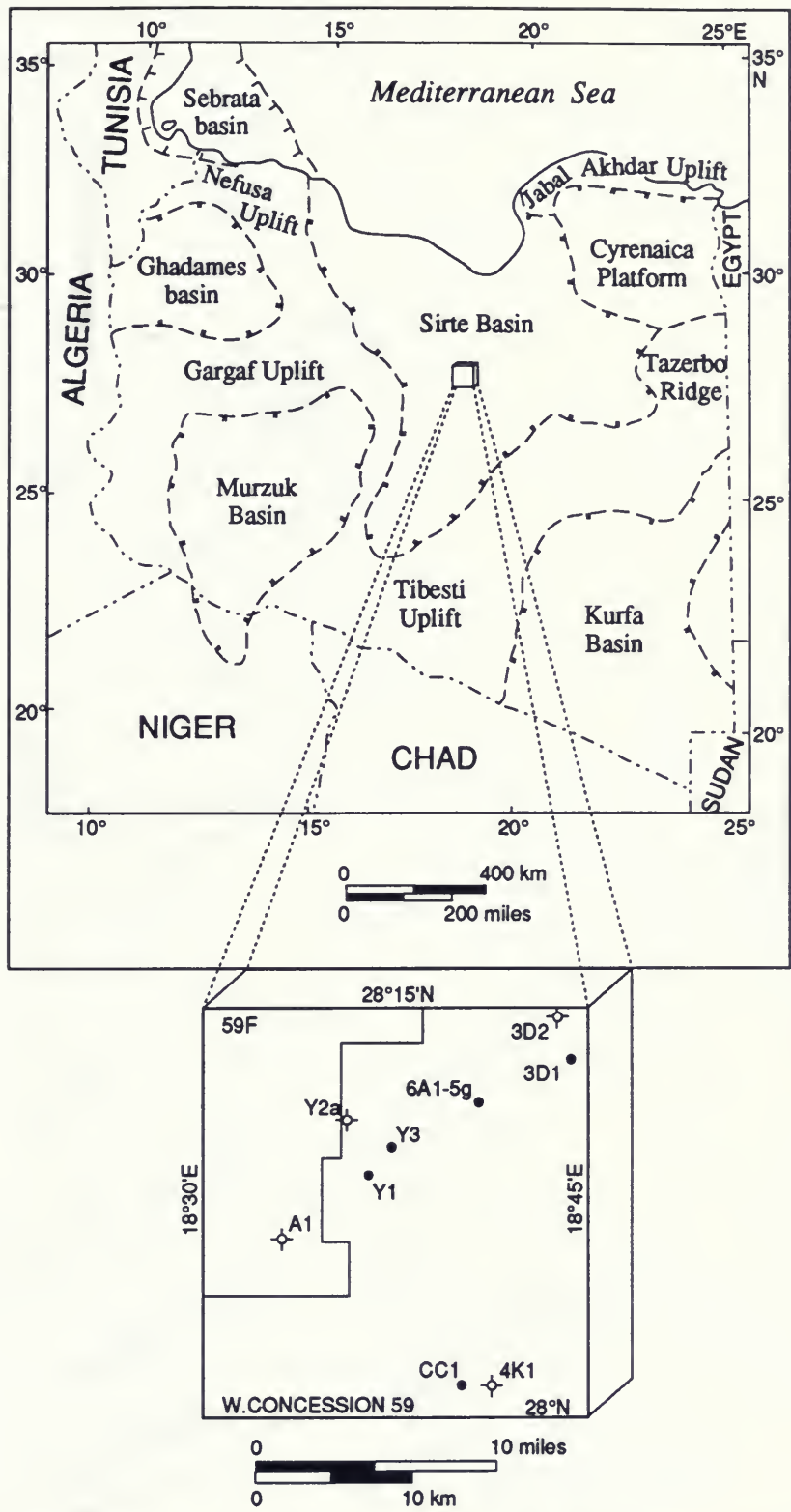


Fig.1 Map of Libya showing major Tectonic Regions
Inset represents study area and drilled wells

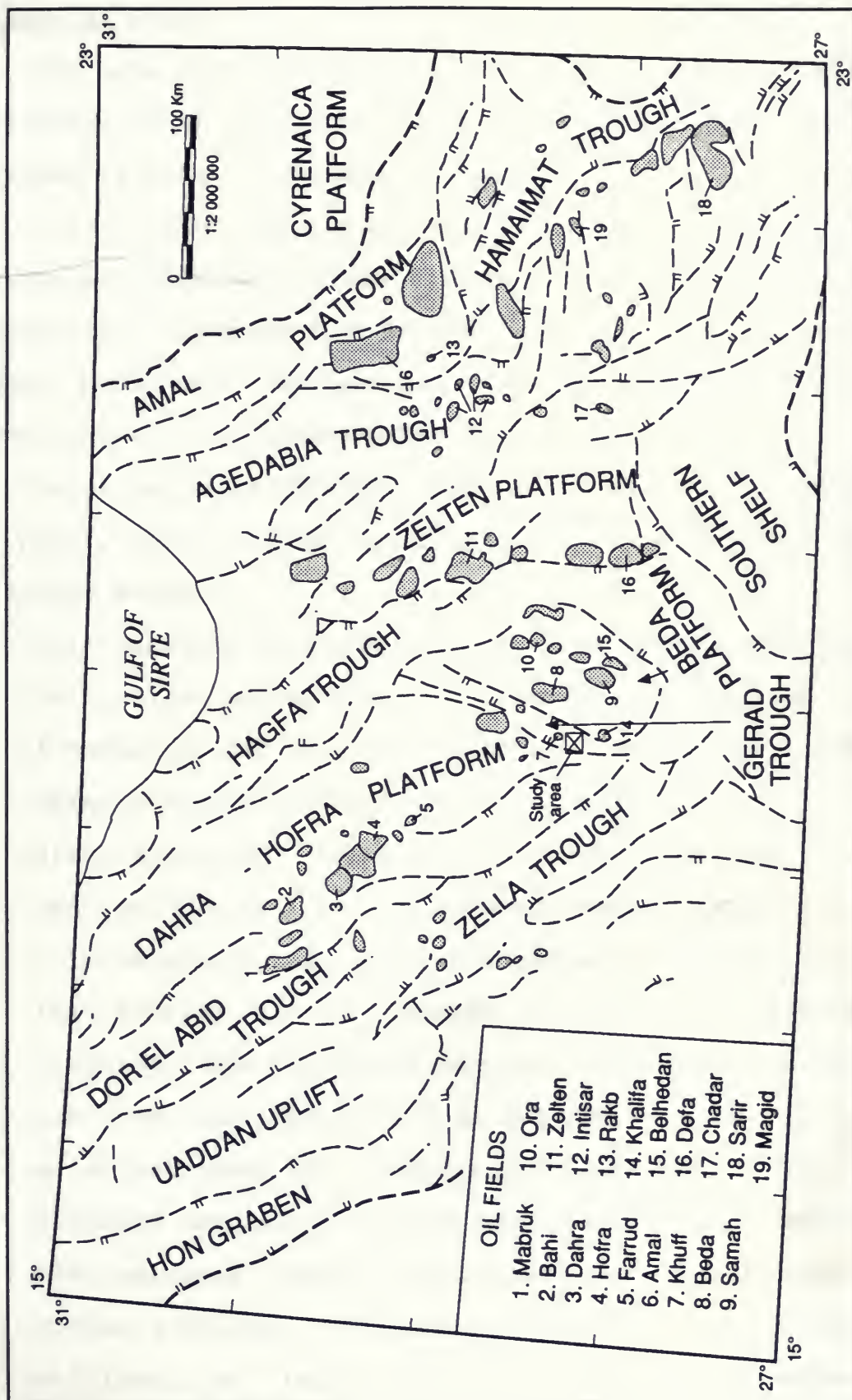


Fig. 2 Major tectonic elements and oil fields of Sirte basin. (modified from Hamyouni et al. 1984)

Methods of Study

The Beda microfacies study is based on geological material, including ditch cuttings, cores, geophysical logs and maps provided by Waha Oil Company of Libya.

The various facilities available at the Department of Geological Sciences of Brock University were utilized in sample preparations, ranging from thin-section cutting, polished core slabs, microfossil extraction, scanning electron microscopy, normal photography and computer facilities.

Cores and ditch cuttings from several wells, including 6A1-59, Y1-59, Y2a-59, Y3-59, A1-59F and CC1-59, were studied by the following methods:

1. Thin-sections were prepared from core samples that were cut into slices and ground to an average thickness of 0.03mm. A total of 200 thin-sections were prepared and examined using a regular petrographic microscope.
2. Stain analysis: Alizarin Red-S stain was used in thin-section staining to distinguish calcite from dolomite. Calcite stains red, whereas dolomite is not affected. The thin-section may be covered in order to protect the staining. The staining solution is prepared by dissolving one gram of Alizarin Red-S in 2ml concentrated HCl and 998 ml of deionized H₂O (Lindholm and Finkelman, 1972).
3. Polished core slab surfaces provided excellent details of rock textures, structures and skeletal constituents.
4. Etched surfaces: A dilute solution of 10% v/v HCl was utilized for visual distinction between limestone and dolomite, based on types of effervescent reactions.

Etching provides valuable information on the rock texture, grain size, identification of non-carbonate grains, and microfossil structures;

5. Microfossil examination: The microfossil content of rock samples from Y1-, Y2a-, Y3-, 6A1-, CC1-59, and A1-59F wells were examined. A total of 250 slides were prepared and the microfossil content was identified under a binocular microscope. Benthonic foraminifera, ostracods, charophytes, dasycladacean algae, molluscs, echinoderms, and bryozoans were identified.

Plates A and B of Appendix I contain the microfossil assemblages and their identifications. The microfossils were extracted from crushed core samples and ditch cuttings by using "Quaternary-O", which is a detergent and an industrial degreaser (Ash and Ash, 1991). The method is described as follows:

- A Add a teaspoon of "Quaternary-O" to a quart of water, or an equivalent of 10ml of "Quaternary-O" to one litre of water in a container with a small amount of rock sample to be disintegrated and cleaned;
- B Allow the solution containing the sample and "Quaternary-O" to boil for three hours, adding water regularly to prevent the solution from drying up and burning the sample;

- C Remove the solution from heat and allow it to cool to room temperature. The residue will settle out on the bottom of the container out of the viscous solution;
- D Gently pour the solution of the container into a 60 mesh sieve placed in a basin. Remove the sieve with residue and decant the solution in the basin;
- E Gently wash and agitate the residue in the sieve several times to ensure that the residue is free from "Quaternary-O" and the mud;
- F Allow the residue to dry in the oven at a minimum temperature of 37.8°C ;
- G The microfossils can be easily picked using a suitable brush and placed on slides for identification;
- H Maps and cross-sections were prepared to demonstrate the microfacies variations, their lateral and vertical continuity. Geophysical well logs and formation tops of wells drilled in and around the study area were also utilized for regional correlations and interpretations.

CHAPTER TWO: GEOLOGY OF SIRTE BASIN

Introduction

There are seven sedimentary provinces in Libya, including the Mesozoic-Tertiary basins of Sirte, Sebrata and the offshore shelf around the Jabal Al-Akhdar Uplift, in addition to the Paleozoic Ghadames, Murzuk, Kufra Basins and Cyrenaica Platform. Several broad uplifts constitute interbasinal boundaries (Fig. 1).

Sirte Basin is the most prolific hydrocarbon producer in Libya and contains most of the discovered hydrocarbon reserves. Oil is trapped in fractured Precambrian basement rocks, Pre-Upper Cretaceous sandstones, and various Upper Cretaceous and Tertiary rocks. Potential hydrocarbon reserves have been discovered in Ghadames, Murzuk and Sebrata Basins and in the northeastern offshore areas of Jabal Al-Akhdar. Minor reserves were discovered in Cyrenaica Platform sediments. However, no commercial hydrocarbon reserves were reported for the Kufra Basin.

Geologic Setting

The Sirte Basin is bounded by the Paleozoic Ghadames and Murzuk Basins to the west; the Paleozoic Kufra Basin to the southeast, and the Cyrenaica Platform to the east and northeast.

Murzuk and Kufra Basins are classified as interior sag basins. They are large continental, intracratonic downwarps, formed by thermal sagging of the continental crust. Ghadames Basin is a foreland basin developed in several tectonic cycles.

It consists of an interior sag basin underlying a marginal sag basin, resulting from folding along converging plates (Clifford, 1986; Selley, 1988). Sirte Basin is classified as an interior fracture basin caused by extensional tectonics. It is characterized by horst and graben structures. Most of the discovered oil fields are associated with highs "horsts", whereas thick shale sequences are associated with lows "grabens" providing the source rocks for the generation of hydrocarbons.

Tectonic Evolution

Several tectonic episodes ranging from Caledonian-Hercynian through Alpine Orogenies resulted in the present day geologic picture of Libya (Hamouni et al., 1984). The Sirte Basin is a rift basin that is probably related to the break-up of Pangaea during the Mesozoic. The primary stage of separation was during the Jurassic (200 - 180 Ma ago) and was marked by a major peak in rift formation (Burke and Whiteman, 1973; Burke and Dewey, 1974). The Sirte dome was initiated after Paleozoic regional uplift as a result of the Hercynian Orogeny.

During the Jurassic through Early Cretaceous, the Sirte dome was subjected to extensional stress resulting in the collapse of the Sirte dome into intricate systems of horsts and grabens trending NNW-SSE (Fig. 2). Precambrian crystalline rocks constitute the bottom of the Sirte Basin (Fig. 3a, b, c).

Initial extreme thinning of the continental crust "lithosphere" is known today in the Red Sea, and where it is succeeded by an arching stage due to lateral extension by normal faulting (Lowell and Genik, 1972; Helwigs, 1976; Harding and

Lowell, 1979). Analagous to the structural history of the Red Sea, the first stage in Sirte Basin's structural evolution was marked by regional arching of the continental lithosphere. This may be caused by thermal convective upwelling in the asthenosphere (Van Houten, 1983). Continued thinning and rifting by normal fault tectonics , subsidence of the newly formed structural features and eustatic sea-level changes led to the inundation of the Sirte Basin by marine waters of the "Paleo-Mediterranean" Tethys Sea from the north during the Late Cretaceous (Barr, 1972; Berggren, 1974; Perrodon, 1983). The Cambro-Ordovician Gargaf quartzite represents pre-rift phase sediments, whereas the Cretaceous and Tertiary sediments represent the post-rift sedimentation phase (Figs. 3a, b, c).

The pre-rift sediments were faulted during the subsequent rifting stage and truncated by an angular unconformity that marks the beginning of rifting. Continental sediments of the Pre-Upper-Cretaceous were being deposited during the rifting stage. Cenomanian transgression resulted in deposition of thick shales, evaporites and carbonates progressively burying and covering the newly formed landscape. Marine transgression and sedimentation continued into the Tertiary and was dominated by carbonate, shale and evaporite deposition. On the grabens accumulated thick sedimentary sections, characterized by shales and argillaceous limestone, whereas the platforms were characterized by high energy carbonates and carbonate build-ups. These sediments represent the post-rifting stage.

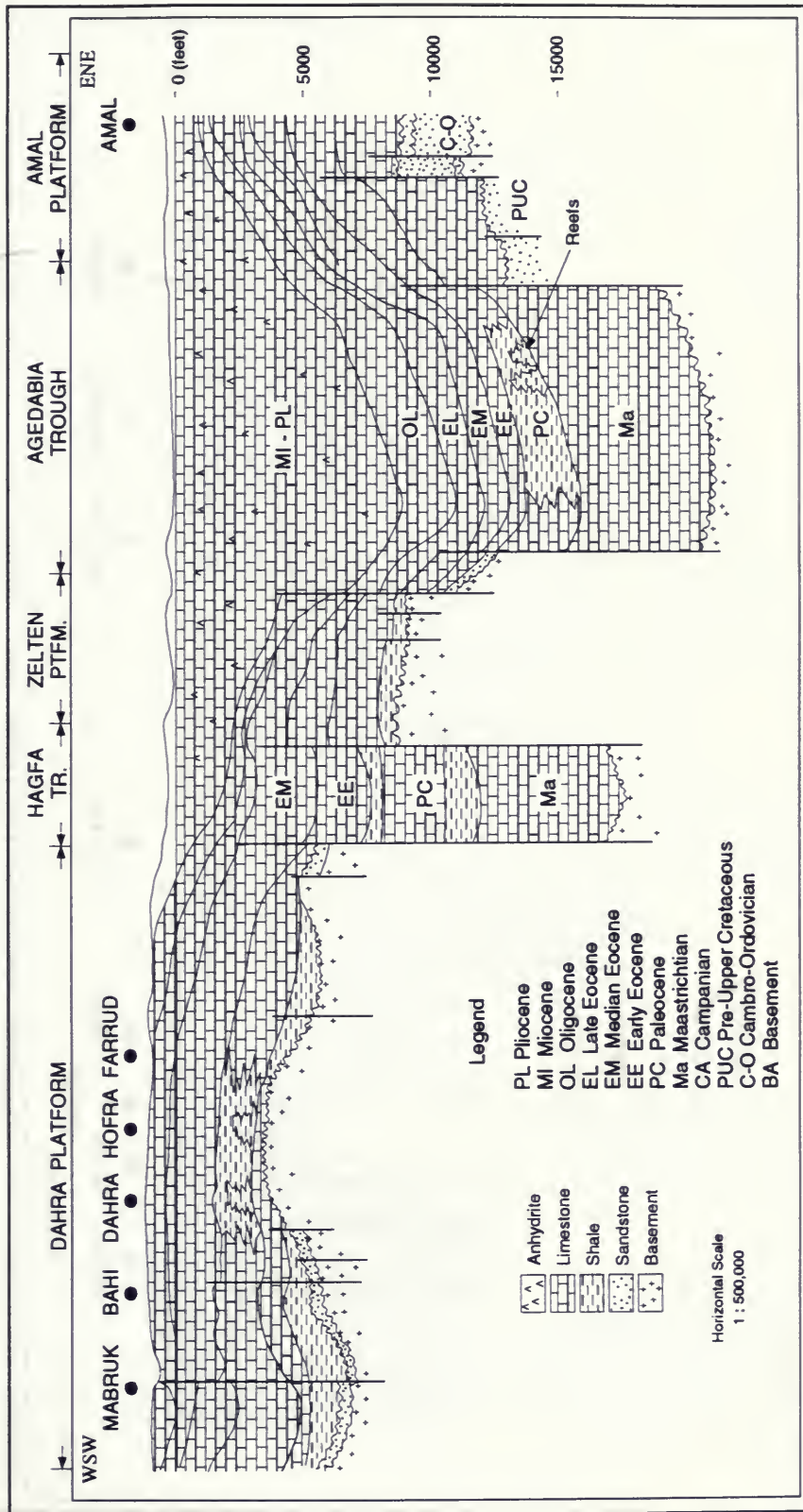


Fig. 3a Structural geologic section of the northern Sirte Basin. (modified from Hamyouni et al. ,1984)

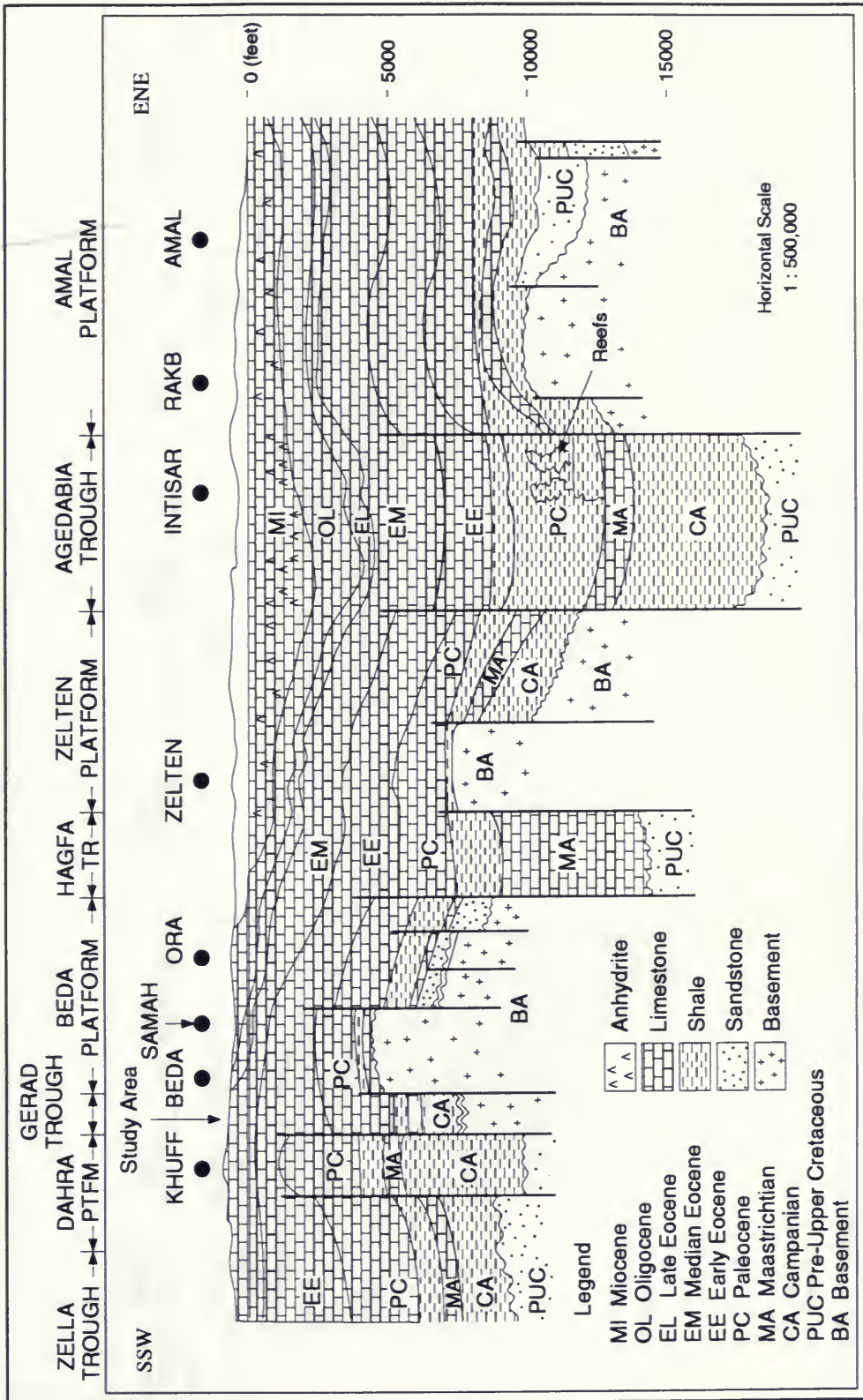


Fig. 3b Structural geologic section of the central Sirte Basin. (modified from Hamyouni et al. , 1984)

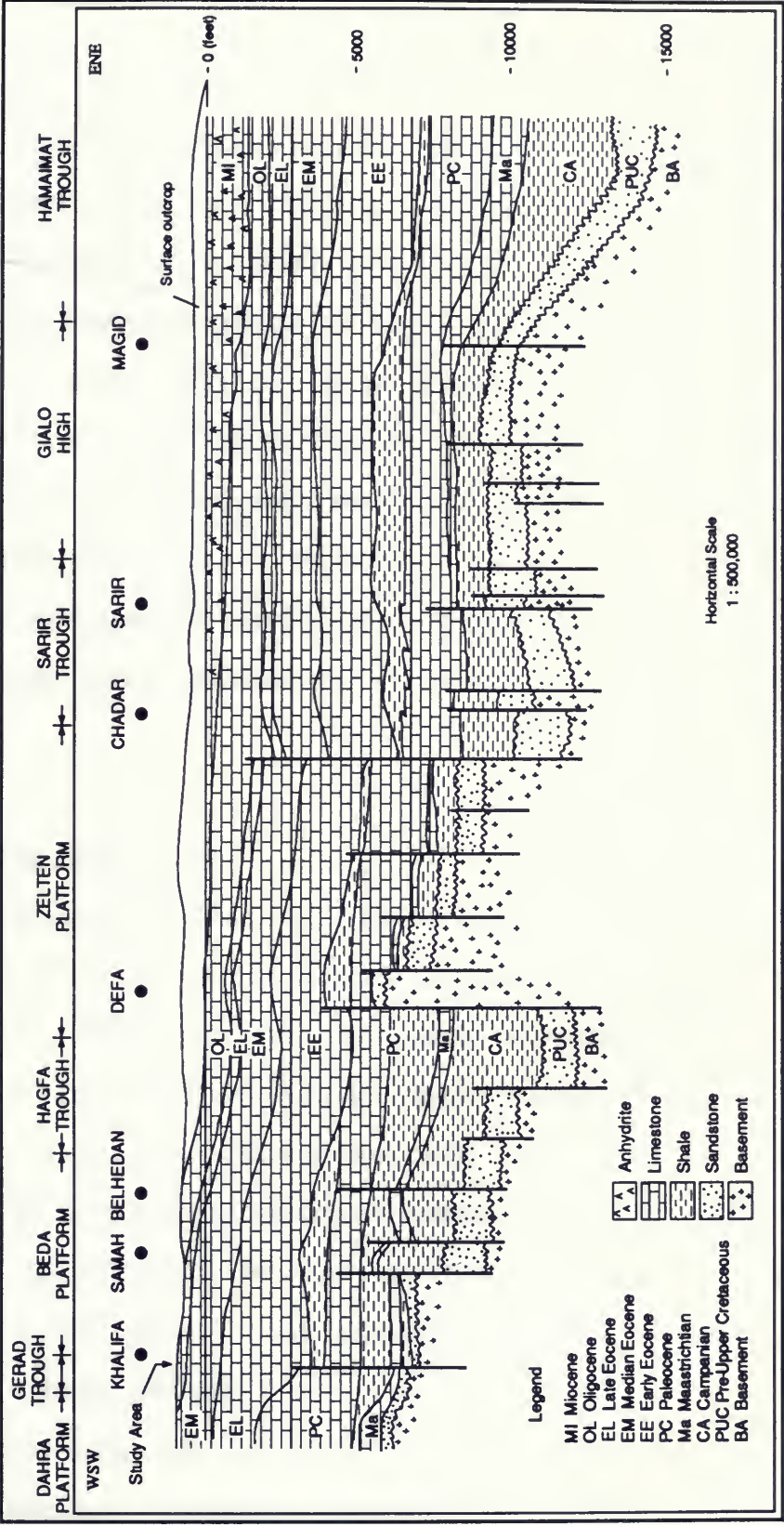


Fig. 3c Structural geologic section of the southern Sirte Basin. (modified from Hamyouni et al. , 1984)

CHAPTER THREE: GENERAL STRATIGRAPHY

Introduction

The Sirte Basin occupies an onshore area of approximately 492,000 km² and contains a thick predominantly marine sedimentary section in excess of 7,620m, ranging in age from Paleozoic to Cenozoic. Average thickness of the sedimentary column is 2,400m (Hamouni et al., 1984). Late Cretaceous Tethys sea water transgressed over the fault blocks from the north, resulting in the deposition of marine sedimentation. The platforms were the site of shallow water deposition of limestones, reefal development and marine sandstones, whereas the troughs were the site of deeper water sediments such as shales and argillaceous limestones.

Stratigraphic Sequences

Hydrocarbon exploration activities in the Sirte Basin by different oil companies resulted in the erection of different stratigraphic nomenclatures by each operator, in order to maintain the confidentiality of their exploration activities. In order to avoid the confusion that has resulted from these discrepancies, the stratigraphic nomenclature proposed by Barr and Weegar (1972) will be implemented throughout this study. The general lithologies, contacts and relative ages are included in Fig. 4 (in back pocket).

The stratigraphic sequence of the study area consists of a thick sedimentary section exceeding 4,500m. A complete sedimentary section was drilled in well A1-59F with a total

depth of 4,510m (14,885 ft.), marking the top of the Pre-Cambrian metamorphic basement (Fig. 5).

The sequence is marked by two major unconformity surfaces; one marked the uplift stage during the Paleozoic, while the other marked the end of Lower Cretaceous sedimentation and the rifting stage. A thick sequence of 912m (3,100 ft.) of continental clastic sediments underlies the Pre-Upper Cretaceous unconformity. The Upper Cretaceous and Tertiary sequences are predominantly marine and consist of alternating successions of deep and shallow marine carbonates, shales, sandstones and evaporites with a maximum thickness of 3,338m (11,014 ft.), encountered in well A1-59F (Fig. 5). However, greater thicknesses are encountered in the rest of the study area where a tremendous increase in the Cretaceous section was indicated by doubling of the thickness of Sirte shale progressing from wells A1-59F to Y1-59 (Figs. 6, in back pocket, and 7). The A1-59F well is located at the edge of the Gerad Trough, whereas the other drilled wells are located towards the center, and their sedimentary sections are consequently thicker as a result of subsidence.

Significant lateral facies variations occurred throughout the Sirte Basin during the Tertiary, which are marked by the development of reefs, shallow water limestones, shales and evaporites. However, no significant lateral facies variations were observed in the study area.

The vertical stratigraphic sequences and basement rocks encountered in the study are based on descriptions provided by

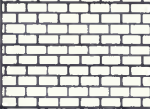

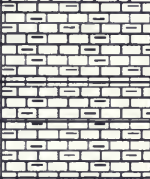

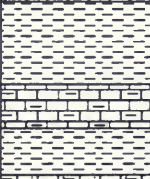


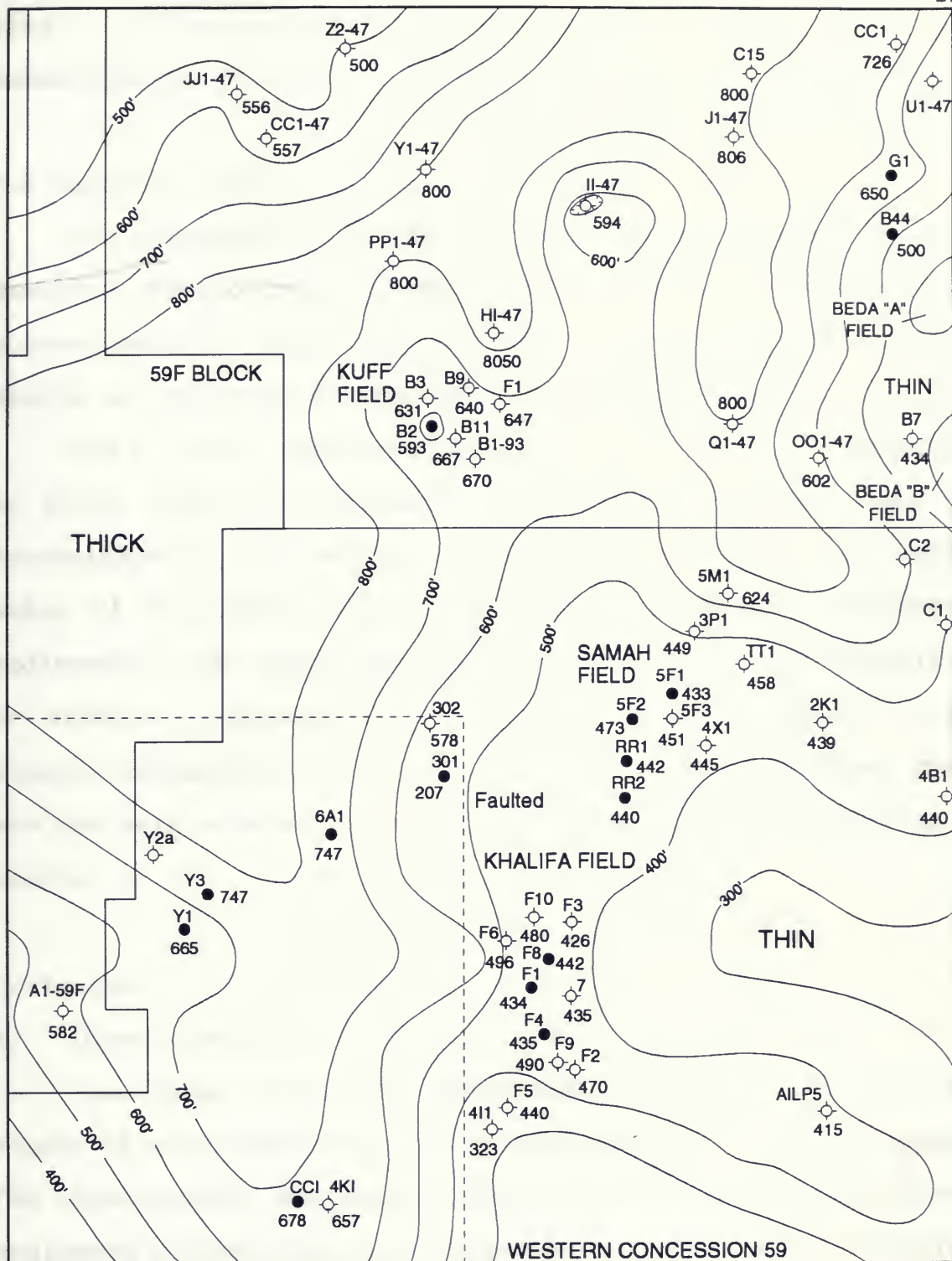
AGE		FORMATION	DEPTH	LITHOLOGY	DESCRIPTION	
TERTIARY	EOCENE	Gialo	+860' +260m		Nummulitic Limestone	
		Gir	1915' 580m		Limestone, Anhydrite and Dolomite	
	PALEOCENE	Kheir	4304' 1300m		Carbonate with Shale	
		Harash	4630' 1400m		Carbonate with Shale	
		Zelten	4905' 1486m		Carbonate with Shale	
		Khalifa	5180' 1570m		Carbonate with Shale	
		"BEDA"	5915' 1793m			Carbonate, Shale, Anhydrite
			Hagfa			6702' 2030m
	CRETACEOUS	L	Kalash	7743' 2346m		Limestone, Shale
			Sirte Shale	8243' 2498m		Shale
			Rachmat	9014' 2731m		Shaley Carbonate with stringers of Sandstone
Etel			9835' 2980m	Carbonate, Shale, Anhydrite and Salt		
Lidam			10828' 3281m	Carbonate and Shale		
Etila			11388' 3450m	Sandstone, Red Shale		
E		Nubian	11874' 3598m		Sandstone and Shale, Red beds	
Pre-Cambrian		Basement	14885' 4510m		Metamorphic rocks	

Fig.5 Columnar section showing the general lithology of the study area as encountered in well A1-59F.



Waha Oil Company and (Barr and Weegar, 1972). They are summarized as follows:

The Basement Rocks

The basement rocks of the study area consist of Pre-Cambrian metamorphic schists and quartzite. Basement was encountered at 4,511m (14,385 ft.) in well A1-59F; greater depths are expected in the rest of the study area.

The basement rocks are unconformably overlain by Paleozoic or Early Cretaceous sediments. Paleozoic sediments were not encountered in the study area and they represent the uplift stage of the Sirte Basin development. Absence of Paleozoic sediments in the study area can be attributed to non-deposition or erosion. Basement rocks were the primary source for the clastic sediments of the Sirte Basin. Fractured basement rocks are the main reservoirs of Amal and Nafoora oil fields (Figs. 2 and 3a, b, c).

Cretaceous

A) Upper Cretaceous

The Upper Cretaceous sequences represent the earliest stages of sedimentation in Sirte Basin during the rifting phase. The stratigraphic sequences consist of thick non-marine clastic sediments of Early Cretaceous age known as the Nubian Formation. The Nubian Formation may unconformably overlie Paleozoic or basement rocks. However, in the study area it unconformably overlies the metamorphic basement.

The Nubian Formation represents the lowermost unit of the stratigraphic series of the study area (Fig. 5). A major unconformity separates the Lower Cretaceous Nubian sediments from the overlying Upper Cretaceous ones.

The Nubian Formation is subdivided into three members: the Upper Sand, the Middle Shale and the Lower Sand Member (Pomeyrol, 1968). This formation reaches a total thickness of 912m (3,011 ft.) in well A1-59F. The Upper Sand Member attains a thickness of 240m (791 ft.) and varies in lithology from fine to medium to coarse grained quartz sand with minor amounts of interstitial clay and feldspars. The Middle Shale Member consists of 312m (1,029 ft.) of red, gray, green and maroon coloured, laminated micaceous shales. This member occasionally contains a considerable percentage of organic material that qualifies it as a good source rock for hydrocarbon generation (Hamouni et al., 1984). The Lower Sand Member is similar in lithology to the Upper Member and attains a thickness of 361m (1,191 ft.) in well A1-59F. The Upper and Lower Sand Members constitute the main reservoirs of giant oil fields, such as Sarir, Bu Attifel, Messla and others in the Sirte Basin (Fig. 2). However, in the study area the Nubian Formation contains no hydrocarbons.

B) Upper Cretaceous

The Upper Cretaceous sedimentary sequences consist of six formations (Fig. 5) forming the Rakb Group and Kalash Formation.

The individual formations are described as follows:

1. The Rakb Group consists of five formations, listed as follows:

a) Etla Formation:

Etla Formation is primarily a reworked clastic unit composed of interbedded siltstone, claystone and sandstone cemented with calcite or dolomite. It is poorly sorted and contains an appreciable amount of red or green interstitial clay and thin interbeds of reddish green, non-calcareous shale. Glauconite, hematite and anhydrite are also common. Fossils were recorded as well.

The Etla Formation is a transgressive marine unit of Cenomanian age and attains a maximum thickness of 169m (560 ft.) in well A1-59F.

b) Lidam Formation:

Lidam Formation consists predominantly of argillaceous limestones with shales and claystone. It is partly dolomitic and pyritic, with occasional traces of anhydrite and siltstone. The maximum thickness of the Lidam Formation in well A1-59F is 169m (578 ft.). The microfossil assemblage is dominated by Cenomanian ostracods and foraminifera. In other parts of the Sirte Basin, it is developed into better facies and is dolomitized, providing excellent reservoirs, such as those of the Masrab oil field (Fig. 2).

c) Etel Formation:

Etel Formation consists of a thick section of interbedded salt, shale, anhydrite, limestone, dolomite and siltstone. The shale is gray-green to brown and occasionally oxidized red, in addition to being calcareous, and partly pyritic with rare glauconite. The dolomite is microcrystalline and ranges in colour from gray to brown and tan. The limestones are micritic, argillaceous, gray to tan in colour, well indurated and fossiliferous. The maximum thickness of this unit in well A1-59F is 300m (993 ft.). The Etel rocks provide the cap for the underlying reservoirs.

d) Rachmat Formation:

Rachmat Formation is primarily a shale sequence with occasional dolomite interbeds toward the bottom, and silt intercalations near the top.

The shale is dark gray and occasionally green or brown, slightly calcareous, glauconitic in part, pyritic, with common limestone interbeds. The maximum thickness of this formation in well A1-59F is 249m (821 ft.), and contains an abundance of benthonic and planktonic foraminifera and ostracods, indicative of Santonian-Coniacian age.

e) Sirte Formation:

This formation consists mainly of dark gray to dark brown, calcareous, carbonaceous and pyritic shale with occasional stringers of limestone. The lower part of Sirte Formation becomes silty with traces of glauconite and dolomite. It is

rich in foraminifera and ostracods. This formation reaches a maximum thickness of 233m (771 ft.) in well A1-59F and ranges in age from Early Campanian to Early Maastrichtian. It is believed to be the source rock for most of the discovered hydrocarbons in the Sirte Basin (Hamayouni et al., 1984).

2. Kalash Formation:

This formation consists mainly of light brown, tan and gray argillaceous limestone with dark gray calcareous shale intercalations. It reaches a maximum thickness of 134m (442 ft.) in A1-59F well. The Kalash Formation contains an abundance of benthonic and planktonic foraminifera and molluscs, indicative of open marine and moderately deep water depositional environments (Barr and Weegar, 1972).

The Kalash Formation was cored in A1-59F and no hydrocarbon shows were encountered. However, it is a prolific reservoir in other parts of the Sirte Basin.

Tertiary

A) Paleocene

The Paleocene sedimentary sequence attains an average thickness of 1,000m (3,300 ft.) in the study area. The facies change dramatically from shales in the troughs to carbonates and local reefs on the platforms throughout the Sirte Basin (Fig. 3).

The Paleocene of the study area is subdivided into early and late stages: Danian and Selandian. The Danian stage is represented by the Beda and Hagfa Formations. The Selandian

"Thanetian" consists of Khalifa, Zelten, and Harash Formations. Kheir Formation straddles the Eocene-Paleocene boundary. The Paleocene formations are listed as follows, in ascending order:

1) Hagfa Formation:

This formation represents the earliest unit of the Paleocene sequence and is Danian in age. Hagfa Formation consists of a thick section of gray, gray-green, gray-brown and black calcareous shale, interbedded with argillaceous limestone in the upper portion of the formation. It is highly fossiliferous and contains an abundance of benthonic and planktonic foraminifera, ostracods, echinoderms and molluscs. The Hagfa Formation reaches a thickness of 310m (1,023 ft.) in well Y1-59 of the study area.

The formation is common throughout the Sirte Basin and it laterally changes into platformal limestones and reefal limestones that constitute the reservoirs of Defa and Intisar oil fields (Fig. 2 and 3).

2) Beda Formation:

The Beda Formation has been informally subdivided into Upper and Lower Members, based on electrical well log and facies change data. The Beda Formation is the subject of this study. The Upper Beda Member is approximately 63m (206 ft.) and the Lower Beda Member averages about 200m (665 ft.) throughout the study area.

In the study area, the Upper Member consists of argillaceous limestone interbedded with dolomite and anhydrite.

However, in other parts of the basin, this member may consist of oolitic limestones and dolomite, providing excellent oil reservoirs throughout the basin. The Lower Member is predominantly limestone, consisting of alternating microfacies with distinct structures and textures. The Beda Formation contains an abundance of benthonic foraminifera, charophytes, dasycladacean algae, ostracods, molluscs, echinoderms, fecal pellets and bryozoans. Algal mats, fenestral fabrics, dolomite and anhydrite are common near the top of the Beda Formation.

The Beda Formation is also known as the "Dasycladacean-Oolitic" limestone (Barr and Weegar, 1972). It is an excellent reservoir throughout most of the Sirte Basin, and it is encountered as a reefal development in Beda field (Fig. 2).

Previous paleontological age dating based on foraminifera indicates a Median Paleocene "Montian" age (Barr and Weegar, 1972) and Montian to Early Thanetian "Selandian" age (Berggren, 1965).

The discovery of the charophyte algae during the course of this study, and the consequent micropaleontologic and stratigraphic interpretations, dictate a revision of the previously assigned age. The new interpretation in the light of this discovery will be discussed in Chapter Four.

3) Khalifa Formation:

Khalifa Formation represents the boundary between the Selandian and the Danian. It has an average thickness of 200m (660 ft.) and consists mainly of argillaceous limestone and dark gray calcareous shale. It is marked by an abundance of faunal

assemblages, dominated by foraminifera, including miliolids and other benthonics and planktonics, indicative of open, shallow to deep marine depositional environments.

Lateral facies changes of Khalifa shale into limestone resulted in the development of reservoir horizons in several locations on the Dahra-Hofra platform. However, in the study area it is predominantly shale and argillaceous limestone that serve as a seal for the underlying Beda reservoir horizons.

4) Zelten and Harash Formations:

These two formations constitute the Jabal Zelten Group. They are considered to be Selandian in age and are predominantly carbonates intercalated with thin shales. The average thickness of this group is 170m (561 ft.) within the study area. The sediments of this group are highly fossiliferous, with an abundance of large and small benthonic foraminifera, and dasycladacean algae, indicative of shallow water depositional environments. These two formations are prolific reservoir rocks and constitute the main reservoirs of the Harash, Zelten, Gialo and several other oil fields in the Sirte Basin.

5) Kheir Formation:

Kheir Formation represents the boundary between Upper Paleocene and Lower Eocene. It consists of calcareous dark gray to greenish gray shale with some limestone, marl and clay. It is extremely fossiliferous and contains an abundance of large and small benthonic and planktonic foraminifera, ostracods,

molluscs, echinoderms and bryozoans. Average thickness of Kheir Formation in the study area is 100m (330 ft.)(Fig. 5).

B) Eocene

The Upper Eocene is represented by the Gir Formation, with an average thickness of 720m (2,376 ft.), consisting of limestone and dolomite interbedded with anhydrite. The lower and upper parts of Gir Formation are fossiliferous. The anhydrite interbeds lack fossils. The Gir Formation represents deposition in shallow marine intertidal to supratidal environments (Fig. 5).

The Middle to Upper Eocene strata of the study area are represented by the Gialo Formation. It attains an average thickness of 300m (990 ft.) and consists of gray to light brown, shallow marine limestone. The Gialo limestone is highly fossiliferous, containing large foraminifera, such as *Nummulites*, in addition to molluscs, echinoderms, ostracods and bryozoans. Gialo limestones are encountered in the subsurface, as well as in surface outcrops throughout the study area (Fig. 5).

CHAPTER FOUR: MICROPALEONTOLOGY

Introduction

Fossils are important indicators of paleoenvironments of deposition. They can be utilized to distinguish marine from non-marine and shallow from deep water environments. Fossils making up part of the sedimentary facies, regarded as grain constituents, and their physical characteristics, such as size, shape, degree of abrasion, rounding, and diagenetic alteration, provide indications of the depositional environment, ecological conditions, depositional processes, as well as diagenetic changes.

Distribution of modern faunal assemblages can be utilized to reconstruct the paleoenvironments of deposition. Several parameters must be taken into consideration when using fossils for paleoenvironmental interpretation, such as the state of preservation, faunal association, diversity, and abundance (Pickerill and Brenchley, 1991).

The Beda Formation in the study area is replete with many benthonic microfossils, such as foraminifera, ostracods, dasycladacean and charophyte algae, molluscs, echinoderms and bryozoans. In this chapter only benthonic foraminifera and charophyte algae will be considered. Benthonic foraminifera are the most widely used microfossils for paleoenvironmental studies and their identification will be limited to generic level. Charophyte algae represents a new finding in the Tertiary of the Sirte Basin and merits some detailed descriptions because of their paleontologic and paleoecologic significance. They are identified to a species level.

Charophytes

Introduction

The charophytes, or stoneworts, are a small group of freshwater green algae that grow submerged on muddy bottoms in ponds, lakes and streams, connected to tidal flat water through a narrow channel, and they range in age from Silurian to Holocene (Khan, 1991).

Charophytes are small plants ranging in height from 15-30cm to 2m. They secrete CaCO_3 on their outer surfaces, calcifying certain parts that are preserved as fossils. The calcified oogonium (gyrogonite or female sac), is the commonly preserved part. It is a spherical to oblong calcareous body with spirally arranged cells, and it attains a maximum diameter of 1.5mm (Tappan, 1980).

Charophytes reproduce by either sexual or vegetative processes. The calcified and fertilized oosporangium (egg), falls to the bottom of their habitat and germinates after a few weeks. Germination may take place through desiccation or through an opening at the apex of the gyrogonite (Tappan, 1980).

Charophytes occur in abundance everywhere in fresh, brackish, quiet and shallow water conditions ranging in depth from 2-30m and can tolerate a wide range of salinity; however optimum growth is at about $26^\circ/\text{‰}$ (Moore, 1991). Modern charophytes need a fresh water stage to regenerate and establish their early growth. However, some species can live in hypersaline waters and can regenerate in brackish water (Riveline, 1991, pers.comm; Feist, 1991, pers.comm.).

Burne et al. (1980) successfully germinated *Lamprothamnium populusum* charophytes under laboratory conditions and salinities greater than those of the Coorong Lagoon in Australia. Germination occurred in less than two weeks in both fresh water and seawater of 35‰ salinity, but no germination took place at higher salinities. However, they suggested that germinated charophytes can survive 60‰ - 70‰ maximum salinity (Burne et al., 1980). They also stated that living charophytes are present in Holocene ephemeral lakes of southern Australia at salinities twice that of seawater (up to 69‰).

The charophytes of the Holocene lakes of southern Australia were found to be associated with ostracods, gastropods and foraminifera. The southern part of Australia is characterized by a semi-arid, Mediterranean type of climate. Living charophytes tolerate differences in salinity by regulating their body pressure through an increase or decrease in their body's ion concentration (Winter and Kirst, 1991).

The occurrence of charophytes is recorded worldwide, except in Antarctica, ranging from sea level to 4,764m in the Himalayas, and from the tropics to Alaska. They are most abundant in temperate regions (Tappan, 1980).

Charophytes thrive in clear, shallow and well oxygenated water, with pH ranging from 5.2 to 9.8, but are common in waters with pH values of 7-8 (Tappan, 1980).

In the Paris Basin, Late Eocene gypsiferous sedimentary sequences contain charophytes in association with miliolids in

many intercalations. The gypsum was interpreted to have been formed as a continental deposit (Riveline, 1991, pers.comm.)

Occurrences

LIVING CHAROPHYTES

Charophytes were reported to be living today in southern Britain and western Ireland in brackish waters of coastal lagoons and ponds with salinities of 26‰ , and water depth of less than 2m (Moore, 1991). They may grow in near-shore shallow water (18m depth) in the Finger Lakes of New York, to about 30m in the Konigsee of Germany and some Japanese lakes (Tappan, 1980). They are found in some of the coastal lagoons and saline lakes adjacent to the Coorong region in Australia, where they are associated with gastropods, ostracods and foraminifera (Burne et al., 1980).

In the National Park of Plitvice Lakes in the Balkans, Yugoslavia, charophytes cover the bottom of lakes and the water depth was reported to be up to 7m (Blazenic et al., 1991).

FOSSIL CHAROPHYTES

Fossil charophytes are found in association with molluscs, foraminifera, ostracods, fish teeth and wood fragments in non-marine sediments. They have also been found in brackish or near shore sediments associated with a typical marine fauna throughout the Phanerozoic (Shaikin, 1991).

Kisielevski (1991) found charophytes in association with ostracods from Triassic marine and continental sediments of the epicontinental basin of Kazakhstan. They also reported them in

the Lower Jurassic non-marine limestone Kata Formation of India, and indicated its deposition in saline water of playa-type lakes. Charophytes of the Kata Formation were associated with ostracods, algal mats, stromatolites, and fish remains (Feist et al., 1991).

Charophyte gyrogonites are found in association with discoidal gypsum, ostracods, molluscs, plant remains, and foraminifera in Purbeckian carbonate sediments of Dorset, England (Late Jurassic - Early Cretaceous; West, 1975). They were also reported from Eocene sediments of the Paris Basin (Feist, 1991, per.comm), the Messinian of Italy (Bellanca and Neri, 1984; Decima et al., 1988; Longinelli, 1979; Rizzini and Dondi, 1979), and from the Holocene saline Coorong lakes of south Australia (Warren, 1990, and Burne et al., 1980).

Bhatia and Brigi (1991) noted charophytes from Early Paleocene red beds of the Lesser Himalayas in association with brackish water fossils, including foraminifera, ostracods, and molluscs. These are indicative of shallow water deposition on a tidal flat environment with periodic influx of fresh water.

CHAROPHYTE ASSEMBLAGE OF THE SIRTE BASIN IN THE FORMATION OF THE STUDY AREA

Charophytes were previously reported from the Lower Cretaceous continental clastic sequence of the Nubian Formation in Sirte Basin (Viterbo, 1968). In the Beda Formation of the study area, the charophytes were encountered in an argillaceous, dark gray one metre thick limestone bed, sandwiched between two massive anhydrite beds. The charophytes were only found in

samples from well 6A1-59 at interval 1,246 - 1,247m (4,840 - 4,844 ft.) and from well CC1-59 at 1,246-1,247m (4,111-4,114 ft.). These two wells are located at the margins of the Gerad Trough and Beda Platform (Fig. 2).

Paleocene charophytes of the Beda Formation are a significant find with important paleoenvironmental, paleoecological and paleontological implications for the Tertiary sequences of the Sirte Basin. The charophyte populations are diverse with 6-7 species, and are indicative of an Early Tertiary "Danian" age for the Beda Formation of the study area. Previously, the Beda Formation based on foraminifera, was assigned a Middle Paleocene "Montian" age (Barr and Weegar, 1972). The finding of the charophytes in the Beda Formation necessitates a review of the previously assigned age and the stratigraphic correlation chart (Barr and Weegar, 1972; Harland et al., 1990, Fig. 4 in back pocket).

SYSTEMATIC PALEONTOLOGY

The charophyte assemblage of the Sirte Basin is composed of six species, grouped in two families (Plate A). The following identifications were provided by Dr. Monique Feist, Laboratory of Paleobotany, University of Montpellier II, France.

FAMILY POROCHARACEAE

1. *Feistiella globosa* (Grambast and Gutiérrez, 1977).

Description:

Gyrogonite is nearly spherical in shape with the base slightly narrower than the apex. The spiral-cells show 5 convolutions (Plate A, Figs 1-2). The colour of the gyrogonite is brown.

Distribution and Range:

This species was previously reported only from the Upper Cretaceous type-locality, from the Cuenca Basin, Spain (Grambast and Gutiérrez, 1977). In the Sirte Basin, its association with the Dano-Montian species *Dughiella wanzuanzensis* shows that it ranges up to the Paleocene. In evaluating the age of the charophyte assemblage, it is interesting to note that the range of Porocharaceae does not pass over the Dano-Montian (Feist, 1979; Massieux et al., 1989).

FAMILY CHARACEAE

1. *Dughiella wanzhuangensis* (Xinlun, 1978)

Description:

Gyrogonite is nearly globular. The apex is somewhat depressed and the spiral-cells are produced into a faint rosette. The base is rounded. The number of convolutions is 7 and well rounded turbecles spaced at nearly regular intervals are found along the spiral-cells (Plate A, Fig 3). The gyrogonite is brown or black in colour.

Distribution and Range:

This species corresponds to the primitive form of *Dughiella bacillaris* Feist-Castel. The range of *D. bacillaris* covers the whole Paleocene.

The primitive form of *D. bacillaris* was reported from the basal Paleocene of southern France (Massieux et al., 1989) and, under the name of *Stephanochara wanghuangensis*, from the Paleocene Shangsü Formation of southern China (Huang, 1989). According to Huang (1989), as well as Russel and Zhai (1987), the Shangsü Formation is dated by mammal faunas as Middle and possibly Early Paleocene, thus Dano-Montian in the International Geological Time Scale (Haq and Van Eysinga, 1987).

2. *Lamprothamnium* sp.

Description:

Gyrogonite is nearly spherical-ovoid in shape with the base slightly narrower than the apex which is wider and depressed. The spiral-cells show 7 convolutions (Plate A, Fig 10). The colour of the gyrogonite is pale brown, gray to black.

Distribution and Range:

(Lower Cretaceous?) Upper Cretaceous-Recent. The different species reported to this genus show but little differences and they are not very useful for biostratigraphy. Their presence is, however, ecologically significant. Representatives of *Lamprothamnium* always occur in brackish environments: saline lakes. This is true for the living representatives (Olsen,

1944; Burne et al., 1980), as well as for fossil ones (Castel and Grambast, 1969; Soulié-Märsche, 1982).

3. ?*Microchara* sp. (n. sp?)

Description:

Gyrogonit is ovoid, tapering towards the base with a slightly flattened apex. Spiral-cells show 5-6 convolutions. They appear distinctly elevated with turbeclles irregularly distributed (Plate A, Fig 10). The colour is brown.

Range:

The genus ranges from Late Cretaceous to Middle Eocene. Its size and ornamentation indicate that this is a Tertiary rather than Cretaceous form.

4. *Stephanochara* sp. A (n. sp?)

Description:

Gyrogonite is spherical-ellipsoid. Spiral-cells show 7-8 convolutions, usually slightly swollen at the apex (Plate A, Fig 4-6). The cells are convex. The colour varies from brown to black.

Range:

The genus ranges from Paleocene to Pliocene.

5. ?*Peckichara* sp. not determinable (one specimen, with broken apex).

Description:

Gyrogonite resembles a flattened spheroid in shape. The length is less than breadth. The number of convolutions is 4-5. The spiral-cells are rough, flat or slightly rounded and the apex is slightly flattened (Plate A, Fig 8-9). The colour varies from pale brown to black.

Range:

Late Cretaceous-Lower Eocene.

STRATIGRAPHICAL IMPLICATIONS

On the whole, the charophyte assemblage of the the Beda Formation in the study area is undoubtedly of Paleocene age. More precisely, in the present state of knowledge on the upper range limit of the family Porocharaceae and the presence of *Dughiella wanzhuangensis*, a species located in a phylogenetic lineage, the age of this assemblage would be Danian.

Benthonic Foraminifera

Introduction

Foraminifera constitute one of the most important groups of microfossils because of their stratigraphic and paleontological value. They are one-celled organisms many of whom secrete calcareous tests, but agglutinated forms cement sand grains and

other particles, together to form arenaceous tests (Haynes, 1981).

Foraminifera are commonly less than 1mm in diameter, but some may be larger, such as fusilinids in the Late Paleozoic and *Nummulites* during the Tertiary. They range from Ordovician to Holocene and were abundant in the Late Paleozoic and from Middle Cretaceous to Holocene (Moore, 1964).

Foraminifera were significant carbonate sediment contributors in the geologic past. Some limestones in the Pennsylvanian and Permian of the southern United States consist entirely of fusilinid tests and form large bioherms and banks. The tests of larger foraminifera such as *Nummulites* and *Orbitoides* from the Cretaceous and Tertiary of the Middle East are also form important carbonate deposits (Wilson, 1975).

Much of the deep ocean floor is covered by an ooze dominated by tests of planktonic foraminifera, including the genera *Globigerina* and *Globorotalia* (Braisner, 1980).

FORAMINIFERAL ASSEMBLAGES OF BEDA FORMATION:

Two hundred and fifty (250) samples of foraminifera representing different intervals of the Beda Formation were picked and examined.

The foraminiferal tests are benthonic and were greatly affected by mechanical abrasion resulting from wave and current action. Diagenetic processes, including recrystallization, dolomitization, cementation, solution leaching, and replacement have greatly influenced the state of preservation.

The Beda Formation in the study area contains a relatively diverse assemblage of calcareous and agglutinated benthonic foraminifera consisting approximately of 33 specimens belonging to 11 families and 33 genera.

The calcareous forms belong to the families Rotaliidae, Anomalinidae, Alabaminidae, Osangulariidae, Nonionidae, Nodosariidae, Miliolidae, and Buliminidae.

The arenaceous forms belong to the families Textulariidae, Verneuilinidae, and Valvulinidae. The family Rotaliidae is the largest and consists of twelve genera. The rotaliids can be further subdivided into small and large forms. Small rotaliids are the most abundant, both in number of genera and percentage with respect to the family Rotaliidae and the total foraminiferal population of the Beda Formation. Small rotaliids include the following genera: *Eponides*, *Discorbis*, *Rotalia*, *Epistomina*, *Elphidium*, *Parrella*, and *Gyroidina*. The genus *Eponides* is the most abundant of the small rotaliids.

The larger rotaliids are represented by *Nummulites* and *Operculina*. *Operculina* is the dominant form of the larger rotaliids. The Miliolidae is the second largest family in number of genera and abundance. The family Miliolidae consists of the following genera: *Quinqueloculina*, *Spiroloculina*, *Triloculina* and *Alveolina*.

The genus *Quinqueloculina* is one of the most abundant taxa of miliolids. Miliolids rank second in abundance after the rotaliids throughout the Beda Formation.

The Anomalinidae is the third most abundant family and consists of *Anomalinoides*, *Cibicides* and *Gavelinella*. *Cibicides* and *Anomalinoides* are the most abundant genera of the Anomalinidae.

The family Nodosariidae consists of five genera; *Lenticulina*, *Marginulina*, *Vaginulinopsis*, *Lagena* and *Robulus*. *Lenticulinas* are the most common nodosariids throughout the Beda Formation.

The family Alabaminidae is represented by genus *Alabamina* and it is rare in this formation.

The family Osangulariidae is represented by genus *Osangularia*, which is rare. The family Nonionidae is represented by genus *Nonion*, and is rare to common. The family Buliminidae consists of two genera, *Bulimina* and *Bolivina*, and these are generally rare in abundance.

The agglutinated forms are rare to common in abundance and are represented by genera from three families. The family Textulariidae consists of the genera *Textularia* and *Spiroplectammina*. They are the most common foraminifera encountered of all the agglutinated forms. The family Valvulinidae consists of the genera *Valvulammina* and *Dorothia* and these are rare in abundance. The benthonic foraminiferal fauna remains essentially uniform throughout the Beda Formation, except for the lower part where agglutinated foraminifera are more abundant.

ECOLOGY OF LIVING BENTHONIC FORAMINIFERA

Benthonic foraminifera attain their highest productivity in nearshore and at midshelf depths (Walton, 1964). Walton (1964) also indicated that the highest concentrations, off Baja California, occur in water depths between 50 and 90m, and between 500 and 600m. Bandy (1964) observed that size and microstructures change with distance from shoreline, water temperature, and depth. Walton (1964) indicated a temperature range of 14 - 20°C and salinity range of 34 - 37‰ for most benthic forms.

The large benthonic foraminifera are confined to tropical and subtropical conditions. The living representatives of the large benthonic foraminifera occur mainly in shallow, warm water on the continental shelf and within the euphotic zone, and in water temperatures not less than 18°C for the warmest month of the year (Adams, 1989). He also suggested that Tertiary forms had no different ecological requirements from the Holocene ones and the vast majority are found in areas of shallow water carbonate sedimentation.

PALEOBIOGEOGRAPHY

The Tethys Sea extended in an east-west direction, linking the Atlantic and Pacific oceans, and served as a migration path for various microfauna travelling in east-west flowing ocean currents (Berggren and Aubert, 1975).

During the Paleocene, most of the northern parts of Libya were covered by waters of the Tethys Sea, which extended southward, through the Sirte Basin, as far as the Tibesti Uplift

(Fig. 1). Tethys Sea sediments contain foraminifera widely spread throughout the Tertiary (Berggren, 1974). Many similarities exist between Paleocene benthonic foraminifera of North Africa, the Gulf Coast United States, the Caribbean and South America (Berggren, 1974).

The Beda Formation contains a rich benthonic foraminiferal assemblage of rotaliids, nonionids, cibicids, miliolids, anomalinids, osangulariids, nodosariids, textulariids, verneuulinids and valvulinids. Such an assemblage has been termed as the "Midway type". It was described from the Midway Group of the Gulf Coast of the United States and its equivalents of the Atlantic coastal plain and the Caribbean region (Cushman, 1951; Kellough, 1965; Berggren, 1974, Fluegeman et al., 1990).

Berggren and Aubert (1975) indicated that benthonic foraminiferal assemblages of *Cibicides*, *Nonionides*, *Rotaliides*, *Discorbids*, *Elphidiellids* and assorted larger foraminifera (*Nummulites*, *Operculina* and *Alveolina*) developed in inner to middle carbonate shelf of the Tethys Sea.

Berggren (1974), in his study of benthonic foraminifera of the Rockall Bank in the North Atlantic, found the genera *Operculina* and *Pararotalia* indicative of inner shelf (0-10m) and middle shelf environments (10-100m).

SYSTEMATIC PALEONTOLOGY

Thirty-three genera of benthonic foraminifera characteristic of the Midway and Tethys carbonate type fauna of the Lower Paleocene Beda Formation are listed. Plate(PL) B of

Appendix I shows some of the benthonic foraminifera of the Beda Formation. These assemblages are listed, as follows:

Family Rotaliidae

Genus *Discorbis* Lamarck, 1804
PL B (6)

Genus *Eponides* Montfort, 1808
PL B (7,8)

Genus *Gyroidina* d'Orbigny, 1826

Genus *Parrella* Finlay, 1939
PL B (9,10)

Genus *Rotalia* Lamarck, 1804
PL B (11,12)

Genus *Epistomina* Terquem, 1883
PL B (13,14)

Genus *Elphidium* Montfort, 1808
PL B (17,18)

Genus *Nummulites* Lamarck, 1801
PL B (16)

Genus *Operculina* d'Orbigny, 1826
PL B (15)

Family Miliolidae

Genus *Quinqueloculina* d'Orbigny, 1826
PL B (1,2)

Genus *Spiroloculina* d'Orbigny, 1826
PL B (4)

Genus *Triloculina* d'Orbigny, 1826
PL B (3)

Genus *Alveolina* d'Orbigny, 1826
PL B (5)

Family Anomalinidae

Subfamily Anomalininae

Genus *Anomalinoides* Brotzen, 1942

PL B (19)

Genus *Cibicides* Thalmann, 1939

PL B (20, 21)

Genus *Gavelinella* Brotzen, 1942

PL B (22, 23)

Family Alabaminidae

Genus *Alabamina* Toulmin, 1941

Family Osangulariidae

Genus *Osangularia* Brotzen, 1940

Family Nonionidae

Subfamily Nonionae

Genus *Nonion* Montfort, 1808

Family Nodosariidae

Subfamily Nodosariinae

Genus *Lenticulina* Lamarch, 1804

Genus *Vaginulinopsis* Silvestri, 1904

Genus *Robulus* d'Orbigny, 1826

Genus *Lagena* d'Orbigny, 1826

Family Textulariidae

Genus *Spiroplectamina* Cushman, 1927

PL B (24)

Genus *Textularia* DeFrance, 1824

Family Verneulinidae

Genus *Gaudryina* d'Orbigny, 1839
PL B (26, 27)

Genus *Clavulinoides* Cushman, 1936
PL B (28)

Genus *Tritaxia* Reuss, 1860

Family Valvulinidae

Genus *Valvulammina* Cushman, 1933
PL B (29)

Genus *Dorothia* Plummer, 1931

Family Buliminidae

Genus *Bulimina* d'Orbigny, 1826

Genus *Bolivina* d'Orbigny, 1839

CHAPTER FIVE: MICROFACIES DESCRIPTIONS

Introduction

Microfacies analysis of the Beda Formation is based on core and drill cutting samples and thin-section examination. A total of 200 thin-sections were prepared from cores representing subsurface rock samples from wells Y3-, Y2a-, 6A1-59, and A1-59F. Rock types were identified using Folk's (1962) and Dunham's (1962) carbonate rock classifications. Microfacies data and sample descriptions are listed in Appendix II. A summary of the microfacies description is provided in table 1. Sedimentary structures, both primary and secondary, were utilized in interpreting conditions and types of depositional environment.

Sedimentary Structures and Textures Common to all Microfacies

Sedimentary structures, both primary and secondary "diagenetic", are important tools for interpreting conditions and types of depositional environments. The sedimentary structures of the Beda Formation include primary organic, inorganic and secondary structures. Primary organic structures include all the fossil constituents encountered throughout the stratigraphic sequence of the Beda Formation. Inorganic features observed include laminations, graded layers, geopetal fabric, composition and colour. Diagenetic processes and products observed in the Beda Formation include recrystallization, solution, cementation, dolomitization,

M i c r o f a c i e s	A T v e r c a g e s (m)	Allochems						Primary Sedimentary Features					Secondary Sedimentary Features					Cement	Matrix	M i n e r a l o g y	Remarks		
		F o r a m i n i f e r a	O s t r a c o d a	Algae	M u l l u s c s	E c h i n o d e r m s	B r y o z o a n s	P e l o i d s	L a m i n a t i o n s	M u d c r a c k s	B u r r o w s	A l g a l m a t s	A n h y d r i t e N o d u l e s	R e p l a c e m e n t	M i c r i t i z a t i o n	F r a c t u r e s	S o l u t i o n					C o m p a c t i o n	S p a r r y C a l c i t e
D a s y c i d a c c e a n	C h a r o p h y t e																						
TMFC1	48.5	R-C	R		C	R			R	C	C	C	C	C	C		R-C	C	C	C	C	Calcite, Dolomite and Anhydrite	Wackestone and Mudstone
MF2	18	C	R-C	R		R		R		C	C	C		C	C		C	C	C	R	C	Calcite and Dolomite	Packstone
MF3	9	R-C	R	R	R	R		R			C			C	C	R	C	C	C	R	C	Calcite and Dolomite	Mudstone
MF4	20	C		C	R-C	R		R			A			C	C		C	C	C	R	R	Calcite	Packstone
MF5	6	C	A		R	R		R	C	C	C	C		C	C	R	R-C	C	C	R	C	Calcite	Wackestone
MF6	12	C-A	R			R								C	C		C	C	C	R-C	C	Calcite and Dolomite	Packstone
MF7	30	C-A	R-C		R		R		R		R			C	R-C			C	C			Calcite	Wackestone and Mudstone
MF8	39	C	R	C	R-C	R		C-A									C	C	C	R		Calcite	Packstone
MF9	14	R	R		R		R							C								Calcite	Wackestone and Mudstone
MF10	6		R		R-C	R		A						C	C			C	C			Calcite	Packstone
MF11	10	R	C	C				R						C			C	C	C			Calcite	Wackestone
MF12	14	C	C																C	C		Calcite	Mudstone

Table 1: Summary of microfacies descriptions. Note: A-abundant, C-common, R-rare.

replacement, compaction, bioturbation, pelletization, micritization, fenestral fabric and fractures.

Recrystallization:

Recrystallization is common in all the examined rock samples of the Beda Formation. It is recognized by the microcrystalline texture of the matrix. The size of microspar ranges between 4-10 μm and may reach up to 40 μm . The micrite matrix is characterized by irregular crystal shapes with occasional development of patchy, coarser crystal mosaic and by the presence of skeletal grains and/or their molds floating in the matrix. Recrystallized grains can be identified by the preservation of their original textures "ghosts" (Plate C1). These are easily differentiated from the leached and subsequently cemented-filled molds (Plate C2) which preserve no original features.

Replacement:

Replacement includes the conversion of high-Mg calcite and aragonite into diagenetic low-Mg calcite, dolomite, anhydrite, gypsum, pyrite, silica and any other replasive mineral or vice versa. Replacement of the unstable calcite grains and retention of microstructures was observed in several samples from the Beda Formation (Plate C3). Dolomite was recorded throughout the Beda Formation with partial to complete replacement of the limestone matrix (Plate C 4a, b, c). In some instances, calcite cement was replaced by dolomite (Plate C5).

Anhydrite, gypsum and pyrite replacement of the matrix and grains was also observed (Plate C4). Calcitization of dolomite was inferred from the molds of dolomite rhombs that were probably dedolomitized and subsequently leached (Plate C5).

Cementation:

Drusy calcite is the most abundant cement in the Beda Formation. It is associated with dissolution features and replacement of chemically unstable grains. The drusy sparite is generally clear and increases in crystal size away from cavity and grain walls (Plates C6, C7). Sparite can result from pressure solution (Plates C8, C9).

Other types of cements include dolomite, anhydrite, gypsum and pyrite. Dolomite cement occurred as a precipitate filling various types of pores (Plate C10a, b). Pyrite cement was recognized in several samples along stylolite surfaces and within intragranular pores of fossils, molds and fractures (Plates C4c, C10b).

Solution:

The microfacies of the Beda Formation are characterized by different solution features, including molds of various types of fossils and mineral crystals (Plate C11, 16a), pseudomorphs of discoidal gypsum (Plate C12), solution enlargement of fractures and pre-existing pores (Plate C13), and stylolite surfaces (Plate C7). Further dissolution was prevented in the Beda Formation once the pores became cemented or filled by

hydrocarbons. Dissolution features are most abundant in the grain-supported microfacies (MF4, MF2).

Compaction:

Compaction includes mechanical and chemical compaction and is indicated by pressure solution features such as on stylolites and between grain surfaces (Choquette and James, 1987).

Mechanical compaction is observed in several samples from the Beda Formation. It is indicated by fracture and breakage of skeletal particles, such as foraminifera and ostracoda tests and fecal pellets (Plates C8, C14). Compaction also developed plastic deformation resulting in bending of elongate grains, and distortion of rounded grains into ellipsoidal shapes (Plates C8, C13). Pressure solution features are observed throughout the Beda Formation (Plates C15a, 15b, 15c, C16b)

Boring and Micrite Envelopes:

Borings lead to grain degradation and destruction and create secondary porosity that facilitates solution leaching and cementation (Tucker and Wright, 1990). Borings are observed in several ostracod and pelecypod shells from the Beda Formation rocks. Microboring destroyed the primary structures of the skeletal grains and produced completely micritized grains (Plates C8, C14, C16). Continued boring leads to dissolution and removal of CaCO_3 and, consequently, the development of micrite envelopes (Bathurst, 1975). They have been recorded throughout the Beda Formation. Micrite envelopes can remain

even after the grains were leached out (Plate C16b). They can act as template for external and internal cementation (Plate C7) and the internal void space is completely or partially cemented by sparite (Plates C7,C16).

Burrowing:

The microfacies of the Beda Formation are extensively burrowed. Several burrowing features are recorded, including horizontal and/or vertical burrows. The burrows are filled with sediments different in textures and colour from the original ones (Plates C17a, b). Mottled structures are also recorded (Plate C17c). Burrowing contributed to the nodular structures of the Beda Formation (Plates C15a,b). Ostracods, gastropods and pelecypods were probably the major burrowers of Beda Formation sediments (Plate C17d).

Fecal Pellets:

Fecal pellets are recorded throughout the microfacies of the Beda Formation in association with ostracods, pelecypods, gastropods, foraminifera, charophytes and dasycladacean algae. They are important contributors to the grain constituents of many packstones and wackestones microfacies (Plate C18a, b). Early recrystallization of fecal pellets and cementation of the matrix resulted in their preservation from being destroyed by compaction (Plate C18a). Pelletization contributed to sediment homogenization and destruction of the primary structures, such as laminations.

Fracturing:

Fractures were recorded in several core samples throughout the study area. They are especially abundant in core samples from well 6A1-59, probably because it is adjacent to a normal fault zone (Fig. 6, in back pocket).

Most of the observed fractures are nearly vertical (PL C19). Fractures enhance the process of solution leaching in carbonate rocks (Moore, 1989). They are solution enlarged in the Beda Formation (Plate C13), and partially or completely filled with cement (Plate C15c).

Fenestral Fabric:

Fenestral structures are recognized in some microfacies of the Beda Formation and are dominantly of planar nature, associated with algal mats (Plate C20a, b). Extensive solution leaching resulted in the enlargement of different pore structures and, consequently, obliterated their original shape.

Descriptions of Microfacies

Detailed examination and description of thin-sections, core samples, drill cuttings, well logs and other available data resulted in the recognition of eleven microfacies and one microfacies complex consisting of three alternating microfacies. The microfacies of the Beda Formation are listed and discussed in ascending order, as follows (Fig. 9): Foraminiferal mudstone (MF12), Dasyclad-pelletal wackestone (MF11), Pelloidal packstone (MF10), Skeletal wackestone-mudstone (MF9), Pellet-dasyclad-foraminiferal packstone (MF8), Foraminiferal wackestone-mudstone

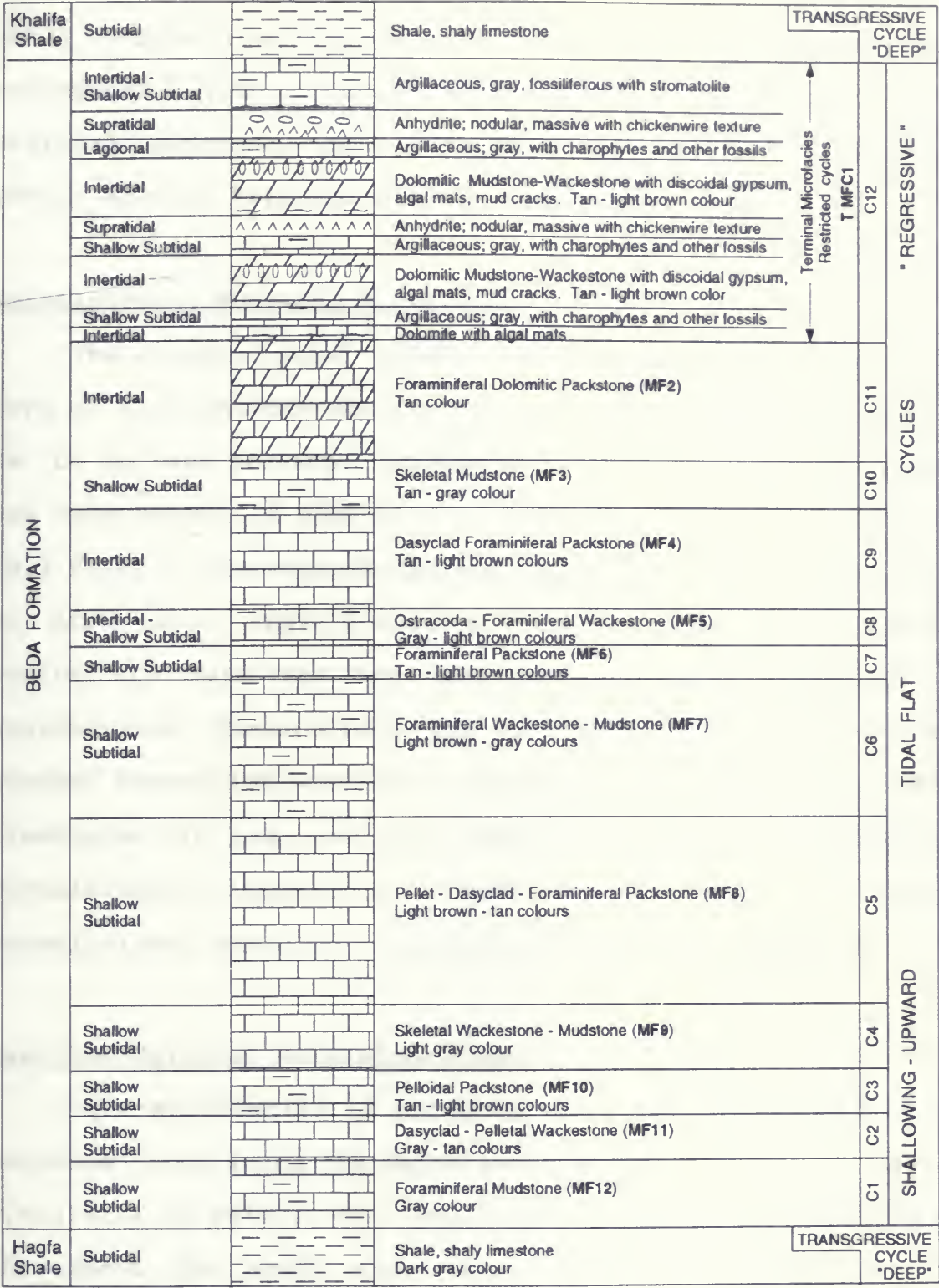


Fig.9 The vertical sequence of the Beda Fm. microfacies

(MF7), Foraminiferal packstone (MF6), Ostracoda-foraminiferal wackestone (MF5), Dasyclad-foraminiferal packstone (MF4), Skeletal mudstone (MF3), Foraminiferal dolomitic packstone (MF2), and the Terminal microfacies complex (TMFC1).

Foraminiferal Mudstone Microfacies (MF12)

The foraminiferal mudstone microfacies marks the lowest part of the sequence and is underlain by the Hagfa shale (Fig. 8a, b, in back pocket). It has an average thickness of 14m and was encountered at depths of 1,724-1,739m (5,690-5,735 ft.) in well Y3-59. This microfacies consists primarily of dense, light to dark gray, argillaceous micrite and is partly pyritic. Grains are rare and are dominated by small benthonic and agglutinated foraminifera and ostracods. It represents a gradual transition between the shales of Hagfa Formation and the limestones of the overlying Beda Formation. The benthonic foraminiferal assemblage consists of the genera *Cibicides*, *Anomalinides*, *Textularia*, *Gaudryina*, with rare miliolids.

Dasyclad-Pelletal Wackestone Microfacies (MF11)

This microfacies is encountered in the lower part of the sequence, comprising the depth interval of 1,702-1,716m (5,618-5,663 ft.) in well Y3-59. The average thickness of MF11 is 10m throughout the study area (Fig. 8, in back pocket). The wackestones of this microfacies gradually changes into the pelloidal packstone microfacies (MF10). The dasyclad-pelletal wackestone microfacies consists of light gray to tan,

argillaceous micrite matrix with scattered grains dominated by dasycladacean algae fragments and pellets. Miliolid foraminifera and ostracods are also recorded and are less common. The various types of grains were completely recrystallized and partly leached as a result of the different diagenetic processes.

This microfacies is not part of the reservoir section because it structurally lies below the oil/water contact, resulting in its complete saturation by formation water.

Pelloidal Packstone Microfacies (MF10)

The pelloidal-packstone microfacies overlies the dasyclad-pelletal wackestone (MF11) and it gradually changes into the overlying skeletal wackestone-mudstone microfacies (MF9). It is encountered at depth interval of 1,706-1,712m (5,630-5,650 ft.) in well Y3-59 (Fig. 8, in back pocket). This microfacies is encountered in the lower part of the sequence only and the grains are dominated by rounded and elliptical pelloids. Other grains include benthonic foraminifera such as miliolids, eponids and agglutinated forms, in addition to gastropods, pelecypod fragments, ostracods and echinoderms. The pelloidal-packstone microfacies consists of light brown to tan recrystallized micrite matrix. The various grains are completely recrystallized and/or are partially leached. Structurally, this microfacies lies far below the oil/water contact, resulting in its complete saturation by formation water.

Skeletal Wackestone-Mudstone Microfacies (MF9)

The skeletal wackestone-mudstone microfacies overlies the pelloidal-packstone microfacies (MF10) and it gradually changes into the pellet-dasyclad-foraminiferal packstone microfacies (MF8). It has an average thickness of 14m (48.2 ft.) and was encountered at depth interval of 1,697-1,706m (5,600-5,630 ft.) in well Y3-59. The drill cuttings consist of light gray lime-mud matrix with scattered and highly fragmented skeletal debris of ostracods, bryozoans, molluscs and foraminifera. The lower part of this microfacies is dominated by mudstones, whereas the upper portion is predominantly a wackestone; and the increase in the amount of grains seems to be gradual in the upward direction. The skeletal wackestone mudstone microfacies of this depth interval is not part of the reservoir because of its poor reservoir qualities and its structural position below the oil/water contact.

Pellet-Deasyclad-Foraminiferal Packstone Microfacies (MF8)

This microfacies underlies the foraminiferal wackestone-mudstone microfacies (MF7) and closely resembles the dasyclad-foraminiferal packstone microfacies (MF4). The packstones of this microfacies gradually change into the overlying wackestone-mudstone microfacies (MF7). It has an average thickness of 39m throughout the study area (depth interval of 1,651-1,697m; 5,450-5,600 ft.). Drill cutting examinations of this microfacies indicate light brown to tan lime-mud matrix, with abundant fecal pellets, dasycladacean algae fragments, miliolids and other smaller benthonic foraminifera, such as eponids,

anomalinids and cibicids. In addition, ostracods and skeletal debris of gastropods, pelecypods, bryozoans and echinoderms are present.

Primary intergranular and intragranular and secondary porosity appear to be completely plugged, primarily by calcite spar and minor anhydrite. The rocks of this microfacies are structurally situated below the oil/water contact. They are completely saturated by formation water.

Foraminiferal Wackestone Mudstone Microfacies (MF7)

This microfacies underlies the foraminiferal packstone microfacies (MF6), and is encountered at depth interval 1,623-1,651m (5,355-5,450 ft.) in well Y3-59 (Fig. 8, in back pocket). It gradually changes into the overlying foraminiferal-packstone microfacies (MF6). The average thickness of this microfacies is 30m throughout the study area.

It differs from the foraminiferal packstone microfacies only in abundance of the fossil content. The skeletal grains and fragments are scattered throughout the micrite matrix. Microfossils are generally rare but dominated by small benthonic and agglutinated foraminifera, such as *Cibicides*, *Eponides*, miliolids, *Lenticulina*, *Textularia*, and *Gaudryina*; in addition to ostracods, and molluscan fragments.

The foraminiferal microfacies consists of light gray, soft and slightly argillaceous wackestone-mudstone. Structurally, this microfacies lies below the oil/water contact. Consequently, it is water-saturated.

Foraminiferal Packstone Microfacies (MF6)

The foraminiferal packstone microfacies occurs at depth interval of 1,609-1,623m (5,310-5,355 ft.) in well Y3-59. The packstones of this microfacies gradually change into the overlying ostracoda-foraminiferal wackestone microfacies (MF5). There is no core control for this microfacies and only drill cuttings were examined. The cuttings consist of light brown to tan lime-mud matrix. The allochems are only partially preserved due to physical and chemical degradation. The cuttings are replete with benthic foraminifera, including miliolids and eponids, in addition to fragmented skeletal grains of different sizes. The matrix seems to be partially dolomitized and clear sparry calcite are also observed. This microfacies lies below the oil water contact of the drilled structures in the study area and it is saturated by formation water (saturation greater than 55%).

Ostracoda-foraminiferal Wackestone Microfacies (MF5)

This microfacies comprises the depth interval of 1,603-1,609m (5,290-5,310 ft.) in well Y3-59. It is overlain by the dasyclad-foraminiferal packstone microfacies (MF4) and underlain by the foraminiferal packstone microfacies (MF6)

This microfacies is relatively thin and consists entirely of light brown to light gray wackestone. It gradually grades up into the overlying dasyclad-foraminiferal packstone microfacies (MF4). The allochems are dominated by small benthonic foraminifera, such as *Cibicides*, *Anomalinides*, *Eponides*,

miliolids and agglutinated forms, including *Textularia*, *Guadryina*, and *Spiroplectammina*. Ostracods are the second most abundant organism, whereas pelecypods, gastropods and echinoderms are rare (Plate C21).

Pelloids are also recorded in several horizons. These are scattered throughout the recrystallized micrite matrix and constitute more than 10% of the rock. This microfacies is intensively burrowed (Plate C15a, b). Irregular or wavy laminations mark the lower 30-40 cms of the microfacies, and horizontal laminations less than 3mm in thickness are well preserved at the top of the microfacies (Plates C22, C23).

Compaction has greatly affected the argillaceous matrix and resulted in the alignment of skeletal grains, stylolites, and nodular textures (Plate C15a). Dolomitization is partial and is probably related to burrowing which provided local porosity enhancement within the sediments. Thin stringers of argillaceous material were encountered throughout this microfacies, indicating a relative increase in the amount of clay in the micrite matrix. Argillaceous seams were further concentrated and accentuated as a result of post-depositional compaction and greatly contributed to porosity and permeability reduction. The micrite matrix is completely recrystallized and replaced by microspar. Sparry calcite, anhydrite and dolomite are the major cements filling molds/vugs, intraskeletal pores, and fractures. Pyrite is a common constituent and replaces ostracods, and is disseminated in the micrite matrix and along stylolite surfaces. Solution leaching contributed to the

development of solution porosity by dissolution of unstable grains and removal of clay and organic matter from the stylolites. The average porosity of this microfacies is estimated at 15%, whereas the average permeability is less than 3md. Oil stains are associated with localized porous zones.

Dasyclad-foraminiferal Packstone Microfacies (MF4)

The dasyclad-foraminiferal packstone microfacies is encountered at depth interval of 1,579-1,603m (5,210-5,290 ft.) in well Y3-59. It abruptly changes into the overlying skeletal-mudstone microfacies (MF3) and overlies the ostracoda-foraminiferal-wackestone microfacies (MF5).

This microfacies varies in colour from light brown to tan and is grain supported. The allochems are dominated by dasycladacean algae, benthonic foraminifera, microgastropods, pelecypods, ostracods, red algae, echinoderms, bryozoans, fecal pellets and undifferentiated skeletal material (Plates C16, C24). The benthonic foraminiferal assemblage consists of large- and small-size populations. The large-size population consists of *Nummulites*, *Operculina*, miliolids and *Alveolina*. The small-size population is represented by *Eponides*, *Cibicides* and other rotaliids. The allochems are recrystallized, leached or completely micritized. The external boundaries of some allochems were preserved subsequent to micritization and dissolution. The matrix is completely recrystallized. Sparry calcite partially or completely occludes the primary intergranular and intragranular and secondary solution

porosities. The sparry calcite cement also lines cavity walls and grains. The drusy spar increases in size away from the edges of the grains and cavity walls. Syntaxial cement was observed on echinodermal plates, however this cement is less common in this microfacies than the drusy spar.

This microfacies is extensively burrowed and all the primary sedimentary structures, if present, were destroyed. Anhydrite is present in minor amounts, but cementing various types of pore systems. Dolomite and pyrite crystals are scattered throughout the matrix. The average porosity of this microfacies is about 21%. It is characterized by primary intergranular, intragranular and secondary solution-enhanced vuggy and moldic porosity. The average permeability is 3md. Light brown oil stains are common throughout this microfacies.

Skeletal Mudstone Microfacies (MF3)

The skeletal mudstone microfacies comprises the depth interval of 1,570-1,579m (5,180-5,210 ft.) in well Y3-59. It is overlain by foraminiferal dolomitic packstone and underlain by dasyclad-foraminiferal packstone microfacies. The rocks of this microfacies are mud supported with minor amounts of skeletal material. They consist predominantly of mudstone grading up into wackestone towards the top of the microfacies, which in turn grades up into the overlying foraminiferal dolomitic packstone microfacies (MF2). The limestone is argillaceous, light to medium gray and extensively bioturbated. Allochems are rare and consist of skeletal debris of foraminifera, ostracoda, molluscs, fecal pellets, echinoderms,

dasycladacean algae, bryozoans, and echinoderms (Plates C25, C4a, C1). The allochems are scattered randomly throughout the micrite matrix.

Dolomitization has moderately affected the micrite matrix and is represented by finely crystalline dolomite (Plate C4a). This microfacies was subjected to early compaction due to the lack of a supporting framework, probably during syndepositional subsidence. Compaction structures such as deformed grains and stylolites are evident (Plates C4a, C15c). Micritization is a common diagenetic feature; micrite envelopes of leached grains and/or wholly micritized grains were observed. Primary structures were completely lost as a result of sediment homogenization through burrowing. Pyrite crystals are scattered throughout the matrix and within several grains and dolomite crystals (Plates C10b, C17c). Most porosity is moldic, vuggy, or fracture. Stylolite surfaces may have acted locally as permeability barriers and porosity reducers. Sparry calcite and anhydrite are the major cements filling the various pores. Fractures, when present, are vertical and filled with calcite or anhydrite cement (Plate C15c). Solution leaching of unstable grains such as foraminifera and fecal pellets resulted in the development of solution porosity. Solution probably took place after recrystallization of the lime-mud matrix, followed by partial cementation of pores. This microfacies is marked by low porosity (8%) and permeability (0.3md). This microfacies is rarely oil stained as a result of its low porosity and permeability.

Foraminiferal Dolomitic Packstone Microfacies (MF2)

The foraminiferal dolomitic packstone microfacies is encountered at depth interval 1,552-1,570m (5,121-5,180 ft.) in well Y3-59 and it abruptly changes into the overlying sediments of the Terminal microfacies complex (Fig. 8, in back pocket, Fig. 9). Pelloids of variable sizes are common in this microfacies including benthonic foraminifera, ostracoda, fecal pellets, dasycladacean algae, bryozoans and molluscs (Plates C18a, C26b).

The benthonic foraminiferal assemblage is represented by miliolids, *Eponides*, *Cibicides* and *Operculina*. Generally, the grains and their shapes are moderately preserved, probably due to early lithification that prevented mechanical deformation by compaction and tectonic activity. The matrix varies from light brown to tan and is partly dolomitized. The dolomite crystals are euhedral to anhedral in shape, and constitute less than 50% of the matrix, and range in size from 0.01-0.03mm.

Dissolution of grains and matrix is evidenced by molds of different biotic constituents and solution enlargement of pre-existing pores (Plate C26a).

Different cement generations are observed in several thin-sections. Recrystallization of the matrix is represented by microspar, whereas coarse, drusy calcite spar fills intergranular and intraskeletal pores, molds, vugs and edges and walls of grains and cavities (Plates C18a, C26b).

Micritization is a common characteristic feature of this microfacies. It is evidenced by micrite envelopes and wholly

micritized grains. The top of this microfacies is marked by fenestral fabric (Plate C20b), indicative of algal mat structures. All the primary structures were destroyed due to intense burrowing by various types of organisms. Anhydrite is a common diagenetic cement and has greatly reduced the rock porosity.

Pyrite crystals are rare. Pyrite lines the internal chambers and the outer surfaces of skeletal grains and/or is disseminated within the recrystallized micrite matrix. Normally graded layers were noted from the foraminiferal dolomitic packstone microfacies. The layers range in thickness from 5 to 10cm. They grade from coarse pelecypod shell hash through medium and fine grained packstone towards the top of the microfacies (Plate C27). These graded layers were recorded from well 6A1-59 only, and their lateral continuity cannot be assessed from the limited core data. The graded layers were encountered twice towards the top of this microfacies.

Porosity is primarily moldic, interparticle, intraparticle and intercrystalline (Plate C26c). It averages about 16%, and permeability ranges between 0 to 10 md. The rocks of this microfacies are heavily stained with light brown oil.

The Terminal Microfacies Complex (TMFC1)

This microfacies complex consists of three microfacies, including the dolomitic mudstone-wackestone, the argillaceous wackestone-mudstone and the anhydrite microfacies.

The terminal microfacies complex gradually overlies the foraminiferal dolomitic packstone (MF2), Figs. 8 (back pocket),

9, and is encountered at depth intervals 1,500-1,522m (4,950-5,121 ft.) in well Y3-59, with an average thickness of 48.5m (160 ft.). This microfacies complex was not completely cored. The available cores from the lower part of the microfacies complex were studied, including those from well Y3-59 of depth intervals 1,539-1,552m (5,080-5,121 ft.), and well 6A1-59, 1,465-1,478m (4,835-4,876 ft.). Detailed description of the terminal microfacies complex is as follows:

1. The Dolomitic Mudstone-Wackestone Microfacies

This microfacies is encountered at the base of the terminal microfacies complex and averages 2m in thickness (Fig. 8, in back pocket). It is dominated by light brown to tan dolomitic mudstone and wackestone with scattered skeletal material, including small benthonic foraminifera, ostracods, gastropods and pelecypods. It is also characterized by the presence of laminar structures, fenestral fabric and discoidal gypsum and its pseudomorphs.

Laminar and fenestral structures are common near the tops and bottoms of some of the beds and are probably algal in origin. The laminae are 0.5-1.2mm thick. The limestone of this unit is partly dolomitized. The dolomite is microcrystalline. The crystals range in size from 0.005-0.03mm (Plates C12, C28, C29, C30).

The original sedimentary structures, if present, were obliterated by burrowing and pelletization by organisms such as ostracods and gastropods. Solution leaching resulted in the development of moldic and vuggy porosity. Leaching of discoidal

gypsum is evidenced by the presence of their pseudomorphs (Plates C12, C31).

Stylolitization and micritization are among the common diagenetic features of this unit. In well A1-59F a thin layer of pelloidal packstone marks the top of this unit. The grains are oval shaped and heavily micritized. The matrix has undergone extensive leaching and the voids are filled with coarse dolomite and sparry calcite cements (Plate C11). Porosity types include intercrystalline, fenestral, solution and fracture. This unit is oil stained and has an average porosity of 15%, whereas permeability ranges from 0.05 to 2 md. Vertical to subvertical mudcracks of up to 2 cm in length were observed (Plate C32). Most of the cracks were filled with anhydrite cement and/or dolomite and calcite. Calcitization of anhydrite, gypsum and dolomite is also recorded as a late diagenetic product.

2. The Argillaceous Wackestone-mudstone Microfacies

This microfacies overlies the dolomitic mudstone-wackestone microfacies in the lower and middle parts of the terminal microfacies complex, and is overlain by or sandwiched between anhydrite layers.

This microfacies is dominated by dark to medium gray, argillaceous, fossiliferous and partly oxidized (reddish-brown) wackestones and mudstones (Fig. 9).

It is occasionally nodular, stylolitic and bioturbated. It ranges in thickness from a few cm to 7m. Allochems include miliolids, small benthonic and agglutinated foraminifera,

charophytes, gastropods, pelecypod fragments, fecal pellets, ostracods, and few fine to medium grained quartz grains. The ostracod shells are thin and smooth. Algal mats are common and are evidenced by the fenestral fabric. Fenestral fabrics were probably the result of decay and rotting of organic matter from algal mats (Plate C20). Solution leaching and fracturing is common.

This microfacies is nondolomitized, except for the area around well A1-59F where partial or complete dolomitization was observed. This microfacies has low porosity and permeability because of its argillaceous nature and, consequently, is not oil stained. Micritized grains and cementation by sparry calcite and anhydrite are present.

3. The Anhydrite Microfacies

The anhydrite microfacies seals the sedimentary sequence of the terminal microfacies complex. It is underlain by argillaceous wackestone-mudstone or dolomitic mudstone-wackestone microfacies. Top of this microfacies is characterized by isolated anhydrite nodules and algal mats (Plates C33a, C33b, C34a). The remaining section shows chickenwire to massive textures (Plate C34b). It ranges in thickness from 2-5m and varies in colour from smokey white to light brown and tan colours. The darker colour probably infer inclusions of organic matter, and clay.

The dark algal partings are lined with dolomite and pyrite crystals (Plate C35). In thin-sections, anhydrite forms radiating rosettes, twinned lenticular, elongate and rectangular

crystal laths. Most of the crystal laths are randomly arranged, they are crossing or subparallel to one another (Plate C34).

Nodular anhydrite or chickenwire textures are common features of the anhydrite microfacies, especially towards the top of Beda Formation (Plate C33a). Most of the nodular texture seems to be lost due to the replacement of micrite around the nodules by anhydrite. Anhydrite appears more massive with some remnants of micrite. The massive textures may have been the result of solution-reprecipitation of gypsum mush. Enterolithic structures are not recorded; however, irregular laminations of anhydrite interbedded with algal mats at the top of the terminal microfacies complex are present (Plate C33a). Anhydrite can easily be identified from electric logs because of its high resistivity (Figs. 8a, b, in back pocket). In well Y3-59, this unit is overlain by a thin unit of pelecypod shell debris in a micrite matrix and cemented by anhydrite (Plate C36). The accumulation of this pelecypod debris was probably the result of a storm event. This microfacies is also characterized by dissolution features and calcitization of anhydrite.

CHAPTER SIX: INTERPRETATION OF DEPOSITIONAL ENVIRONMENTS

Introduction

The microfacies of Beda Formation were defined and interpreted primarily on the basis of the observed sedimentary structures, textures and fossil content. The environmental interpretation takes into account the rock textures, grain types, skeletal constituents, sedimentary structures, diagenetic features and the overall facies association, their vertical and lateral continuity.

The standard microfacies (SMF) system devised by Wilson (1975) and Flugel (1982) recognizes twenty-four standard microfacies and are assigned to nine standard carbonate facies belts (Fig. 10). It is utilized as a reference to place the interpreted microfacies of the Beda Formation in their possible depositional environmental context.

Microfossils as Indicators of the Paleoenvironments

The carbonate rocks of the Beda Formation consist of a wide range of grain constituents that are dominantly skeletal and/or the product of organic activity. Such grains not only provide indications of paleogeographic and paleoecological conditions but also about diagenetic changes. The microfossils of the Beda Formation provided valuable information regarding water depth, temperature, salinity and energy.

Fossil abundances and degree of abrasion of tests was utilized to determine whether the fossils were autochthonous or allochthonous. The presence of large abundances and relatively

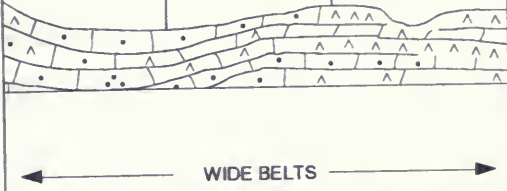
SHELF LAGOON OPEN CIRCULATION	RESTRICTED CIRCULATION SHELF AND TIDAL FLATS	EVAPORITES ON SABKHAS - SALINAS	FACIES PROFILE
7	8	9	
			2ND ORDER SEDIMENTARY BODIES
TIDAL DELTAS LAGOONAL PONDS TYPICAL SHELF MOUNDS COLUMNAR ALGAL MATS. CHANNELS AND TIDAL BARS OF LIME SAND.	TIDAL FLATS. CHANNELS NATURAL LEVEES PONDS ALGAL MAT BELTS.	ANHYDRITE DOMES. TEPEE STRUCTURES LAMINATED CRUSTS OF GYPSUM. SALINAS (EVAPORATIVE PONDS) SABKHAS (EVAPORATIVE FLATS)	
8 WHOLE SHELLS IN MICRITE 9 BIOCLASTIC WACKESTONE COATED 10 GRAINS IN MICRITE 16 PELSPARITE 17 GRAPESTONE ONKOIDS IN 18 MICRITE FORAM, DASYCLADACEAN GRAINSTONE	16, 17, 18 19 FENESTRAL PELOIDAL LAMINATE MICRITE 24 RUDSTONE IN CHANNELS 21 SPONGIOSTROME MICRITE 23 NON LAMINATE PURE MICRITE 22 ONKOIDAL MICRITE	20 STROMATOLITIC MICRITE. 23 NON LAMINATE, PURE MICRITE NODULAR-PEARL ENTEROLITHIC ANHYDRITE. SELENITE BLADES IN MICRITE.	STANDARD MICROFACIES

Fig.10 Standard Microfacies and their depositional environments (after Wilson, 1975).

well preserved skeletal grains suggests possible local accumulation.

The fossil assemblages of the Beda Formation are predominantly benthonic foraminifera, ostracods, dasycladacean and charophytes algae, molluscs, echinoderms, and bryozoans. Most of these microfossils indicate shallow, clear, warm and highly oxygenated water conditions characteristic of shallow shelf depositional environments.

The major microfossils are discussed in detail in the micropaleontology chapter (Chapter Four); others are indicated throughout the microfacies descriptions chapter (Chapter Five). A summary of the fossil constituents of the Beda Formation, their ecological and depositional environments are included in Tables 2 and 3.

Type of Fauna	Type of environment, salinity and temperature	Average Depth	Maximum Depth
Coralline Red Algae	Normal, open marine shelf and bay	<25m very shallow	200 - 250m
Codiacean Algae	Warm, shallow marine, variable salinity, variable water circulation	10m	100m
Dasycladacean algae	Warm, shallow, variable salinity (up to 50-60‰), quiet lagoon waters	3 - 5m, below low tide	12 - 15m
Charophyte algae	Fresh water, but may wash into coastal marine and brackish water	shallow	< 10m
Blue-green-cyanophytes (Algal mats)	Highly variable, fresh to hypersaline	intertidal	45m?

Table 2: Ecological Conditions and Environments of Major Groups of Calcareous Algae (Ginsburg et al., 1971; Wilson, 1975).

TYPE OF FAUNA	SALINITY AND TEMPERATURE	WATER DEPTH AND ENVIRONMENT TYPE
Benthonic Foraminifera: Nummulites, miliolids, operculinas	34-27°/‰, 2-27°C world wide distribution, marine and brackish waters	Most benthonic foraminifera are abundant in shallow water (0-90m) of middle shelf and are less abundant in deeper water. Indicative of depths (0- 10m), inner shelf(lagoons)
Ostracods	Up to 80°/‰. Live in most aquatic environments, both fresh and marine.	Abundant in shallow marine water of continental shelf, but some species range to bathyal and abyssal depths
Molluscs Pelecypods Gastropods	marine to fresh water	Abundant and better preserved in neritic zones (burrowing and sessile in nature). They thrive in agitated near-shore intertidal waters < 30m deep and can be found in deeper water (600m).
Bryozoans	marine	Abundant in shallow continental shelf and may extend to abyssal depths, attached. Optimal conditions are shallow water, calcareous shale or muddy environments (benthonic in habitat)
Echinoderms	Marine	Abundant in shallow water (inner shelf), and can be found at abyssal depths.

Table 3: Ecologic Conditions and environments of Benthonic Foraminifera, Ostracods, Molluscs, Bryozoans, and Echinoderms (Compiled from Milliman, 1974; Bathurst, 1975; Braiser, 1980; Tasch, 1980; Boucot, 1981; Briggs et al., 1990).

Foraminiferal Mudstone Microfacies (MF12)

This microfacies is marked by mud-supported textures and gray colours. It marks the beginning of the shallowing upward sequence, and transition from the deep water, shaly condition of the Hagfa Formation, into the relatively clear, shallower, normal marine conditions of the Beda Formation (Figs. 8, in back pocket, 9). The benthonic faunal assemblage of ostracods, small benthonic calcareous and agglutinated foraminifera, is indicative of inner to middle shelf environments, with maximum water depths of 100 m, open marine and low energy, subtidal conditions (Table 3). This microfacies is similar to Wilson's (1975) facies Belt 7 and SMF 8 and 9 (Fig. 10).

Dasyclad-Pelletal Wackestone Microfacies (MF11)

This microfacies consists of bioclastic light gray to tan wackestones, indicative of shallow water and oxidizing conditions. The skeletal constituents include fragments of dasycladacean algae, miliolids, ostracods and fecal pellets. The presence of dasycladacean algae and miliolids indicate water depths of less than 15 m (Table 2). The dasyclad-pelletal wackestone microfacies is interpreted to have been deposited in a shallow subtidal environment, characterized by shallow, clear, warm, low energy, open marine, and normal salinity water conditions. It is similar to Wilson's (1975) facies Belt 7 and SMF 8 and 9 (Fig. 10).

Pelloidal Packstone Microfacies (MF10)

This microfacies is dominated by grain-supported textures and by light brown to tan sediments, indicative of shallow water and oxidizing conditions. The grain constituents consist of pelloids of rounded and elliptical shape. Other grains include benthonic foraminifera, such as miliolids, eponids and agglutinated types with pelecypods, gastropods, dasycladacean algae fragments, ostracods and echinoderms. This microfacies is interpreted to have been deposited in shallow, warm, clear, normal salinity water, of low energy within the subtidal zone of the tidal flat environment and is similar to Wilson's (1975) facies Belt 7 and 8 and SMF 9, 10, and 19 (Fig. 10).

Skeletal Wackestone-mudstone Microfacies (MF9)

The rock textures and the microfossil constituents of this microfacies are similar to dasyclad-foraminiferal packstone (MF4) and foraminiferal packstone (MF6). It is interpreted to have been deposited in the shallow subtidal environment. It fits the SMF type 8, 9, and facies Belt 7 in Wilson's (1975) facies model (Fig. 10).

Pellet-Dasyclad-Foraminiferal Packstone Microfacies (MF8)

This microfacies resembles the dasyclad-foraminiferal packstone microfacies (MF4) and is characterized by its light oxidized colours and the abundance of fecal pellets, dasycladacean algae fragments and benthonic foraminifera. Skeletal fragments of pelecypods, echinoderms and ostracods are also recorded.

The pellet-dasyclad-foraminiferal packstone microfacies is interpreted to have been deposited in a shallow subtidal environment within the shallow shelf setting and it resembles Wilson's (1975) facies Belt 7 and 8 and SMF type 10, 16, 18 and 19 (Fig. 10).

Foraminiferal Wackestone-Mudstone Microfacies (MF7)

This microfacies consists of light gray wackestone and mudstone with scattered biotic grains of small benthonic foraminifera, ostracods and molluscan fragments. It is interpreted to have been deposited in a shallow subtidal environment within a shelf setting characterized by shallow, warm, normal salinity waters. The absence of dasycladacean algae, bryozoans and echinoderms may indicate the possibility of restricted conditions. The foraminiferal wackestone-mudstone microfacies is similar to Wilson's (1975) facies Belt 7 and 8 and SMF 9, 10 and 19 (Fig. 10).

Foraminiferal Packstone Microfacies (MF6)

This microfacies is a light brown and tan packstone. The grain constituents are predominantly benthonic foraminifera, especially miliolids and *Eponides* with common occurrence of ostracods. The allochems are abraded, the result of abrasion in agitated water. Recrystallization, cementation and partial dolomitization of the matrix are common diagenetic features. The rock textures, light colours, diagenetic features, and microfossil content are indicative of deposition in a shallow

subtidal environment, characterized by moderate to low energy, shallow water, and fluctuating salinity conditions, as indicated by limited fauna and the absence of dasycladacean algae. This microfacies resembles Wilson's (1975) facies Belt 7, 8 and SMF 8, 9, 10, 16 and 19 (Fig. 10).

Ostracoda-foraminiferal Wackestone Microfacies (MF5)

This microfacies consists of small benthonic and agglutinated foraminifera and ostracods with minor abundance of molluscs, echinoderms and fecal pellets. Sedimentary structures include horizontal and irregular lamination that were developed by tidal storms and algal mats, burrowing and compaction features such as nodular textures and stylolites, light gray colour, solution porosity, dolomitization, cementation and pyrite. The biotic constituents and the sedimentary structures and textures indicate shallow marine, low energy condition. The ostracoda-foraminiferal wackestone microfacies is interpreted to have been deposited in a subtidal shallow marine environment and possibly in tidal channels and/or lagoon.

This microfacies is similar to Wilson's (1975) Belt 7 and 8 and SMF 8, 9, 19 and 19 (Fig. 10). Similar diagnostic criteria were described from the modern and ancient deposits characteristic of subtidal zones of shallow shelf environments (Shinn, 1983; Enos, 1983; Wilson and Jordan, 1983; Logan et al., 1970; Cloyd et al., 1990; Brown et al., 1990).

Dasyclad-foraminiferal Packstone Microfacies (MF4)

This microfacies is characterized by grain supported limestone textures with abundant benthonic foraminifera such as miliolids, *Nummulites*, *Operculina*, *Eponides* and *Cibicides*, in addition to dasycladacean algae, ostracods, echinoderms, pelecypods, gastropods and bryozoans.

Solution, micritization, fecal pellets, bioturbation and cementation by calcite and anhydrite are common. The biotic constituents especially the dasycladacean algae, *Nummulites*, *Operculina* and miliolids are indicative of warm, clear, shallow marine water with depths less than 15m (Tables 2, 3). Micritization, pelletization, burrowing, solution leaching, light oxidizing colours are secondary supporting evidence of shallow water conditions. The sedimentary structures, textures and the microfossil content of the dasyclad-foraminiferal packstone microfacies indicate deposition under shallow marine, clear, warm, normal salinity, low to moderate energy conditions in an intertidal to shallow subtidal environment of deposition. This microfacies corresponds to Wilson's (1975) facies Belt 7 and 8 and SMF 10, 16, 18 and 19 (Fig. 10).

Holocene and ancient analogues of this type of depositional environments and their distinguishing criteria were described in several references, such as Roehl(1967); Logan et al.(1970); Shinn et al.(1969); Tucker and Wright(1990).

Skeletal Mudstone Microfacies (MF3)

This microfacies is characterized by light gray micrite. The average thickness of this microfacies is 10m. The presence of some skeletal grains such as foraminifera, ostracods, dasycladacean algae fragments, molluscs, echinoderms, bryozoans in association with fecal pellets, micrite envelopes, pyrite, extensive burrows, indicates accumulation in shallow marine, normal salinity, clear and low to moderate energy water indicative of lower intertidal to subtidal environment.

Holocene analogues of this microfacies have been reported in shallow subtidal and intertidal zones from low energy tidal flats, lagoons and bays (Roehl, 1967; Logan et al., 1970; Shinn et al., 1969; Wilson and Jordan, 1983; Tucker et al., 1990). This microfacies is similar to the standard microfacies types 8 and 9, 19 of Wilson (1975) and Flugel (1982) and the environments of Belt 7 in Wilson (1975) (Fig. 10).

Foraminiferal-Dolomitic Packstone Microfacies (MF2)

This microfacies was identified in all the wells. The biotic assemblage especially the dasycladacean algae, algal mats, foraminifera and the sedimentary structures, such as the light colours, micrite envelopes, fenestral fabrics and fecal pellets; are all indicative of shallow water deposition, possibly in high to low intertidal zones of tidal flats.

Anhydrite inclusion and dolomitization are characteristic of modern tidal flats of the Arabian Gulf (Shinn, 1983; Wilson and Jordan, 1983; Shinn, 1968; Shinn et al., 1969; Roehl, 1967).

Dolomitization was probably early diagenetic and may have resulted from the downward percolation of Mg-rich brines. Solution porosity, drusy calcite spar and light oxidizing colours in carbonate rocks indicate subaerial exposure and meteoric water infiltration (Read, 1973).

This microfacies is similar to Wilson (1975), Belt 7 and 8, and Wilson's (1975) and Flugel (1982) SMF 10, 18, 19 (Fig 10).

Terminal Microfacies Complex (TMFC1)

The terminal microfacies complex consists of a cyclic sequence of dolomitic mudstone-wackstone, argillaceous wackestone-mudstone and anhydrite microfacies.

The depositional history of this complex can be subdivided into several intermittent phases, namely brackish, restricted marine and evaporitic environments. The brackish phase is represented by the argillaceous mudstone-wackestone microfacies, the restricted marine is represented by the dolomitic mudstone-wackstone and the evaporitic phase by the anhydrite microfacies.

1. The Dolomitic Mudstone-Wackestone Microfacies

The dolomitic mudstone-wackstone microfacies is characterized by the presence of benthonic foraminifera, ostracods, fecal pellets and pelecypod fragments. Sedimentary structures include laminations, algal mats, discoidal gypsum and its pseudomorphs and mudcracks. The mudstones and wackestones were probably formed during periods of low energy.

The presence of discoidal gypsum and its pseudomorphs suggest a progressive rise of water salinity. The occurrence of

algal mats, mudcracks, oxidation surfaces, light colours, dissolution features, dolomitization, dedolomitization, and dissolution within the dolomitic mudstone-wackestone microfacies indicate deposition at or near sea-level and in environments characterized by intermittent flooding and drying. These characteristics correspond to tidal flat environments, with ponds, lagoons, and supratidal sabkhas similar to the Holocene region of southern Australia (Burne et al., 1980; Warren 1990), the coastal ponds described from Shark Bay, western Australia (Logan, 1961, Logan et al., 1964; Logan et al., 1970) and to Andros Island, Bahamas (Roehl, 1967; Ginsburg, 1975; Shinn et al., 1965).

2. The Argillaceous Wackestone-mudstone Microfacies

The argillaceous wackestone-mudstone microfacies is characterized by its distinct dark to medium gray colour, the presence of charophyte algae in association with pelecypods, gastropods, ostracods, benthonic foraminifera and fecal pellets. Sedimentary features include nodular textures, stylolites, bioturbation, in addition to reddish-brown colours indicative of oxidation and subaerial exposure. Charophytes gyrogonites are regarded as evidence for the presence of fresh water (Burne et al., 1980). Charophyte algae inhabits environments with water depths of 2-15m and can be found at maximum depths of 30m (Table 2).

The argillaceous wackestone-mudstone microfacies was deposited under restricted conditions; possibly isolated coastal lagoon within the shallow shelf setting of the Beda and Dahra-

Hafra platforms. Such an environment was characterized by shallow, quiet and low salinity brackish water. The fresh water may reflect seasonal rainfall and runoff. This microfacies is similar to Wilson's (1975) Belt 9, and Wilson's (1975) and Flugel (1982) SMF 16 and 19 (Fig. 10).

3. The Anhydrite Microfacies

The anhydrite microfacies is characterized by nodular and massive textures. Anhydrite and gypsum were formed under extreme supersaturation as a result of rapid evaporation in mud flats, lagoons or ponds (Warren, 1989). The hypersaline conditions were developed during low stands of sea-level when the connection between the depositional environment and the open sea was severed.

In Holocene environments, nodular anhydrite develops in carbonate sediments of the capillary zone above the ground water table in supratidal flats or sabkhas (Warren, 1989; Hardie et al., 1983). Anhydrite nodules formed as an early diagenetic replacement within the pre-existing limestone sediments. Gypsum crystal mush is being converted into nodular anhydrite within the middle supratidal zone (Schreiber et al., 1986). Continued precipitation of anhydrite nodules and their coalescence produces the nodular texture known as chickenwire (Dean et al., 1975; Warren, 1989).

Dehydration, dissolution and reprecipitation of gypsum to form anhydrite contributed to relatively thick sections of anhydrite within the Beda Formation (more than one metre). Such diagenetic changes may result because of slight changes in sea-

level, ground water level and influx of surface water. Perhaps all or some of these factors had an influence on changing the salinity of the interstitial brines. Gypsum was replaced by anhydrite during compaction and dewatering during shallow burial of the sabkha sequence (Shearman and Fuller, 1969). Great volumes of anhydrite can be produced by direct precipitation-replacement processes and produce nodular textures.

The anhydrite microfacies indicates low energy sedimentation in intertidal to supratidal environments, on a shallow shelf characterized by tidal flats with sabkhas, lagoons and ponds. This microfacies is similar to Wilson's (1975) Belt 9 and SMF 23 (Fig. 10).

Summary of the Environmental Conditions During Deposition of the Beda Sediments and Allochems

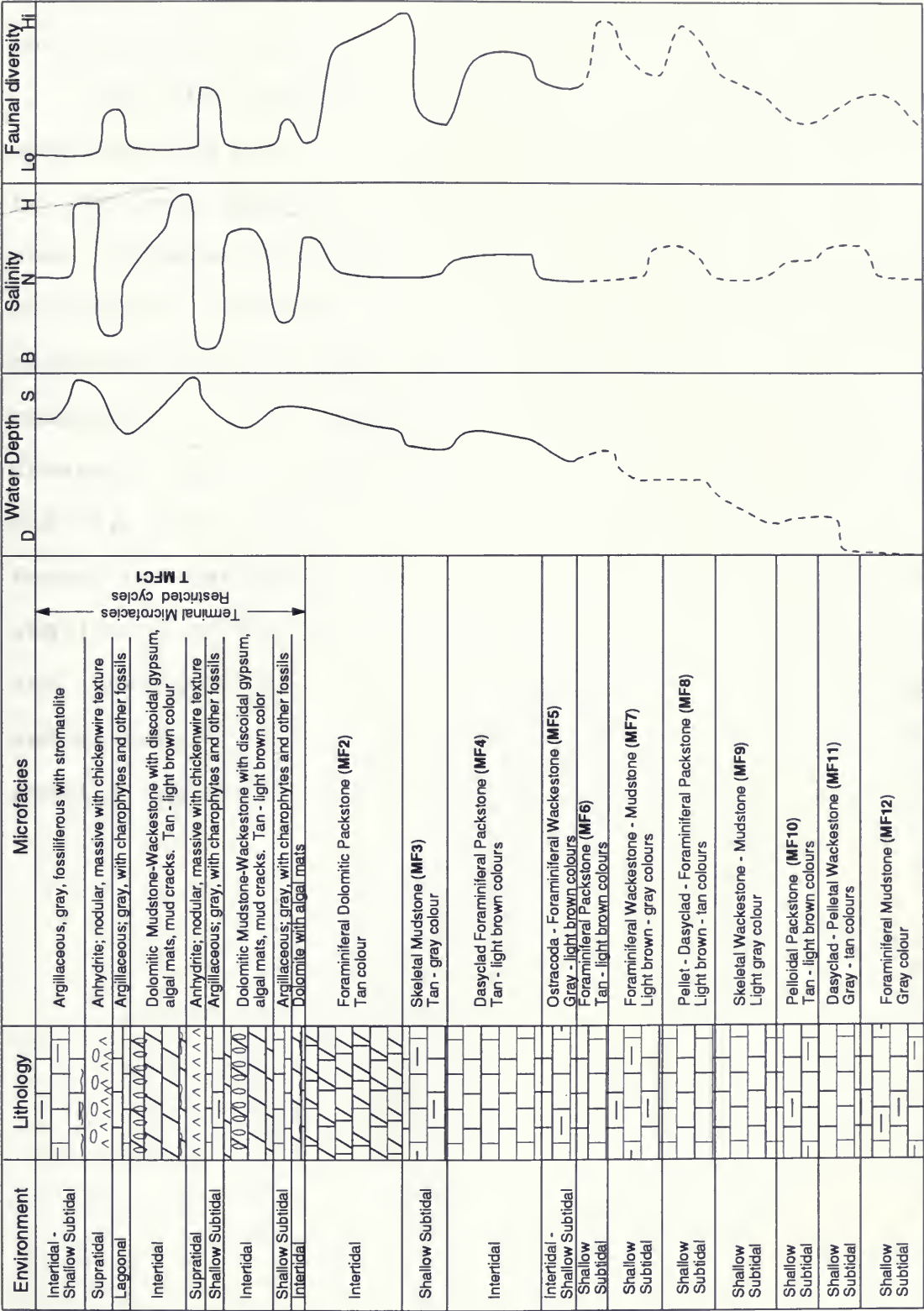
The Beda Formation is characterized by the regular repetition of the shallow subtidal mud-supported to intertidal grain-supported limestone microfacies several times within the vertical sequence. The sequence is marked at the top by hypersaline, brackish and restricted carbonate sediments of the terminal microfacies complex (TMFC1; Fig 11). The microfacies association of the Beda Formation reflects a typical low to moderate energy sequence of tidal flat and lagoonal facies (James, 1984; Enos, 1983; Shinn, 1983; Wilson, 1975).

The presence of charophytes in the terminal microfacies complex suggests the development of brackish conditions due to an influx of fresh water and water depths less than 15m. Anhydrite and gypsum indicate sabkha conditions whereas

dasycladacean algae and benthonic fossil assemblages indicate shallow water deposition. There are no major depositional breaks in the microfacies vertical sequence of the Beda Formation, suggesting that the sequence may have been the product of alternating migration of tidal flat and lagoonal facies.

During deeper water and subtidal low energy conditions, mud-supported limestones, with limited fossil content and allochems were deposited. However, when the Gerad Trough "lagoon" was filled with sediments, shallower intertidal conditions prevailed and grain-supported limestones were deposited. These limestones are characterized by an abundance of dasycladacean algae and other benthonic fossils, indicative of clear, warm, shallow water with relatively high energy conditions (Fig 11).

The shallowing-upward sequence of the Beda Formation microfacies reveals a regular upward changing pattern as a result of major and long-term relative sea-level fluctuations that may have involved the whole basin and, therefore, may be of wider global significance. However, with the major long-term shallowing upward cycles, there are smaller cycles due to local tectonic events. The long-term cycle was probably related to more regional changes in sea-level that affected the whole basin and produced transgressive-regressive-transgressive cycles of Hagfa Shale, Beda Formation carbonates and Khalifa Shale (Fig 9). The long-term and larger-scale cycles involved hundreds of metres in sediment thickness, while the individual smaller-scale sediment cycles are only a few metres thick.



Note : D - deep, S - shallow; B - brackish, N - Normal, H - hypersaline; lo - low, Hi - high

Fig.11 Summary diagram of environmental conditions during deposition of Beda sediments and allochems.

Changes in climate, salinity, temperature, water depth, circulation patterns and other factors have had great effects on microfacies changes of the Beda Formation (Fig 11).

When the sedimentation rates were high on the platform and sea-level was not rising fast, the whole shelf setting was close to sea-level and shallow water conditions prevailed. However, when exchange with open sea was periodically restricted or completely blocked, it resulted in the development of hypersaline lagoons with anhydrite and fresh water influx during emergence. With subsequent sea-level rise, the platforms drowned, and in these deep water conditions deposition of Khalifa Shale followed the end of Beda Formation. Beda Formation carbonate deposition was the result of gradual shallowing of the early Danian sea that was about 100-200m deep and shallowed to 15m during most of the Beda Formation sedimentation. This was suggested by the presence of benthonic fossils, sedimentary structures and textures.

CHAPTER SEVEN: GENERAL PALEOGEOGRAPHY

Sirte Basin

Sirte Basin is an epicratonic embayment developed at the rim of the continental margin of North Africa at the end of the rift-drift sequence (Sanford, 1970; Burke, 1972; Walcott, 1972).

During the Paleozoic, the Sirte Basin area was a large, north-south trending regional uplift "dome" that influenced Paleozoic sedimentation. The regional dome collapsed in the middle of the Cretaceous period into NW-SE horst and graben structures forming the early Sirte embayment (Barr, 1972; Berggren, 1974) and opened to the Tethys "Paleo-Mediterranean".

The sedimentary sequence of the Sirte Basin consists of basal sands, evaporites, shales and carbonates of Paleozoic and Early Cretaceous age that are overlain unconformably by Upper Cretaceous and Paleocene shales, carbonates and evaporites (Fig. 5). The sediments are thickest in troughs, while thinner carbonate deposits, reefs and banks developed on the adjacent platforms. During the Eocene, Sirte Basin received about 1 km of interbedded carbonates and evaporites. In the final phase, during the Oligocene and Miocene, Sirte Basin was filled by terrigenous, marine carbonate and evaporite sediments.

The history of the basin was marked by intermittent periods of structural activity. Initial subsidence of basin bottom sediments was rapid during the Late Cretaceous with marine transgressions from the north. The bottom of the basin was extensively faulted and marked by metamorphic and localized volcanic activities during the Tertiary and Cretaceous periods.

The type and rate of sedimentation was greatly controlled by the concurrent tectonic episodes resulting in uplift, tilting and subsequently influenced sediment subsidence and/or erosion.

Paleogeography of the Study Area

The study area is located in the Gerad Trough which developed as a NE-SW trending extensional graben. It is more than 150 km long and 15 km wide (Fig. 2). Presently, regional dip is to the west-south-west and plunging in a south-westerly direction. The Gerad Trough was a shallow graben throughout deposition of Beda Formation sediments and may have connected the Zella and Hagfa Troughs which are adjacent to the Beda and Dahra-Hofra platforms (Fig. 2). The faunal assemblages, sedimentary structures, textures and the vertical sequence indicate that the Gerad Trough was characterized by shallow, restricted water conditions within a broad shallow shelf setting extending across the Dahra-Hofra and Beda platforms (Fig. 12).

Locally, the Gerad Trough is marked by several horsts and grabens; a result of extensional tectonism. The area was tectonically active throughout the Tertiary Period. The sedimentary sequence was tilted to the east-south-east during the Danian, and tilting continued during the Tertiary. Presently the sequence is tilted to the west-south-west (Fig. 8, Fig. 6, in back pocket). This indicates the renewal of tectonic activities subsequent to deposition of Beda Formation sediments.

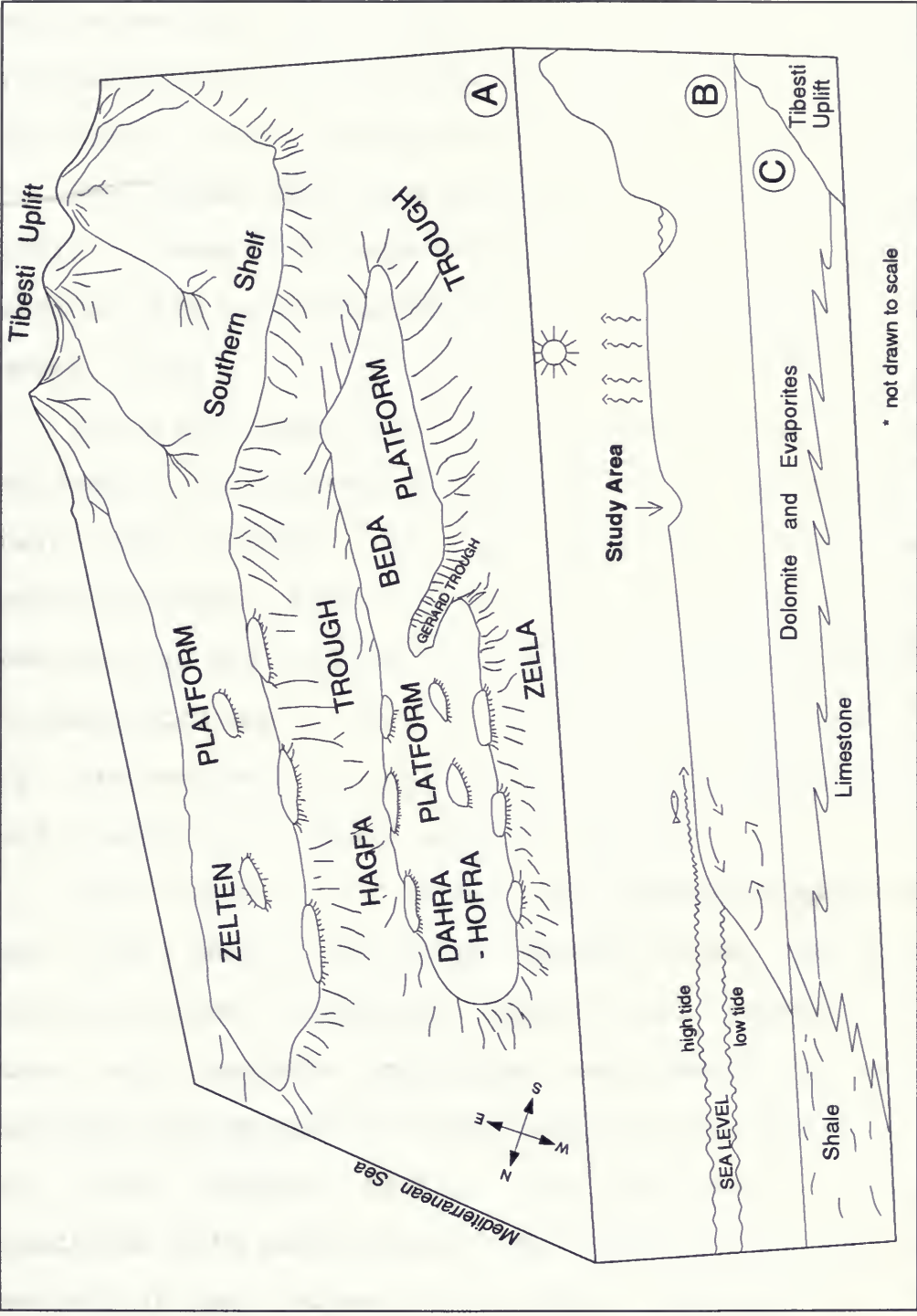


Fig.12 A) A sketch of tectonic elements of Sirte basin. B) Profile of tectonic elements. C) General stratigraphy of Beda Formation.

The General Model of Deposition

The Sirte Basin was a shallow inland sea with clear, shallow and warm water conditions that permitted the deposition of extensive carbonate sediments. The Sirte paleogeography can be compared to the modern Arabian Gulf.

The Arabian Gulf is a shallow sea (20-80m deep), landlocked within a desert climate with limited oceanic influence and surface water salinities of 39-40‰ in the open gulf (Wilson and Jordan, 1983).

Sirte Basin has many of the characteristics of an epeiric sea model with isolated platforms such as the one depicted by Irwin, 1965; Heckel, 1972; Klein and Ryer, 1978; Cram, 1979; Pratt and James, 1986. Tidal flats and patch reefs developed over much of the isolated platforms and were surrounded by open to restricted marine waters within the trough areas (Figs. 2, 12). The sediment accreted vertically and migrated laterally to form a shallowing upward sequence (Fig. 9).

Tidal currents and storms are considered to have been the most likely source of energy, whereas tidal flat progradation would have been the dominant depositional process. The Bahama Banks are isolated platforms surrounded by open waters characterized by shallow water carbonate sedimentation (Shinn et al., 1969; Hardie, 1977). Shallow water carbonates are associated with extensional fault blocks in the Red Sea and in the Gulf of Suez (Purser et al., 1987). They are being deposited on tilted fault blocks formed during rifting with reefs developing along their edges in a gulfward direction. The Leduc

Formation of Western Canada represents deposition on an ancient isolated platform (Wilson, 1975).

The Beda Formation model in the study area 'represents an isolated shelf, surrounded by shallow water and characterized by patch reefs, tidal flats and lagoons (Fig. 12). It is similar to present day Andros Island, Bahamas (Shinn et al., 1969; Ginsburg, and Hardie, 1975).

The presence of anhydrite and gypsum in the study area indicates dry climatic conditions with intermittent wet periods, as evidenced by the presence of charophyte algae.

The Beda Formation carbonates were deposited in variable salinity conditions. The Terminal microfacies near the top of the Beda Formation were deposited under restricted water flow conditions. This restriction probably resulted from physical barriers in the offshore area, sea-level changes or tectonic activity. The restricted circulation resulted in the development of hypersaline lagoons and sabkhas. The periodic influx of fresh water enhanced the development of brackish condition and the flourishing of charophytes.

The seasonal influx of fresh water indicates wet climatic conditions during the Danian for the Sirte Basin. However, periodic replenishment of the shelf by marine waters allowed the precipitation of marine limestones and the occurrence of the restricted marine fauna such as ostracods, gastropods, algal mats and foraminifera intermixed with the brackish-fresh water charophytes.

The Major Controls of Beda Formation Sedimentation

The major controls of the Beda Formation carbonate deposition were sea-level change, tectonism and climate. Sea-level change and rates of tectonic subsidence are the most important controlling factors of carbonate platform cyclicity (Bice, 1988). Climate determines the water temperature, salinity, nutrient supply, storm tides, wave activity and circulation patterns (Wilson, 1975).

Shallow water carbonates were extensively developed over the platforms of the Sirte Basin, and most of the terrigenous clastic sediment influx generated from the highlands such as the Tibesti Uplift was prevented from reaching the platforms by their entrapment in the deeper trough areas surrounding the platforms (Fig. 12).

The rise and fall of Tethys sea-level in the Sirte Basin have had great influences on rock textures, facies sequences, and diagenesis. It controlled the degree of subaerial exposure and meteoric diagenesis that resulted in solution leaching and the development of secondary porosity, dolomitization and anhydrite precipitation within the Beda Formation sediments.

A rapid rise in sea-level resulted in deposition of the Hagfa shale during an early Danian transgression followed by a gradual shallowing period that lasted until the end of the Danian, and was followed by Beda Formation sediment deposition. A subsequent sea-level rise during Early Selandian was responsible for superjacent deposition of the Khalifa shale on Beda Formation sediments.

Temperature and salinity are important factors affecting shallow-water carbonate secreting organisms (Lees, 1975; Boucot, 1981; Hudson, 1990; Pickerill and Brenchley, 1991). Green algae such as dasycladacean and charophytes, benthonic foraminifera, ostracods, coralline red algae, bryozoans, echinoderms and molluscs can survive in waters with temperatures of 15-10°C (Bosence, 1980; Farrow et al., 1984; Rao and Green, 1982; Nelson, 1978).

In tropical waters the number of species is five to ten times greater than those of cold regions (Pickerill and Brenchley, 1991). Salinity and temperature fluctuations influenced the abundance and number of species of the Beda Formation microfacies. The intertidal microfacies are generally characterized by an abundance of benthonic foraminifera, dasycladacean algae, ostracods, molluscs, bryozoans and echinoderms. The subtidal microfacies have considerably fewer fossils.

Hypersaline, restricted conditions that developed during the deposition of the terminal microfacies complex (TMFC1) limited the presence of dasycladacean algae, bryozoans, and echinoderms (Logan, 1961; Hoffman et al., 1969; Friedman et al., 1973). The faunal diversity of organisms tolerant of hypersaline conditions such as foraminifera (miliolids), ostracods and gastropods was low. Algal mats can exist under normal, hypersaline and brackish conditions (Hoffman et al., 1969). They were encountered throughout different salinity conditions within the Beda Formation.

Charophyte algae need fresh to brackish water for its reproduction stage and were only encountered in the brackish sediments of the terminal microfacies complex. The anhydrite microfacies lacked these fossils.

Water depth is very important in shallow marine environments. Carbonate sedimentation is extensive at water depths less than 15m because of high biological activity and productivity (James, 1984; Tucker and Wright, 1990; Kendall and Schlager, 1981). The presence of daycladacean algae, charophytes, large benthonic foraminifera such as *Nummulites* and *Operculina* and algal mats indicate water depths of less than 30m for some of the depositional environments of Beda Formation such as the terminal microfacies complex and the dasyclad-foraminiferal packstone microfacies.

The light penetration related to water depth also controls the photic zone which, in turn, controls the growth of photosynthetic organisms such as algae and seagrass. Endolithic algae played a major role in degrading the grain constituents of the Beda Formation microfacies through their microboring activity as evidence by micritized grains and micrite envelopes.

The photic zone may reach a depth of 250m in modern tropical settings and in shelf areas of the North Sea, but normally the depth ranges from 22-45m (Hudson, 1990). On Florida shelf and the Bahama Platform, production rates of biogenic carbonates are highest in waters less than 15m deep (Shinn, 1983; Wilson and Jordan, 1983; Enos, 1983).

It is evident from the above discussion that the study area was characterized by shallow water depositional environments on shelves with less 100m during the deposition of Beda Formation sediments.

The Gerad Trough, where the study area is located, was probably a shallow lagoon characterized by quiet, poor to moderate water circulation, in addition to hypersaline conditions, as noted by anhydrite deposition at the top of the Beda Formation (Figs. 11, 13).

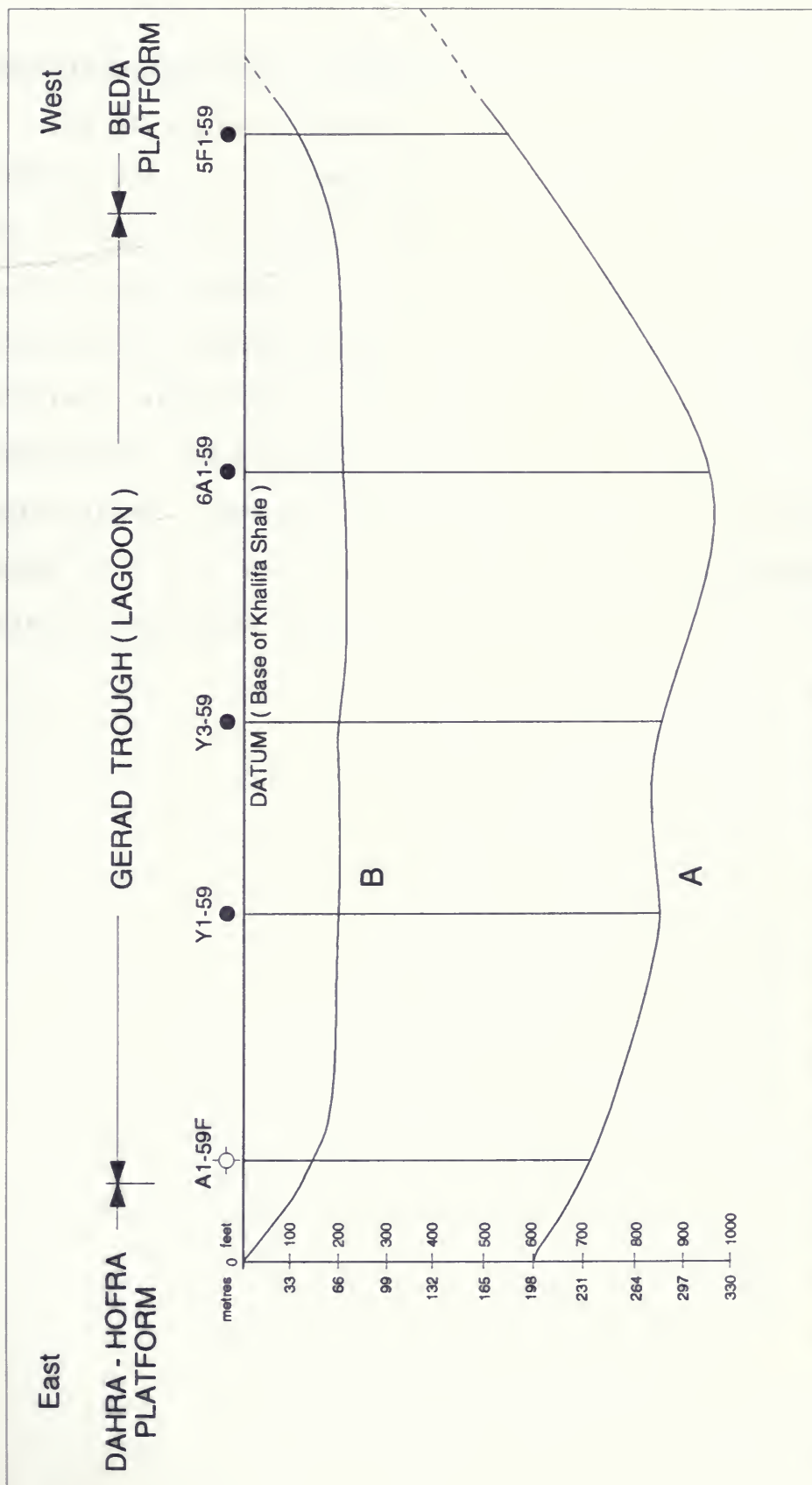


Fig. 13 Reconstruction of the paleogeography of the study area.

A) Paleotopography of Hagfa shale at the onset of Beda sedimentation relative to Khalifa Shale datum.
 B) Paleotopography of Lower Beda Member.

CHAPTER EIGHT: PETROLEUM GEOLOGY

Petroleum Exploration History in the Study Area

Seven exploration wells were drilled by Waha Oil Company to confirm seismically defined structures in the study area. These wells are A1-59F, 6A1-, CC1-, 4K1-, Y1-, Y2a-, and Y3-59 (Fig. 14, in back pocket). The primary objective was to test the hydrocarbon potential of the Beda Formation. Almost all the drilled structures are normal northwest-southeast fault controlled anticlinal features or "horsts". Hydrocarbon exploration results and reservoir properties are summarized in table 4. The drilling results of the individual wells are briefly discussed below.

Borehole	Reservoir Rocks	Porosity Type	Trapping Mechanism	Hydrocarbon Tests
A1-59F	Foraminiferal dolomitic packstone(MF2)	Moldic, inter-granular and inter-crystalline	Structural	Dry
Y1-59	Dolomitic mudstone-wackestone(TMFC1) and foraminiferal dolomitic packstone(MF2)	As above	Structural	Tested oil
Y2a-59	Foraminiferal dolomitic packstone(MF2)	As above	Structural	Dry
Y3-59	Dolomitic mudstone-wackestone(TMFC1) and foraminiferal dolomitic packstone(MF2)	As above	Structural	Tested oil
6A1-59	As above	Inter-crystalline , fracture, moldic	Structural	Tested oil
CC1-59	As above	Moldic, inter-granular, inter-crystalline	Structural	Tested oil
4K1-59	As above	As above	Structural	Dry

Table 4: Summary Of Petroleum Geology In The Study Area

A1-59F

The A1-59F well was drilled to evaluate a seismically defined anticlinal feature. The structural anomaly is bounded by two major normal faults trending northwest-southeast with the down-thrown sides to the west producing a tilted horst block (Figs. 6, 14, in back pocket). The A1-59F well is located 7.25 km west-south-west of the Y1-59 well and 25 km west of the Khalifa field. The well was drilled to a total depth of 4,547m (15,004 ft.). Hydrocarbon shows were encountered at depth interval 1,578-1,588m (5,207-5,241 ft.) within the Beda Formation.

This interval was explored further by drillstem-test No. 2 and produced salt water (Fig. 6, in back pocket). The well was abandoned. The reason for A1-59F being dry can be attributed to the non-sealing fault on the eastern side of the structure which has permitted the oil to migrate up-dip through the porous rocks of Beda Formation into the adjacent higher structure of the Y-59 area (Fig. 6).

Y-59 Structure

Three wells were drilled to test the Y-59 structure. These wells are Y1, Y2a and Y3-59 (Figs. 6, 14, in back pocket). The Y-59 structure represents a horst block bounded by northwest-southeast trending faults.

The Beda Formation was the primary exploration target. The Y1-59 well was the first drilling exploration of the Y-structure. It was drilled to a total depth of 3,322m (10,963 ft.) below sea-level. Beda reservoirs showed oil from several

intervals, as indicated by drill-stem test 1, 2, 3, 4 (Fig. 6, in back pocket).

Y2a-59 was the second well to be drilled in the study area. It was drilled to a total depth of 1,325m (4,373 ft.). No oil shows were encountered in the Beda Formation and drill-stem testing recovered salt water. The Y2a-59 well was drilled off-structure which is the main reason for it being non-producing.

The Y3-59 well was drilled to define and extend the north-eastern production limits of the Y-structure from the Beda reservoir. The well showed oil from the Beda Formation and the results of drill-stem tests are indicated in Fig. 6.

CC1-59

The CC1-59 well was drilled in the early 1960's to explore a structural high in the southern part of the study area and test the hydrocarbon potential of the Beda Formation. The well showed oil from different depths within the Beda reservoir. However, the well was plugged and abandoned on the basis of non-commercial quantities of oil.

4K1-59

Well 4K1-59 was drilled in 1974 to evaluate a seismic structural feature in the southern part of the study area. The well was drilled to a total subsea depth of 1,654m (5,457 ft.). Although oil stains were encountered from the Beda reservoir, the interval was not tested for its hydrocarbon potential and the well was plugged and abandoned.

6A1-59

The 6A1-59 well was drilled during 1989 to test a seismically defined tilted horst block located approximately 7.25 km northeast of the Y3-59 well. The anticlinal feature is bounded by two major normal faults trending northwest-southeast with the down-throw to the west and east respectively (Figs. 6, 14, in back pocket). Oil was confirmed from various intervals within the Beda reservoir, as indicated by drill-stem tests 3 and 4.

Porosity and Permeability

Porosity and permeability development in carbonate rocks is greatly influenced by the depositional environment and facies. Permeability is the result of interconnected porosity of a rock (Choquette and Pray, 1970), and is measured in millidarcy (md).

Porosity and permeability determination is a major objectives of the microfacies analysis of the Beda Formation, in order to predict the porous and permeable trends for potential hydrocarbon reservoirs.

Porosity types and their development history are the result of interactive biological, sedimentary and diagenetic processes that have influenced the carbonate rocks throughout their depositional history. Diagenetic processes such as solution leaching and dolomitization result in the development of secondary porosity throughout the burial history of the rock.

Porosity and permeability of the Beda Formation have been analyzed through standard laboratory core analysis, well logs,

petrographic, visual and electron scanning microscopy examination of thin-sections, core slabs and rock samples.

Analysis of the Beda Formation microfacies indicates the presence of six important porosity types. Moldic porosity is the predominant type, followed in decreasing order of abundance and importance by intercrystalline, intragranular, intergranular, vuggy, fenestral and fracture porosity. The predominance of moldic and intercrystalline porosities over the other types is the result of pervasive diagenetic processes, such as solution leaching and dolomitization. Cementation by sparry calcite and anhydrite has greatly decreased the effective porosity through pore plugging and decreasing connectivity.

Almost all of the microfacies are characterized by moldic and intragranular porosity. Intercrystalline porosity is limited to the dolomitized zones within the terminal microfacies complex (TMFC1) and the foraminiferal dolomitic packstone microfacies (MF2). Porosity varies from one microfacies to another and it averages about 15% in the oil producing horizons of the Beda Formation.

Permeability is generally low and best developed in the dolomitic limestone microfacies. Porosity and permeability development in the producing intervals was dependent upon the degree of dolomitization and solution leaching. Permeability of Beda reservoir rocks of the terminal Microfacies Complex (TMFC1) and the foraminiferal dolomitic packstone (MF2) of the study area averages about 2 md. Such permeability is considered low but still economic, provided that artificial fracturing and

acidizing of the reservoir rock be utilized during the development stage of the field to enhance flow.

The dolomitic limestone microfacies developed the best reservoir qualities as a consequence of matrix dolomitization and preferential dissolution of the metastable carbonate grains and fossils. Permeability, of the reservoir rocks, was developed when the isolated pores, such as molds, became interconnected as a result of those secondary diagenetic processes.

Source and Seal Rocks

Marine transgression of the Sirte Basin during the Early Cretaceous resulted in the deposition of thick and dark shales in the deeper parts of the basin and carbonates in the shallower areas. The Campanian Sirte shale is believed to be the source of most of the hydrocarbon accumulation in the Sirte Basin (Hamayouni et al., 1984; Clifford, 1986). The oil was generated in these trough shales and migrated updip into the reservoir rocks. Most of the discovered oil is trapped in reefs developed along the edges of platforms and in structural traps that resulted from the draping of sedimentary strata across normal fault blocks in the platform and trough areas of the Sirte Basin.

The Paleocene sedimentary sequence contains major carbonate build-ups and other prolific carbonate reservoirs such as the Beda Formation. The Beda Formation is marked at the top by the presence of thick anhydrite beds of the terminal microfacies

complex and is overlain by the Khalifa shale providing the seal for oil entrapment in the underlying Beda reservoir rocks of the foraminiferal dolomitic packstone (MF2) and the dolomitic mudstone-wackestone microfacies of the terminal Microfacies Complex (TMFC1).

CONCLUSIONS

1. Petrographic and paleontologic analysis of the Paleocene sediments of the Beda Formation of western concession 59 and 59F block resulted in the delineation of one microfacies complex and eleven individual microfacies types. They are as follows in ascending order:

MF12-	Foraminiferal Mudstone Microfacies ,
MF11-	Dasyclad Pelletal Wackestone Microfacies ,
MF10-	Pelloidal Packstone Microfacies ,
MF9-	Skeletal Wackestone-mudstone Microfacies ,
MF8-	Pellet-dasyclad Foraminiferal Packstone Microfacies ,
MF7-	Foraminiferal Wackestone-mudstone Microfacies ,
MF6-	Foraminiferal Packstone Microfacies ,
MF5-	Ostracoda-foraminiferal Wackestone Microfacies ,
MF4-	Dasyclad-foraminiferal Packstone Microfacies ,
MF3-	Skeletal Mudstone Microfacies ,
MF2-	Foraminifera Dolomitic packstone Microfacies , and
TMFC1-	The Terminal Microfacies Complex .

2. The grains, allochems, biotic constituents, sedimentary structures and textures suggest that the limestones were deposited on a broad shallow shelf characterized by tidal flats and shallow lagoons. Water depth variations were probably the result of sea-level changes and tectonic activity. Deposition was severely

restricted at the end of Beda Formation deposition due to physical blockage and/or drop in sea-level. The restricted conditions resulted in the development of subaerial exposure and fresh water influx as indicated by the presence of charophytes in addition to the development of sabkha environments.

The microfacies of the Beda Formation represent a shallowing-upward sequence consisting of alternating shallow subtidal and intertidal carbonate cycles which are marked at the top by supratidal sabkha deposits.

The deposition of Beda Formation was terminated by the drowning of the platforms by the Upper Paleocene transgression and the deposition of Khalifa shale.

3. The Beda Formation conformably overlies the Hagfa shale and is conformably overlain by Khalifa shale.
4. The discovery of the charophytes confines the age of Beda Formation to Early Paleocene "Danian". The discovery of the charophytes in the Paleocene of Sirte Basin indicates that the species *Feistiella globosa* ranges up to the Paleocene; earlier this species was reported only from the Late Cretaceous.
5. The Beda Formation thickens markedly from 121m (400 ft.) over the platforms to over 242m (800 ft.) in the study

area. The local thickening of the Beda Formation is structurally controlled and confined to the Gerad Trough.

6. Seismic maps show several structural closures at the Beda level. These closures coincide with thick sections of the Beda Formation with relatively good reservoir potential; especially near the top where grain supported and dolomitized microfacies were encountered. Average porosity in this zone is 15-20% and permeability is above 3 md. The reservoir rocks of the Beda Formation are capped by the overlying anhydrite of the terminal microfacies complex and by the shales of Khalifa Formation.

7. Oil is produced from moldic, intergranular and intercrystalline pores. Dissolution and dolomitization have enhanced reservoir porosities and consequently its permeability. In some horizons porosity was reduced due to plugging by anhydrite as a result of sabkha diagenesis supplemented by sparry calcite cement occlusion.

RECOMMENDATIONS

1. The Beda microfacies study focussed on an area in the southwest of the Sirte Basin. However, the study should be expanded to cover wider areas and expand regionally across the southwestern margins of the basin.
2. The discovery of the charophyte algae near the top of the Beda Formation marks the presence of brackish water environments due to freshwater influx during the Danian in southwestern Sirte Basin. Certain charophyte species restrict the age of the Beda Formation to Danian; this age restriction, as well as the regional distribution of the charophytes should be investigated by collecting data on a wider scale throughout Sirte Basin. The charophyte zone may prove to be a good stratigraphic marker of paleoenvironmental and paleoecological significance.
3. Additional wells should be drilled to test the delineated structures in the study area. The microfacies analysis of Beda Formation indicates the presence of good reservoir properties throughout the study area.

REFERENCES

- Adams, C. G., 1989. Foraminifera as indicators of geological events. *Proc. Geol. Assoc.*, 100., 297-311.
- Adams, J. E. and Rhodes, M. L., 1960. Dolomitization by seepage refluxion. *Am. Assoc. Petrol. Geol. Bull.*, 44, 1912-1920.
- Aitken, J. D., 1967. Classification and environmental significance of crypt-algal limestones and dolomites, with illustrations from the Cambrian and Ordovician of south-western Alberta. *J. Sediment. Petrol.*, 37, 1163-1178.
- Allen, J. R. L., 1984. Sedimentary structures: their character and physical basis. *Development in Sedimentology*, 30, Elsevier, Amsterdam, 663 pp.
- Ash, M. and Ash, I., 1991. Handbook of Industrial Chemical Additives: An International Guide by Product, Trade Name, Function and Supplier, VHC Publisher, New York, 859 pp.
- Ball, M. M., Shinn, E. A. and Stockman, K. W., 1967. The geologic effects of Hurricane Donna in South Florida. *J. Geol.*, 75, 583-597.
- Bandy, O. L., 1964. General correlation of foraminiferal structure with environment. In: *Approaches to Paleoecology*, J. Imbrie and N. D. Newell (eds.), 75-90, New York: John Wiley.
- Barr, F. T. and Weegar, A. A., 1972. Stratigraphic Nomenclature of the Sirte Basin, Libya. *Petrol. Explor. Soc. Libya*, 179 pp.
- Barr, F. T., 1972a. Cretaceous biostratigraphy and planktonic foraminifera of Libya. *Micropaleontology*, 18, 1-46.
- Bathurst, R. G. C., 1975. Carbonate Sediments and their Diagenesis. Elsevier, Amsterdam, 658 pp.
- Behrens, E. W., 1969. Hurricane effect on hypersaline bay. In: *Int. Symp. Coastal Lagoons (Mexico, 1967)* A. Ayala-Castanares and F. B. Phleger (eds.). UNAM-UNESCO, 301-312.
- Bellanca, A. and Neri, R., 1986. Evaporite carbonate cycles of the Messinian, Sicily: Stable isotopes, mineralogy, textural features and environmental implications. *J. Sediment. Petrol.*, 56, 614-621.
- Berggren, W. A., 1965. The Paleocene biostratigraphy of the Waha-Defa area and central concession 71. *Stratigraphic Report No. 59.*, Oasis Oil Co. of Libya, Inc., 15pp.

- Berggren, W. A., 1974. Late Paleocene-Early Eocene benthonic foraminiferal biostratigraphy and paleoecology of Rockall Bank. *Micropaleontology*, 20, 426-448.
- Berggren, W. A., 1974. Paleocene benthonic foraminiferal biostratigraphy and paleoecology of Libya (Sirte Basin) and Mali. *Micropaleontology*, 20, 449-465.
- Berggren, W. A. and Aubert, J., 1975. Paleocene benthonic foraminiferal biostratigraphy, paleobiogeography, and paleoecology of Atlantic-Tethyan regions: Midway-type fauna. *Paleogeog. Paleoclimat. Paleoecol.*, 18, 73-192.
- Bhatia, S. B. and Brigi, H., 1991. Early Intetian charophytes from Shimla Hills, Lesser Himalayas. *Bull. Soc. Bot. France*, 138, 7-14.
- Bice, D., 1988. Synthetic stratigraphy of carbonate platform and basin systems. *Geology*, 16, 703-706.
- Bisson, M. A. and Kirst, G. O., 1980. *Lamprothamnium*, a euryhaline charophyte: 1 - osmotic relations and membrane potential at steady state. *J. Exp. Bot.*, 31, 1223-1235.
- Blazencic, J. Blazencic, Z., Crizan, M. and Stevanovic, B., 1991. Ecological study of charophytes from the national park of Plitvice Lakes. *Bull. Soc. Bot. France*, 138, 15-24.
- Blindow, I., 1991. Reasons for the decline of charophytes in eutrophicated lakes in Scania (Sweden). *Bull. Soc. Bot. France*, 138, 95.
- Bosence, D. W. J., 1980. Sedimentary facies, models and production rates of coralline algal gravels, Western Ireland. *Geol. J.*, 15, 91-111.
- Boucot, A. J., 1981. *Principles of Benthic Marine Paleoecology*. Academic Press, New York, 463 pp.
- Braiser, M. D., 1980. *Microfossils*. George Allen and Unwin, London, 193 pp.
- Briggs, E. G. and Crowther, P. R., 1990. *Paleobiology*. Blackwell, Oxford, 583 pp.
- Brotzen, F., 1940. Flintrannas och trindelrannas geologi. *Sveriges Geol. Undersok.* 34, 1-33.
- _____, 1942. Die Foraminiferengattung *Gavelinella*. *Nov. Gen. und die Systematik der Rotalliiformes*: *Sveriges Geol. Undersok.* 36, 1-60.

- Brown, M. A., Archer, A. W. and Kvale, E. P., 1990. Neap-spring tidal cyclicity in laminated carbonate channel-fill deposits and its implications: Salem limestone (Mississippian), South-central Indiana, U.S.A. *J. Sediment. Petrol.*, 60, 152-159.
- Burke, K., 1972. Longshore drift, submarine canyons and submarine fans in development of Niger Delta. *Am. Assoc. Petrol. Geol. Bull.*, 56, 1975-1983.
- Burke, K. and Whiteman, A. J., 1973. Uplift, rifting and the break-up of Africa. In: *Implication of Continental Drift to the earth sciences*, D. H. Tarling and S. K. Runcorn (eds.). 2, Academic Press, London, 1035-1045.
- Burke, K. and Dewey, J., 1974. Two plates in Africa during the Cretaceous. *Nature*, 249, 313-316.
- Burne, R. V., Bauld, J. and DeDeckker, P., 1980. Saline lake charophytes and their geological significance. *J. Sediment Petrol.*, 50, 281-293.
- Butler, G. P., 1970. Holocene gypsum and anhydrite of Abu Dhabi Sabkha, Trucial Coast: An alternative explanation of origin. In: *Third Symposium on salts*, J. L. Rau and L. F. Dellirig (eds.), 120-152. Northern Ohio Geol. Soc., Cleveland, Ohio.
- Carter, R. M., Abbott, S. T., FalThorpe, C. S., Haywick, D. W. and Henderson, R. A., 1991. Application of global sea-level and sequence-stratigraphic models in Southern Hemisphere Neogene Strata from New Zealand. In: *Sedimentation, Tectonics and Eustasy, sea-level changes at active margins*, D. I. M. MacDonald (ed.). Spec. Public., no. 12 of the International Association of Sedimentologists, 41-65, Blackwell Scientific Publications.
- Castel, M. and Grambast, L., 1969. Charophytes de l'Eocène des Cordières. *Bull. Soc. géol., France*, 7, 936-943, 30-32
- Choquette, P. W. and James, N. P., 1987. Diagenesis in limestones - 3, the deep burial environment. *Geoscience Canada*, 14, 3-35.
- Choquette, P. W. and Pray, L. C., 1970. Geologic nomenclature and classification of porosity in sedimentary carbonates. *Am. Assoc. Petrol. Geol. Bull.*, 54, 207-250.
- Clifford, A. C., 1986. African Oil - past, present and future. In: *M. T. Halbouty (ed.). Future Petroleum Provinces of the World*, M.T. Halbouty (ed.). *Am. Assoc. Petrol. Geol. Mem. No. 40*, 339-372.

- Cloyd, K. C., Demicco, R. V. and Spencer, R. J., 1990. Tidal channel, levee, and crevasse-splay deposits from a Cambrian tidal channel system: A new mechanism to produce shallow-upward sequences. *J. Sediment. Petrol.*, 60, 73-83.
- Cram, J. M., 1979. The influence of continental shelf width on tidal range: Paleo-oceanographic implications. *J. Geol.*, 87, 441-447.
- Curtis, H., 1979. *Biology*, Worth Publications Inc., New York, 1043 pp.
- Cushman, J. A., 1927. Some new genera of the foraminifera. *Cushman Lab. Foram. Research. Contrib.*, 2, 77-81.
- _____, 1933. Two new genera *Pernirina* and *Hogenowella* and their relationships to genera of the *Valvulinidae*. *Am. J. Sci.*, 26, 19-26.
- _____, 1936. New genera and species of the families *Vernuilinidae* and *Valvulinidae* and of subfamily *Virguliniinae*. *Cushman Lab. Foram. Research, Spec. Publ.* 6, 71 pp.
- _____, 1951. Paleocene Foraminifera of the Gulf Coastal region of the United States and adjacent areas. *U.S. Geological Survey Professional Paper*, 232. 75 pp.
- d'Orbigny, Aleide Dessalines, 1826. Tableau méthodique de la classe des Céphalopodes. *Ann. Sci. Nat. Paris*, 7, 245-314.
- _____, 1839. Voyage dans l'Amérique Méridionale-Foraminifères: 5, 86pp. Pitores-Levrault et c^e (Paris), V. Levrault.
- Dean, W. E., Ali, Y. A. and Hilmy, M. E., 1975. Sedimentological significance of nodular and laminated anhydrite: *Geology*, 3, 367-372.
- Decima, A., McKenzie, J. A. and Schreiber, B. C., 1988. The origin of "evaporative" limestones: An example from the Messinian of Sicily (Italy). *J. Sediment. Petrol.*, 58, 256-272.
- Defrance, M. J. L., 1824. *Dictionnaire des Sciences Naturelles*. 32, 1-567. F. G. Levrault (Paris).
- Dunham, R. J., 1962. Classification of carbonate rocks according to depositional texture. In: *Classification of carbonate rocks*: *Am. Assoc. Petrol. Geol. Mem. No. 1*, 108-121.

- Enos, P., 1983. Shelf environments. In: Carbonate Depositional environments, P. A. Scholle; D. G. Bebout; C. H. Moore (eds.) Am. Assoc. Petrol. Geol. Mem. No. 33, 269-291.
- Evans, G., Schmidt, V., Bush, P. and Nelson, H., 1969. Stratigraphy and geologic history of the Sabkha, Abu Dhabi, Persian Gulf. *Sedimentology*, 12, 145-159.
- Farrow, G. E., Allen, N. H and Akpau, E. A., 1984. Bioclastic carbonate sedimentation on a high-latitude, tide-dominated shelf, Northeast Orkney Islands, Scotland. *J. Sediment. Petrol.*, 54, 374-393.
- Feist, M., Bhatia, S. B. and Yadagiri, P., 1991. On the oldest representative of the family Characeae and its relationships with the Porocharaceae. *Bull. Soc. Bot. France*, 138, 25-32.
- Feist, M., 1979. Charophytes at the Cretaceous-Tertiary boundary. New data and present state of knowledge. Cretaceous-Tertiary Boundary Events Symposium, II Proceedings, 88-94, Christensen and Birkelund (eds.), Copenhagen Univ.
- Finlay, H. J., 1939. New Zealand Foraminifera, key species in stratigraphy. *Royal Soc. New Zealand, Trans.*, 68, 504-543.
- Fluegeman, Jr. R. H., Berggren, W. A. and Madeleine, B., 1990. Paleocene benthonic foraminiferal biostratigraphy of the eastern Gulf coastal plain. *Micropaleontology*, 36, 56-64.
- Flügel, E., 1982. *Microfacies analysis of limestones*, Springer-Verlag, Berlin, 633 pp.
- Folk, R. L., 1962. Spectral subdivision of limestone types: In: *Classification of carbonate rocks*: Am. Assoc. Petrol. Geol. Mem. No. 1, 87-97.
- Friedman, G. M., Amiel, A. J., Braun, M. and Miller, D. S., 1973. Generation of carbonate particles and laminites in algal mats - examples from sea marginal hypersaline pool, Gulf of Aqaba, Red Sea. *Am. Assoc. Petrol. Geol. Bull.*, 51, 541-557.
- Friedman, G. M. and Sanders, J. E., 1978. *Principles of Sedimentology*, John Wiley and Sons, New York, 792 pp.
- Ginsburg, R. N., 1957. Early diagenesis and lithification of shallow water carbonate sediments in South Florida. In: *Regional Aspects of Carbonate Deposition*, R. J. LeBlanc and J. C. Breeding (eds.). *Soc. Econ. Paleont. Miner. Spec. Publ. No. 5*, 80-90.

- Ginsburg, R. N., Rezak, R. Wray, J. L., 1971. Geology of calcareous algae (notes for short course). Sediments I, 61 pp., Comparative Sedimentology Lab., University of Miami, 1971.
- Ginsburg, R. N., 1975. Tidal deposits: A casebook of recent examples and fossil counterparts. Springer-Verlag, New York, 428 pp.
- Ginsburg, R. N. and Hardie, L. A., 1975. Tidal and storm deposits, northwestern Andros Island, Bahamas. In: Tidal deposits: A casebook of recent examples and fossil counterparts, R. N. Ginsburg (ed.), 201-208. Springer-Verlag, New York.
- Grambast L. and Gutierrez, G., 1977. Especies nuevas de Charophytes du Crétacé terminal de la Province de Cuenca (Espagne). Paléobiologie continentale, 8, 34pp.
- Hamouni, E. A., Amr, I. A, Riani, M. A., El-Ghull, A. B. and Rahoma, S. A., 1984. Source and habitat of oil in Libyan Basins. A report presented at a conference on source and habitat of oil in the Arab countries, sponsored by the Organization of Arab Petroleum Exporting Countries (OAPEC) In Kuwait, Sept., 1984. 125-180.
- Haq, B. and Van Eysinga, F. W., 1987. Geological Time Table. Elsevier, Amsterdam.
- Hardie, L. A., 1977. Sedimentation on modern carbonate tidal flats of northwest Andros Island, Bahamas: The Johns Hopkins Univ. Press, Baltimore, The Johns Hopkins Univ. Stud. in Geology, 22, 202 pp.
- Hardie, L. A. and Garrett, P., 1977. General environmental setting. In: Sedimentation on the modern carbonate tidal flats of northwest Andros Island, Bahamas, L. A. Hardie (ed.), 12-49, The Johns Hopkins Univ. Stud. in Geology, 22. The Johns Hopkins University Press, Baltimore.
- Hardie, L. A., Lowenstein, T. K. and Spencer, R. J., 1983. The problem with distinguishing between primary and secondary features in evaporites. Sixth International Symposium on Salt, 1, 13-39.
- Harding, T. P. and Lowell, J. D., 1979. Structural styles, their plate-tectonic habitats, and hydrocarbon traps in petroleum provinces. Am. Assoc. Petrol. Geol. Bull., 63, 1016-1058.
- Harland, W. B., Armstrong, R. L., Cox, A. V., Craig, L. E., Smith, A. G. and Smith, D. G., 1990. A Geologic Time Scale, 1989, Cambridge University Press, Cambridge, 263pp.

- Harris, P. M., Kendall, C. G. St. C. and Lerche, I., 1985. Carbonate cementation - A brief review. In: Carbonate Cements, N. Schneidermann and P. M. Harris (eds.), Soc. Econ. Paleont. Miner. Spec. Publ. No. 36, 79-95.
- Haynes, J. R., 1981. Foraminifera. John Wiley and Sons, New York, 433 pp.
- Heckel, P. H., 1972. Possible inorganic origin for stromatolites in calcilutite mounds in the Tully limestone, Devonian of New York. J. Sediment. Petrol., 42, 7-18.
- Helwigs, J., 1976. Shortening of continental crust and orogenic belts and plate tectonics. Nature, 260, 768-770.
- Hoffman, P. F., Logan, B. W. and Gebelein, C. D., 1969. Biological versus environmental factors governing the morphology and internal structure of recent algal stromatolites in Shark Bay, W. Australia (Abs.). Bull. Geol. Soc. Am., 1, 28-29.
- Horodyski, R. J. and Harr, S. P. V., 1975. Holocene calcareous stromatolites from Laguna Mormona (Baja California), Mexico. J. Sediment. Petrol., 45, 894-906.
- Horodyski, R. J. and Bloeser, B., 1977. Laminated algal mats from a coastal lagoon, Laguna Mormona, Baja California, Mexico. J. Sediment. Petrol., 47, 680-696.
- Huang, R. J., 1988. Charophytes of Nanxiong Basin, Guandong and its Cretaceous-Tertiary Boundary. Acta Palaeontologica Sinica, 27, 468-474. English abridged version. Beijing.
- Hubbard, R. J., 1988. Age significance of sequence boundaries on Jurassic and early Cretaceous rifted continental margins. Am. Assoc. Petrol. Geol. Bull., 72, 49-72.
- Hudson, J. D., 1990. Salinity from faunal analysis and geochemistry. In: Paleobiology: A Synthesis, Briggs, D. E. G. and Crowther, P. R. (eds.), Blackwell Scientific Publications, London, 406-410.
- Illing, L. V., Wells, A. J., Taylor, J. C. M., 1965. Penecontemporary dolomite in the Persian Gulf. In: Dolomitization and limestone diagenesis, L. C. Pray and R. C. Murray (eds.), Soc. Econ. Paleont. Miner. Spec. Publ. No. 13, 89-111.
- Irwin, M. L., 1965. General theory of epeiric clear water sedimentation. Am. Assoc. Petrol. Geol. Bull., 49, 445-459.

- James, N. P. and Choquette, P. W., 1984. Diagenesis of Limestone - the meteoric diagenetic environment. *Geoscience Canada* 11, 161-194.
- James, N. P., 1984a. Shallowing-upward sequences in carbonates. In: *Facies Models*, R. G. Walker (ed.). 213-228. *Geoscience Canada*.
- Kellough, G. R., 1965. Paleoecology of the foraminifera of the Wills Point Formation (Midway Group) in northeast Texas. *Trans. Gulf Coast Assoc. Geol. Soc.*, 15, 73-152.
- Kendall, C. G. St. C. and Schlager, W., 1981. Carbonates and relative changes in sea-level. *Mar. Geol.*, 44, 181-212.
- Khan, M., 1991. Charophytes in time and space: zonal distribution pattern. *Bull. Soc. Bot. France*, 138, 33-45.
- Kinsman, D. J. J., 1969. Modes of formation, sedimentary associations and diagnostic features of shallow-water and supratidal evaporites. *Am. Assoc. Petrol. Geol. Bull.*, 53, 830-840.
- Kisielevski, F. J., 1991. The Triassic charophytes of western Kazakhstan. *Bull. Soc. Bot. De France*, 138, 47-52.
- Klein, G., 1965. Dynamic significance of primary structures in the Middle Jurassic great Oolite series, southern England. In: *Primary sedimentary structures and their hydrodynamic interpretation*, G. V. Middleton (ed.), *Soc. Econ. Paleont. Miner. Spec. Publ.*, No. 12, 173-191.
- Klein, G. de V. and Ryer, T. A., 1978. Tidal circulation patterns in Precambrian, Paleozoic and Cretaceous epeiric and mioclinal shelf seas. *Bull. Geol. Soc. Am.*, 89, 1050-1058.
- Lamarch, J. B., 1801. *Systeme des animaux sans Vertebres*. *Museum Natl. Histoir Nat. Paris, Ann.*, 2, 432 pp.
- _____, 1804. *Suite des mémoires sur les fossiles des environs de Paris*. *Museum Natl. Hist. Nat. Paris, Ann.*, 5, p. 349-357.
- Land, L. S., MacKenzie, F. T. and Gould, S. J., 1967. Pleistocene history of Bermuda. *Bull. Geol. Soc. Am.*, 78, 993-1006.
- Lees, A., 1975. Possible influences of salinity and temperature on modern shelf carbonate sedimentation. *Mar. Geol.*, 19, 159-198.
- Levy, Y., 1977. Description and mode of formation of the supratidal evaporites facies in the northern Sinae coastal plain. *J. Sediment. Petrol.*, 47, 463-474.

- Lindholm, R. C. and Finkelman, R. B., 1972. Calcite staining: semiquantitative determination of ferrous iron. *J. Sediment. Petrol.*, 42, 239-242.
- Logan, B. W., 1961. Cryptozoan and associated stromatolites from the Recent, Shark Bay, W. Australia. *J. Geol.*, 69, 517-533.
- Logan, B. W., Davies, G. R., Read, J. F. and Cebulski, D. E., 1970. Carbonate sedimentation and environments, Shark Bay, W. Australia. *Am. Assoc. Petrol. Geol. Mem. No. 13*, 223.
- Logan, B. W., Hoffman, P. and Gebelein, C. D., 1974. Algal mats, Crypt-algal fabrics and structures, Hamelin Pool, W. Australia. *Am. Assoc. Petrol. Geol. Mem. No. 22*, 140-173.
- Logan, B. W., Rezaki, R. and Ginsburg, R. W., 1964. Classification and environmental significance of algal stramatolites. *J. Geol.*, 72, 68-93.
- Longinelli, A., 1979. Isotope geochemistry of some Messinian evaporites: Paleoenviromental implications. *Paleogeog. Paleoclimat. Paleoecol.*, 29, 95-123.
- Lowell, J. D. and Genik, G. J., 1972. Seafloor spreading and structural evolution of the southern Red Sea. *Am. Assoc. Petrol. Geol. Bull.* 56, 247-259.
- Massieux M. Tambareau Y. and Villatte J., 1989. Nouveaux gisements à charophytes du Dano-Montien Nord-Pyrénéen. *Rev. Micropal.*, 32, 140-150.
- Miller, K. B., Brett, C. E and Parsons, K. M., 1988. The paleoecologic significance of storm generated disturbance within a Middle Devonian muddy epeiric sea. *Palaaios*, 3, 35-52.
- Milliman, J. D., 1974. *Marine Carbonates*. Springer-Verlag, Berlin, 375 pp.
- Montfort, D. de., 1808. *Conchyliologie Systématique et classification methodique des coquilles*. *Soc. Geol. France, Bull.*, 1, 400-409.
- Moore, C. H., 1985. Upper Jurassic subsurface cements: A case history. In: *Carbonate Cements*, P. M. Harris and N. Schneidermann (eds.), *Soc. Econ. Paleont. Miner. Spec. Publ. No. 36*, 291-308.
- Moore, C. H., 1989. *Carbonate diagenesis and porosity*. Elsevier Publications, Amsterdam. 338 pp.
- Moore, C. H. and Druckman, Y., 1981. Burial diagenesis and porosity evolution, Upper Jurassic Smackover, Arkansas and Louisiana. *Am. Assoc. Petrol. Geol. Bull.*, 65, 597-628.

- Moore, J. A., 1991. *Lamprothamnium populasum*, a pioneer in the conservation of characeae and their habitats. Bull. Soc. Bot. France, 138, 73-74.
- Moore, R. C. (ed.), 1964. Treatise of invertebrate Paleontology, Part C, Protista 2. The Geological Society of America and the University of Kansas Press, Vol. 1 and 2, 900 pp.
- Nelson, C. S., 1978. Temperate shelf carbonate sediments in the Cenozoic of New Zealand. Sedimentology, 25, 737-771.
- Olsen, S., 1944. Danish Charophyta: chronological, ecological and biological investigations. Kongel. Danske. Vid. Selsk. Bot. Skr., 3, 1-140
- Perkins, R. D. and Halsey, S. D., 1971. Geologic significance of microboring fungi and algae in Carolina shelf sediments. J. Sediment. Petrol., 41, 843-853.
- Perrodon, A., 1983. Dynamics of oil and gas accumulation. Bulletin Des Centres De Recherches Exploration-production, ELF-Aquitane, Mem., 5, 368 pp.
- Pettijohn, F. J., 1957. Sedimentary Rocks. Harper and Row, New York, 718 pp.
- Pickerill, R. K. and Brenchley, P. J., 1991. Benthic macrofossils as paleoenvironmental indicators in marine clastic facies. Geoscience Canada, 18, 119-138.
- Plummer, H. J., 1931. Some Cretaceous Foraminifera in Texas. Univ. Texas Bull. 3101, 109-203.
- Pomeyrol, R., 1968. Nubian Sandstone. Am. Assoc. Petrol. Geol. Bull., 52, 589-600.
- Pratt, B. R. and James, N. P., 1986. The St. George Group (Lower Ordovician) of Western Newfoundland: Tidal flat island model for carbonate sedimentation in shallow epeiric seas. Sedimentology, 33, 313-343.
- Purser, B. H., Soliman, M. and M'Rabet, A., 1987. Carbonate, evaporite, siliciclastic transitions in Quaternary rift sediments of the northwestern Red Sea. Sediment. Geol., 53, 247-268.
- Rao, C. P. and Green, D. C., 1982. Oxygen and carbon isotopes of Early Permian cold-water carbonates, Tasmania, Australia. J. Sediment. Petrol., 52, 1111-1125.
- Read, J. F., 1973. Carbonate cycles, Pillara formation (Devonian), Canning Basin, W. Australia. Bull. Can. Petrol. Geol., 21, 38-51.

- Reading, H. G., 1986. Facies. In: Sedimentary Environments and Facies, H. G. Reading (ed.), 4-19, Blackwell, Oxford.
- Reuss, A. E., 1860. Uber Ataxophragmium, eine neue Foraminiferengattung aus der Familie der Uvellideen. K. Bohm. Gesell. Wiss. Prag. Math. Naturw. Cl., Sitzungsber, 40, 147-238.
- Rizzini, A. and Dondi, L., 1979. Messinian evolution of the Po Basin and its economic implications (Hydrocarbons). Paleogeog. Paleoclimat. Paleoecol., 29, 41-74.
- Roehl, P. O., 1967. Stony Mountain (Ordovician) and interlake (Silurian) facies analogs of recent low energy marine and subaerial carbonates, Bahamas. Am. Assoc. Petrol. Geol. Bull., 51, 1979-2032.
- Russell De and Zhai R. J., 1987. The Paleogene of Asia: mammals and stratigraphy. Mem. Mus. Nat. Hist. Nat., Sci. Terre, t. 52, 120p. Paris.
- Sanford, R. M., 1970. Sarir oil field, Libya-desert surprise. In: Geology of Giant Petroleum fields, M.T. Halbouty, (ed.), Am. Assoc. Petrol. Geol. Mem., 14, 447-476.
- Sassen, R. and Moore, C. H., 1988. Framework of hydrocarbon generation and destruction in eastern Smackover trend. Am. Assoc. Petrol. Geol. Bull., 72, 649-663.
- Scholle, P. A. and Halley, R. B., 1985. Burial diagenesis: out of sight, out of mind. In: Carbonate cements, N. Schneidermann and P. M. Harris (eds.). Soc. Econ. Paleont. Miner. Spec. Publ. No. 36, 309-334.
- Schreiber, B. C., Tucker, M. E. and Till, R., 1986. Arid shorelines and evaporites. In: Sedimentary Environments and facies, H. G. Reading (ed.), 189-223. Blackwell, Oxford.
- Scoffin, T. P., 1987. An Introduction to Carbonate Sediments and Rocks. Chapman and Hall, New York, 274 pp.
- Selley, R. C., 1985. Elements of Petroleum Geology. Freeman and Company Publications, New York, 447 pp.
- Selley, R. C., 1988. Applied Sedimentology. Academic Press, London, 446 pp.
- Shaikin, I. M., 1991. Rates of evolution of charophytes in Phanerozoic. Bull. Soc. Bot. France, 138, 75-93.
- Shearman, D. J., 1966. Origin of marine evaporites by diagenesis: Inst. of Min. and Metall. Trans. Ser. B, 75, 208-215.

- Shearman, D. J. and Fuller J. G., 1969. Anhydrite diagenesis, calcification and organic laminites, Winnipegosis formation, Middle Devonian, Saskatchewan. Bull. Can. Petrol. Geol., 17, 469-525.
- Shinn, E. A., 1968a. Practical significance of birdseye structures in carbonate rocks. J. Sediment. Petrol., 38, 215-223.
- Shinn, E. A., 1968b. Selective dolomitization of recent sedimentary structures. J. Sediment. Petrol., 38, 612-616.
- Shinn, E. A., 1983. Tidal flat environment. In: Carbonate Depositional Environment, P. A. Scholle, D. G. Bebout and C. H. Moore (eds.). Am. Assoc. Petrol. Geol. Mem. 33, 173-210.
- Shinn, E. A., Ginsburg, R. N. and Lloyd, R. M., 1965. Holocene supratidal dolomite from Andros Island, Bahamas. Soc. Econ. Paleont. Miner. Spec. Publ. No. 12, 112-123.
- Shinn, E. A., Lloyd, R. M. and Ginsburg, R. N., 1969. Anatomy of modern carbonate tidal flat, Andros Island. J. Sediment. Petrol., 39, 1202-1228.
- Silvestri, A., 1904. Forme nuove a poco conosciute di protozoi miocenici piemontesi. Accad. Pont. Nouvi Lincei, Atti, 39, 4-15.
- Soulie-Marsche, I., 1982. Charophytes as lacustrine biomarkers during the Quaternary in North Africa. J. Afric. Earth Sci., 12, 341-351. Pergamon Press.
- Stross, R. G., 1979. Density and boundary regulations of the *Nitella* meadow in Lake George, New York. Aquatic Botany, 6, 285-300.
- Tasch, P., 1980. Paleobiology of the invertebrates. John Wiley and Sons, New York, 975 pp.
- Tappan, H., 1980. The Paleobiology of Plant Protists, W. H. Freeman and Company, San Francisco, 102 pp.
- Terquem, O., 1883. Sur un nouveau genre de Foraminifères der Fuller's-earth de la Moselle. Soc. Géol. France, Bull., 3, 37-39.
- Thalman, H.E., 1939. Bibliography and index to new genera, species and varieties of Foraminifera. J. Paleont., 9, 715-743.
- Toulmin, L. D., 1941. Eocene smaller foraminifera from the salt mountain limestone of Alabama. J. Paleont. 15, 567-611.

- Tucker, M. E., 1981. Sedimentary petrology, An Introduction. Blackwell Scientific Publications, 252 pp.
- Tucker, M. E. and Wright, V. P., 1990. Carbonate sedimentology. Blackwell Scientific Publications, London, 482 pp.
- Van Houten, F. B., 1983. Cretaceous rifting above a fixed mantle hot spot, Sirte Basin, north-central Libya. *Geology*, 11, 115-118.
- Viterbo, I., 1968. Lower Cretaceous charophytes from the subsurface "Nubian Complex" of the Sirte Basin, Libya (Abstract), 3rd African Micropaleont, Coll., Cairo, Abst. Papers, p. 25.
- Walcott, R. I., 1972. Gravity flexure and growth of sedimentary basins at a continental edge. *Bull. Geol. Soc. Am.*, 83, 1845-1848.
- Walker, R. G., 1984a. Shelf and shallow marine sands. In: *Facies Models*, 2nd edition: Geoscience Canada, R. G. Walker (ed.). Reprint Series 1, 141-170.
- Walton, W. R., 1964. Recent foraminiferal ecology and paleoecology. In: *Approaches to Paleoecology*, J. Imbrie and N. D. Newell (eds.). 151-237. John Wiley and Sons, New York.
- Wanless, H. R., 1979. Limestone response to stress-pressure solution and dolomitization. *J. Sediment. Petrol.*, 49, 437-462.
- Ward, W. C. and Halley, R. B., 1985. Dolomitization in a mixing zone of near-seawater composition, late Pleistocene, northeastern Yucatan Peninsula. *J. Sediment. Petrol.*, 55, 407-420.
- Warren, J. K., 1988. Sedimentology of Coorong Dolomite in the Salt Creek region, South Australia. *Carbonates and Evaporites*, 3, 175-199.
- Warren, J. K., 1989. *Evaporite Sedimentology*. Prentice-Hall, Englewood Cliffs, New Jersey, 285 pp.
- Warren, J. K., 1990. Sedimentology and mineralogy of dolomite Coorong lakes, South Australia. *J. Sediment. Petrol.*, 60, 843-858.
- Warren, J. K. and Kendall, G. G. St. C., 1985. Comparison of marine (subaerial) and saline (subaqueous) evaporites: ancient and modern. *Am. Assoc. Petrol. Geol. Bull.*, 69, 1013-1023.

- West, I. M., 1975. Evaporites and associated sediments of the basal Purbeck Formation (Upper Jurassic) of Dorset. Proc. Geol. Assoc., 85, 205-225.
- West, I. M., 1979. Review of evaporite diagenesis in the Purbeck Formation of southern England. In: Symposium de sédimentation Jurassique Européen. Spec. Publ. Assoc. Sediment. Français 1, 407-416.
- Wilgus, C. K., Hastings, B. S., Kendall, C. G. St. C., Posamentier, H., Ross, C. A. and Van Wagoner, J. (eds.), 1988. Sea-level changes - an integrated approach. Soc. Econ. Paleont. Miner. Spec. Publ. No. 42, 407 pp.
- Wilson, J. L., 1975. Carbonate Facies in Geologic History. Springer-Verlag, New York, 471 pp.
- Wilson, J. E. and Jordan, C., 1983. Middle shelf environments. Am. Assoc. Petrol. Geol. Mem. 33, 297-343.
- Winter, U. and Kirst, G. O., 1991. Vacuolar composition during sexual reproduction and salinity stress in charophytes. Bull. Soc. Bot. France, 138, 85-93.

APPENDICES

Appendix I: Plates A, B, and C

Appendix II: Sample Descriptions of Beda Formation, Y3-59 Well

APPENDIX I

Plate A: Charophyte Algae

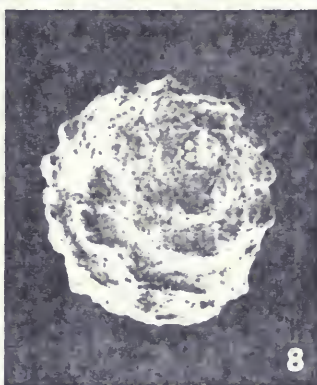
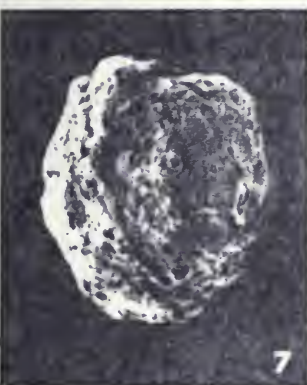
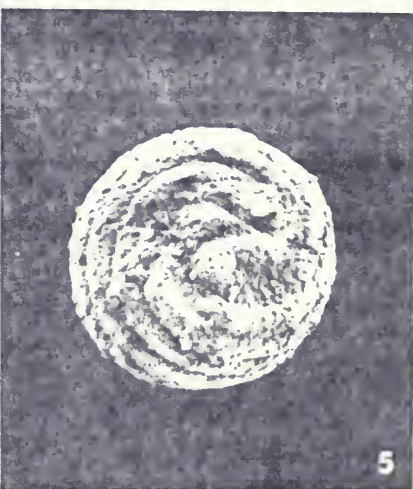
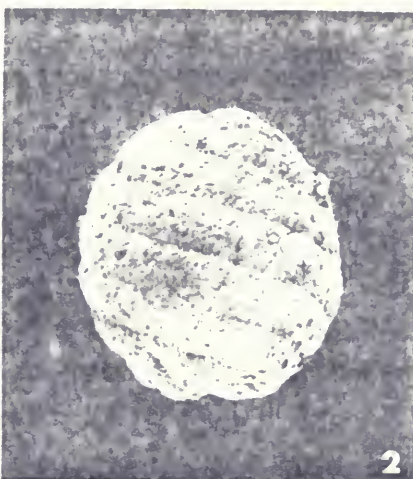
Plate B: Foraminifera

Plate C: Microfacies

PLATE A: CHAROPHYTE ALGAE

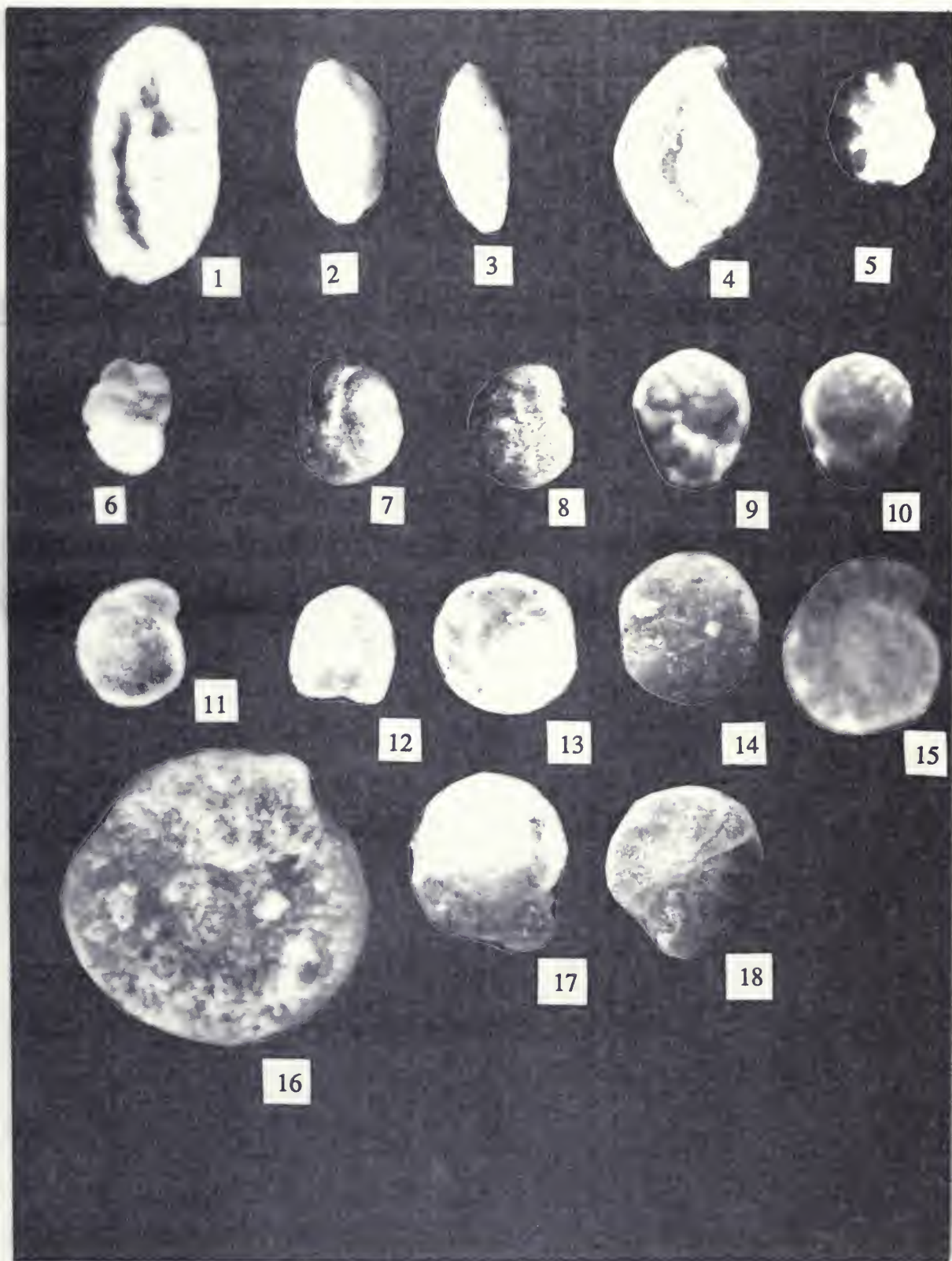
Figures

- 1 - 2 *Feistiella globosa*, lateral views, X 34.
- Dughiella wanzuangsensis*, lateral view, X 47.
- 3 - 6 *Stephanochara* sp. A Feist. 4, lateral view; 5, apical
 view; 6, basal view. X 56.
- ? *Peckichara* sp., lateral view, X 65.
- 8 - 9 ? *Microchara* sp., lateral views, X 65.
- 10 *Lamprothamnium* sp., view from the apex, X 56.



gures

- | | | | |
|------|---|--------|--------------------------|
| 2 | <i>Quinqueloculina</i> d'Orbigny, 1826. | X750. | Dorsal View |
| | <i>Triloculina</i> d'Orbigny, 1826. | X750. | Dorsal View |
| | <i>Spiroloculina</i> d'Orbigny, 1826. | X750. | Dorsal View |
| | <i>Alveolina</i> d'Orbigny, 1826. | X540. | Side View |
| | <i>Discorbis</i> Lamarck, 1804. | X1200. | Side View |
| 8 | <i>Eponides</i> Montfort, 1808. | X750. | Dorsal and Ventral Views |
| 10 | <i>Parella</i> Finlay, 1939. | X750. | Ventral and Dorsal Views |
| , 12 | <i>Rotalia</i> Lamarck, 1804. | X750. | Dorsal and Ventral Views |
| , 14 | <i>Epistomina</i> Terquem, 1883. | X1200. | Dorsal and Ventral Views |
| | <i>Operculina</i> d'Orbigny, 1826. | X540. | Side View |
| | <i>Nummulites</i> Lamarck, 1801. | X750. | Dorsal View |
| , 18 | <i>Elphidium</i> Montfort, 1808. | X750. | Ventral and Dorsal Views |



Figures

- 9 *Anomalinoides* Brotzen, 1942. X750. Dorsal View
- 0, 21 *Cibicides* Thalmann, 1939. X750. Dorsal and Ventral
Views
- 2, 23 *Gavelinella* Brotzen, 1942. X750. Dorsal and Ventral
Views
- 4 *Spiroplectammina* Cushman, 1927. X1200. Dorsal View
- 5 *Textularia* DeFrance, 1824. X900. Dorsal View
- 6, 27 *Gaudryina* d'Orbigny, 1839. X1200. Dorsal View
- 8 *Clavulinoides* Cushman, 1936. X540. Dorsal View
- 9 *Valvulammina* Cushman, 1933. X1200. Front View

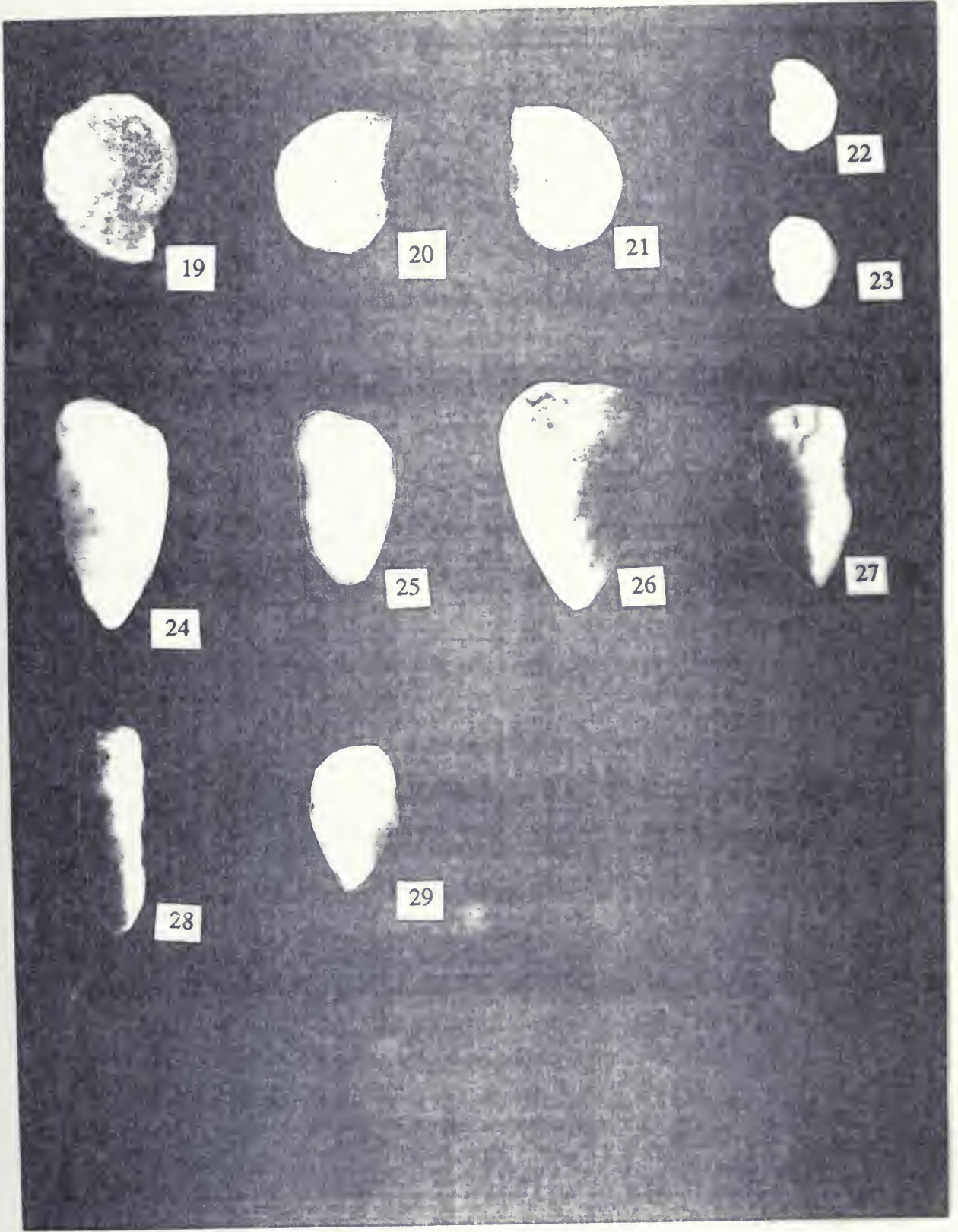


PLATE C: MICROFACIES

Figures

Thin-section photomicrograph under plane light showing recrystallized skeletal grains of echinoderm plates and foraminifera (MF3) at a depth of 1560m in well Y3-59.

Thin-section photomicrograph under polarized light showing solution leached and subsequently cemented molds of pelecypod shell fragments (MF3) at a depth of 1565m in well Y3-59.

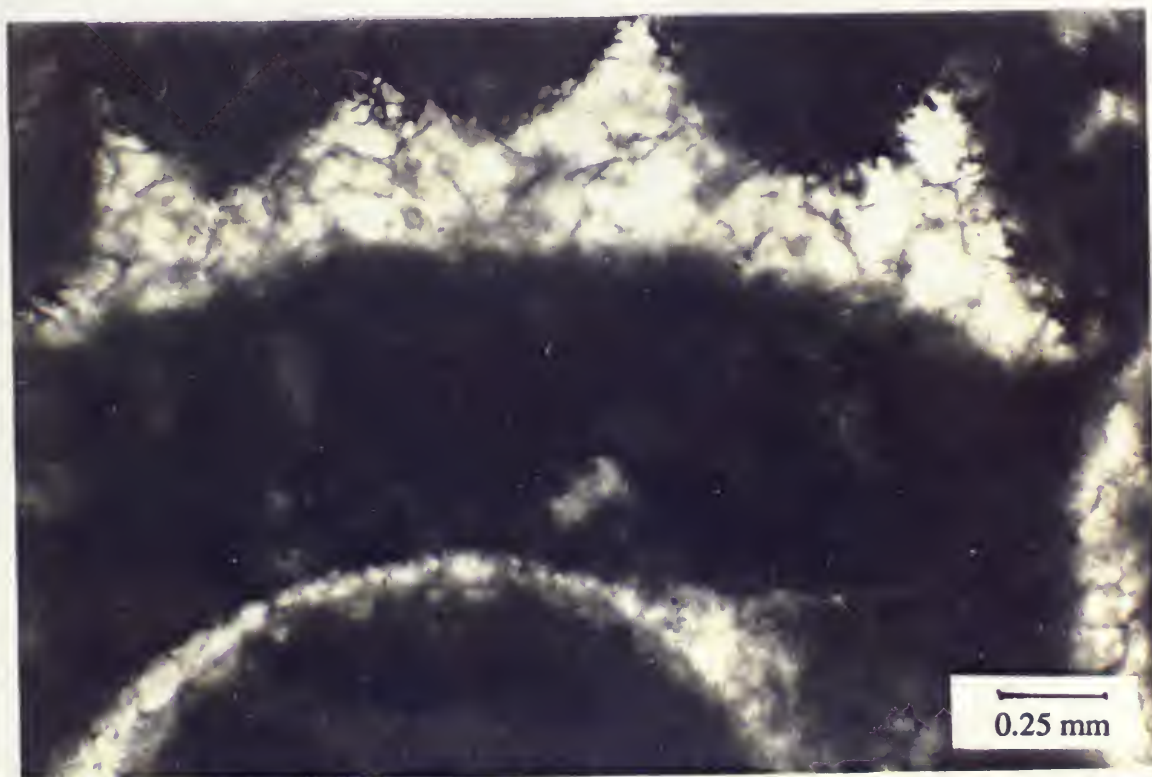
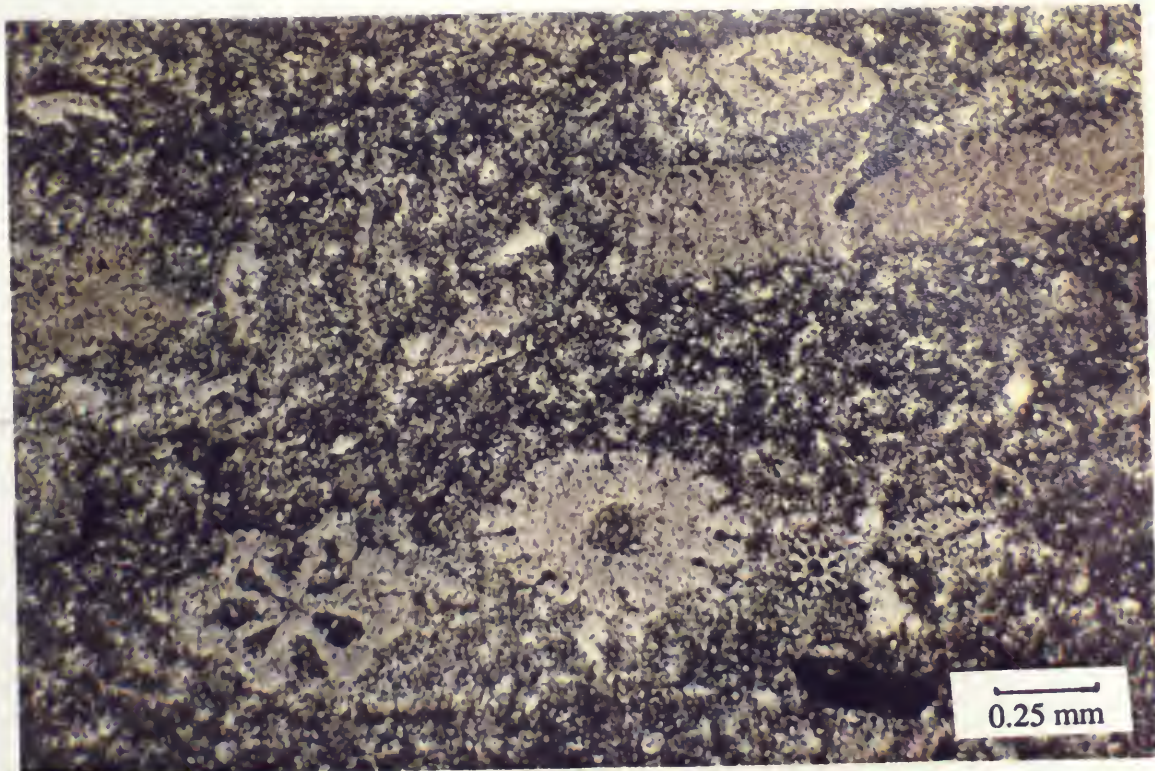


PLATE C

Figure

Thin-section photomicrograph under plane light showing coralline red-algae fragment showing the fine cellular structures. The red-algae fragments are altered from high-Mg to low-Mg calcite during diagenesis with good preservation of the cellular structure. The dark spots on the surface of the fragment are microborings that were probably the product of endolithic algae during the process of micritization(MF4) at a depth of 1575m in well Y3-59.

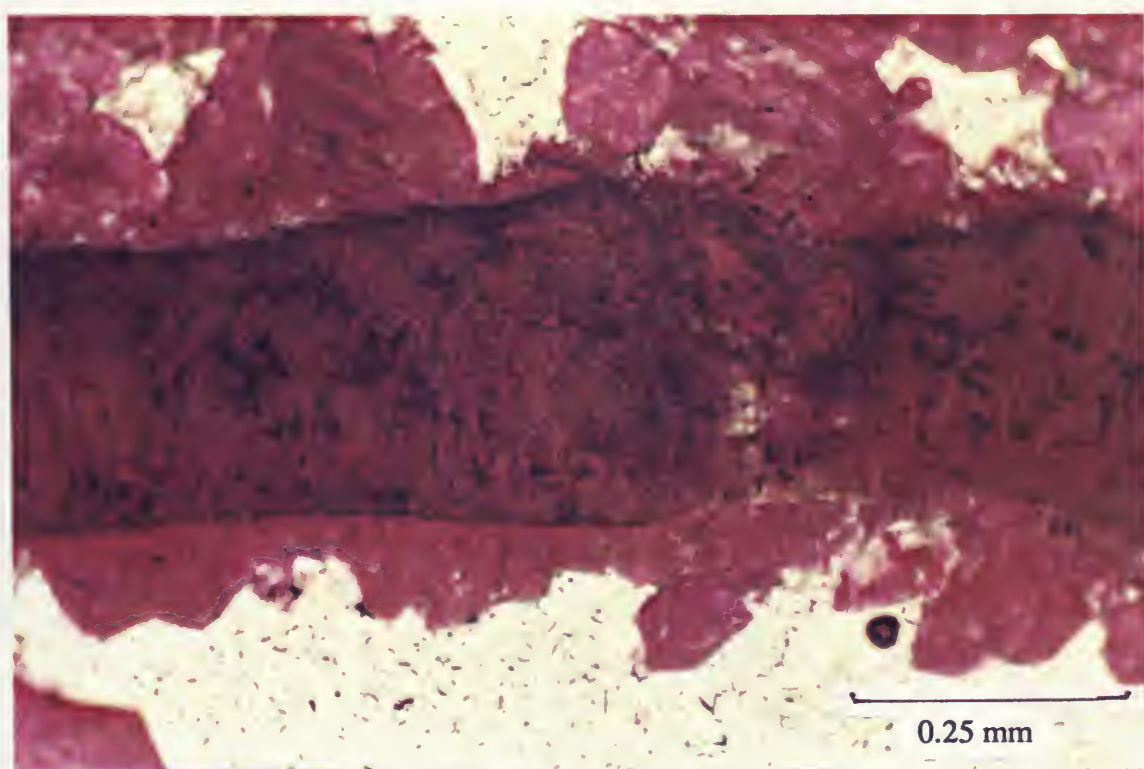


PLATE C

figures

Thin-section photomicrograph under plane light from the skeletal mudstone (MF3) at a depth of 1563.5m in well Y3-59. Replacement of limestone matrix by microcrystalline dolomite with partial solution leaching of grains and micrite matrix. Intense, bedding-parallel compaction resulted in flattening and crushing of thin-walled ostracode shells.

Thin-section photomicrograph under polarized light showing replacement of micrite matrix by anhydrite(TMFC1) at a depth of 1538m in well Y3-59.

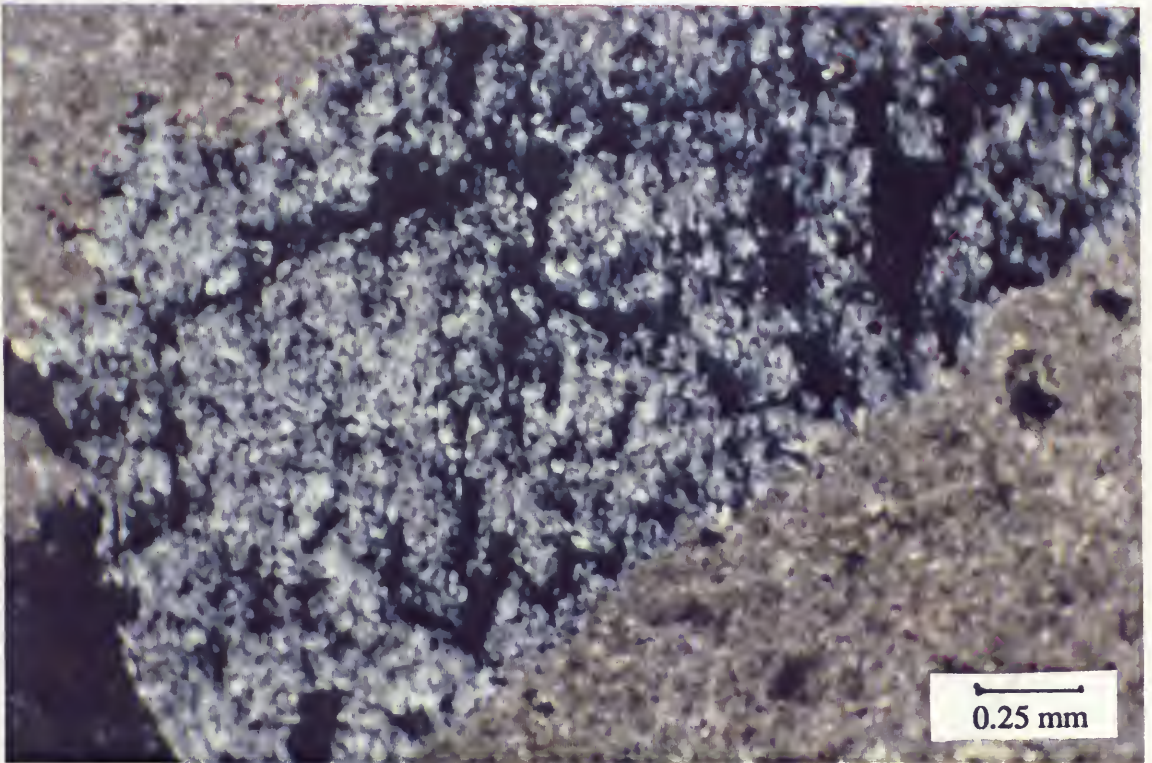
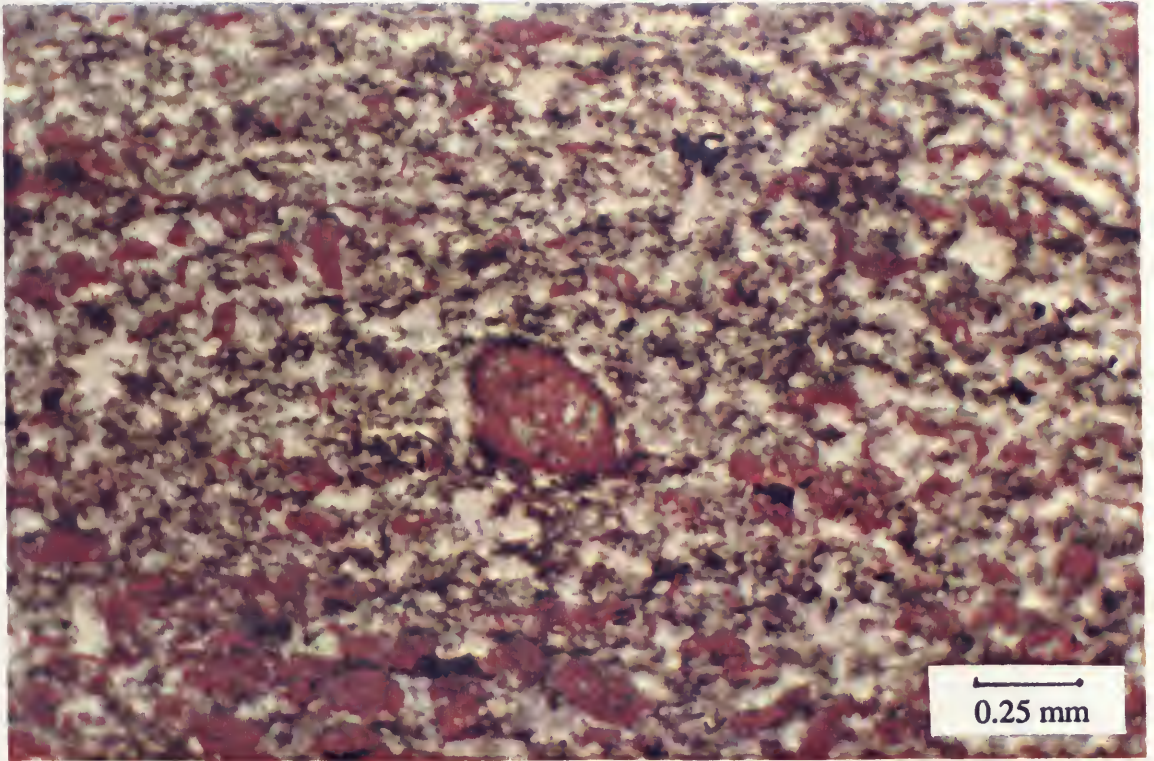


PLATE C

figures

Thin-section photomicrograph under polarized light replacement of a skeletal fragment by anhydrite(TMFC1) at a depth of 1565m in well Y3-59.

Molds of euhedral dolomite crystals that were dedolomitized and subsequently leached out(TMFC1) at a depth of 1466m in well 6A1-59.
Scanning Electron Microscopy photomicrograph(2000X).

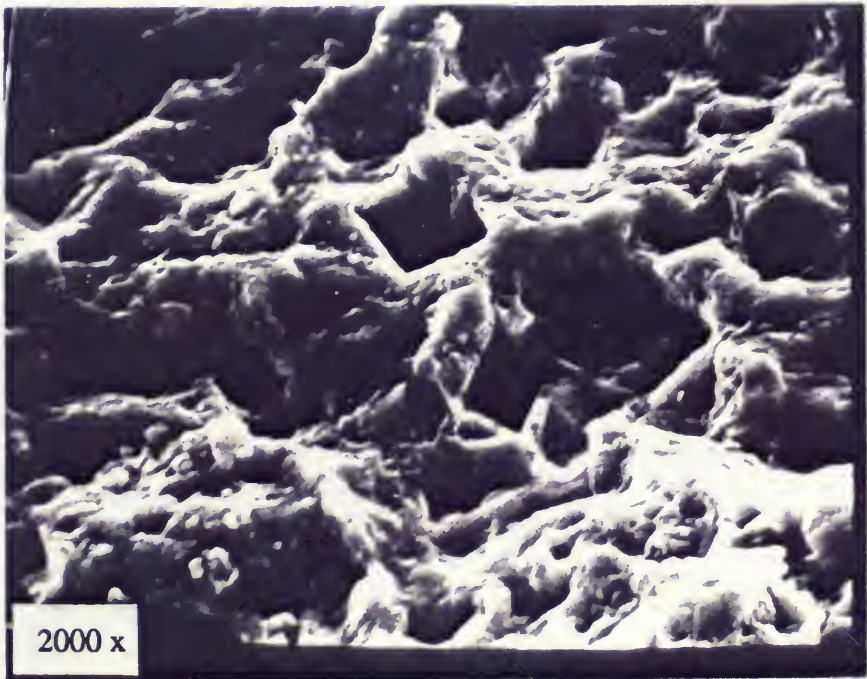
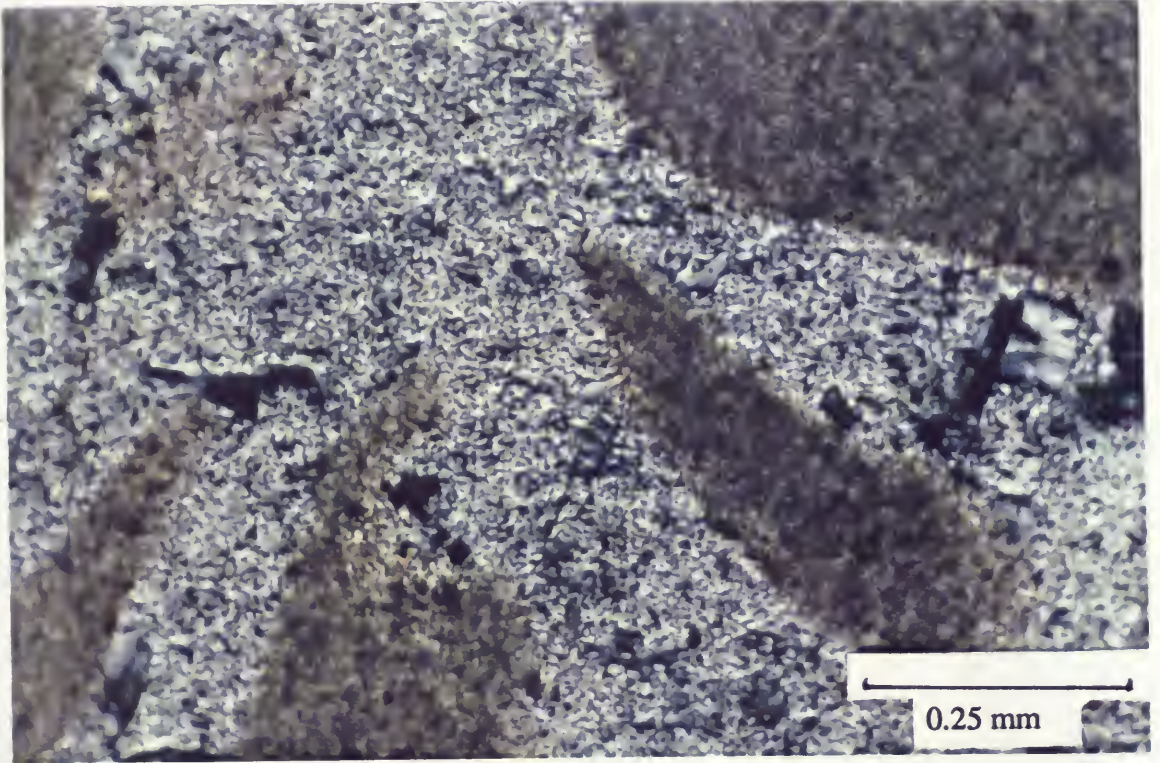


PLATE C

figure

Thin-section photomicrograph under plane light showing cavity filling of gastropod shell by the sediment during deposition and the void space was later infilled by sparry calcite cement. Also note the partial replacement of calcite cement and matrix by microcrystalline dolomite(MF4) at a depth of 1570m in well Y3-59.

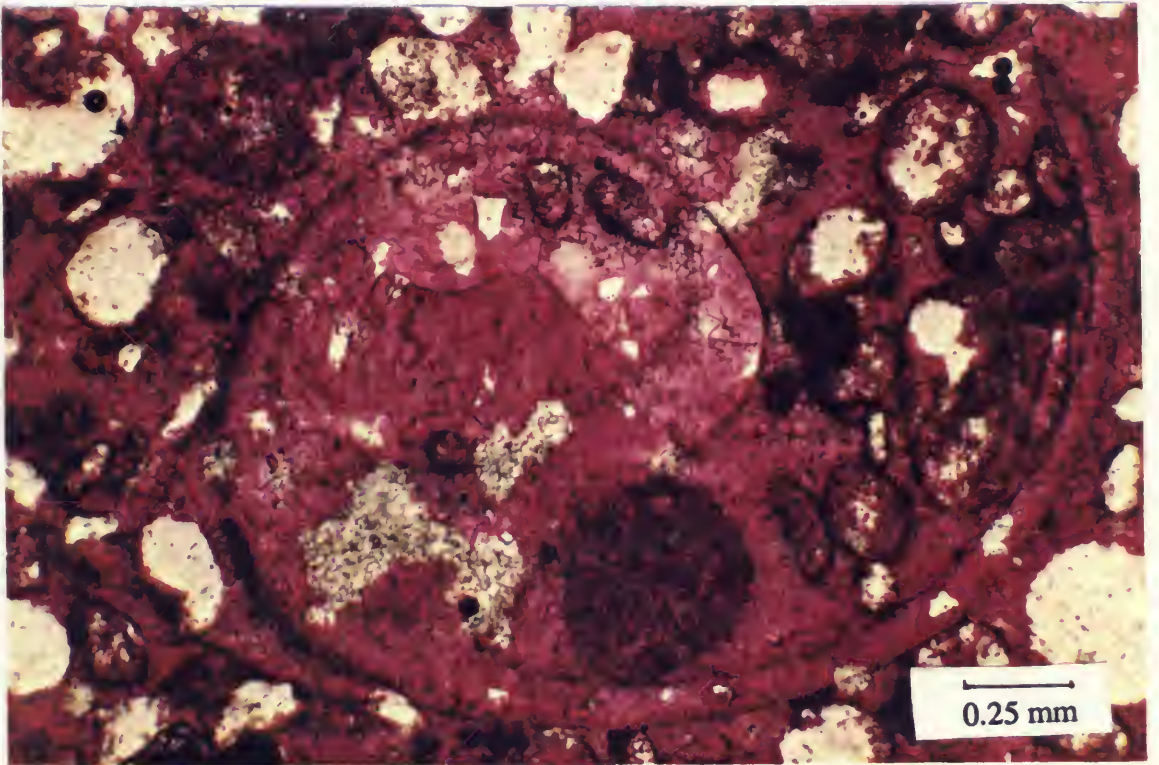


PLATE C

Figures

Thin-section photomicrograph under plane light showing drusy calcite cement(MF3) at a depth of 1555m in well Y3-59. An ostracod shell showing coarse sparry calcite cavity filling. Fine-grained cement fringe on the internal edges of the shell is followed by coarse calcite spar. Note dissolution along the stylolite surface next to the ostracod shell.

Thin-section photomicrograph under plane light showing broken micrite envelopes of bivalves are considered as an evidence for compaction and deformation of the sediment prior to cementation(MF4) at a depth of 1571.2m in well Y3-59. Note sparry cement fringe around the edges of bivalve fragments and blocky cement in cavities. Almost all the skeletal grains were completely micritized and partially dissolved. The skeletal grains consist of miliolids, pelecypods, dasycladacean algae and pelloids.

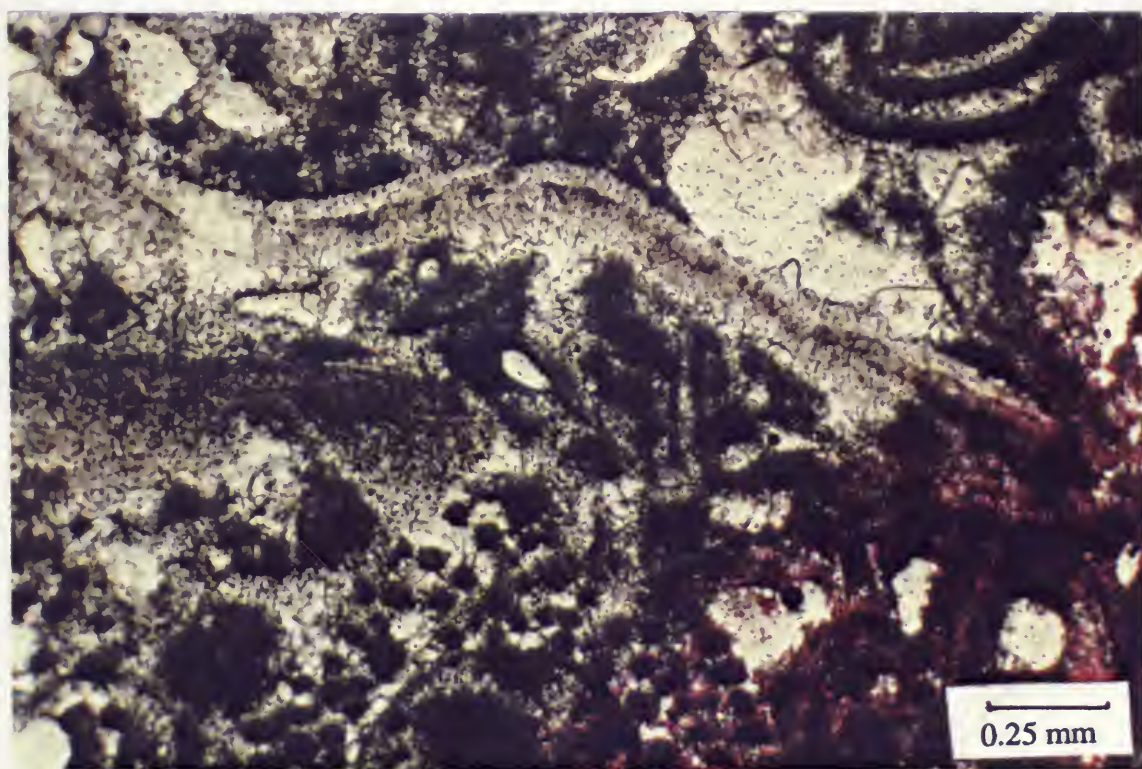
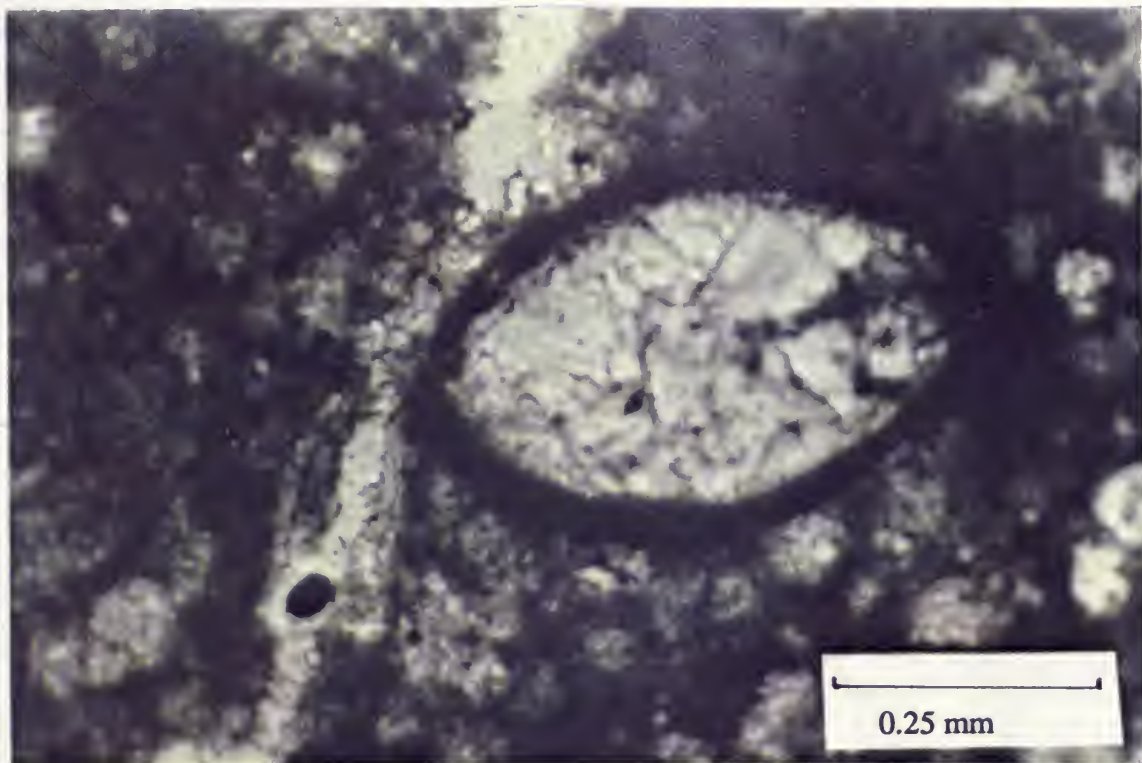


PLATE C

figures

Thin-section photomicrograph under plane light showing solution leaching of stylolite zone and precipitation of late diagenetic sparry calcite cement (MF5) at a depth of 1586.4m in well Y3-59. Partial loss of volume of a carbonate pelloid as indicated by the truncation of the upper right edge. Stylolites are associated with compaction and provide late diagenetic calcite cement in limestones (Wanless, 1979). Note the agglutinated foraminifera in the lower right corner of the photomicrograph.

0a

Thin-section photomicrograph under plane light showing large dolomite rhomb associated with a fracture in MF5 at a depth of 1587m in well Y3-59. The fracture provided porosity for Mg-rich fluids to infiltrate the sediment and precipitate dolomite cement.

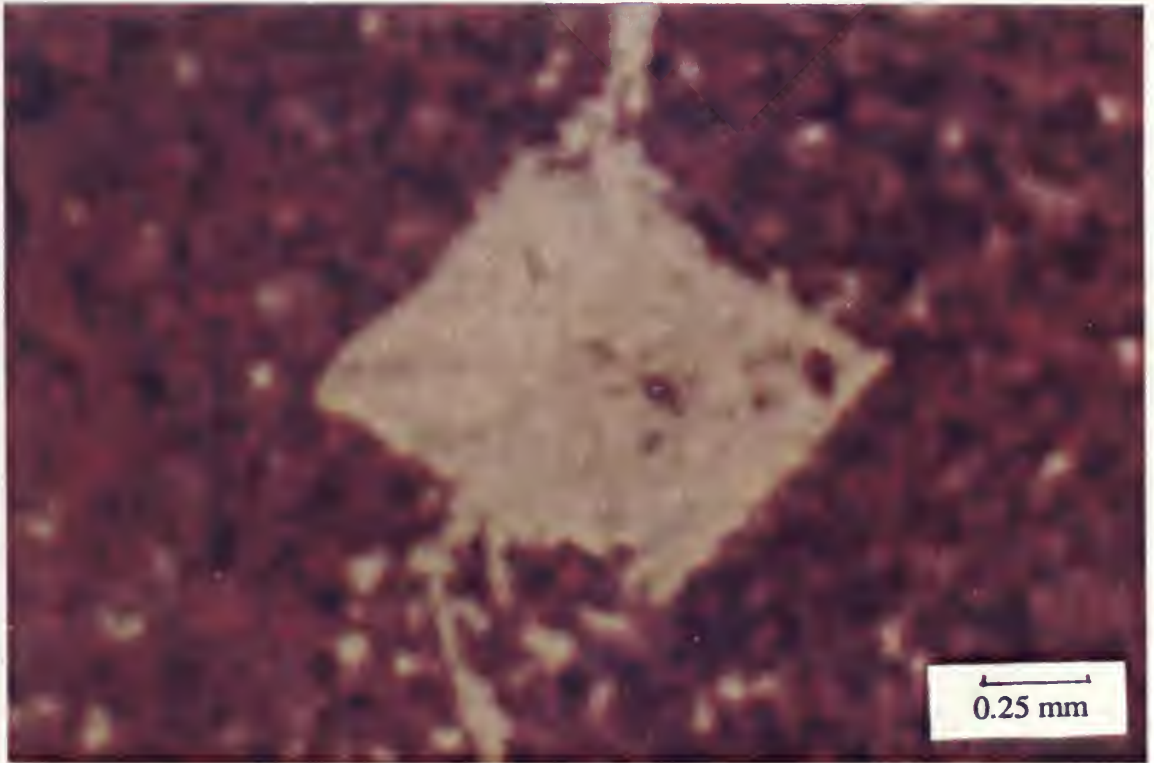
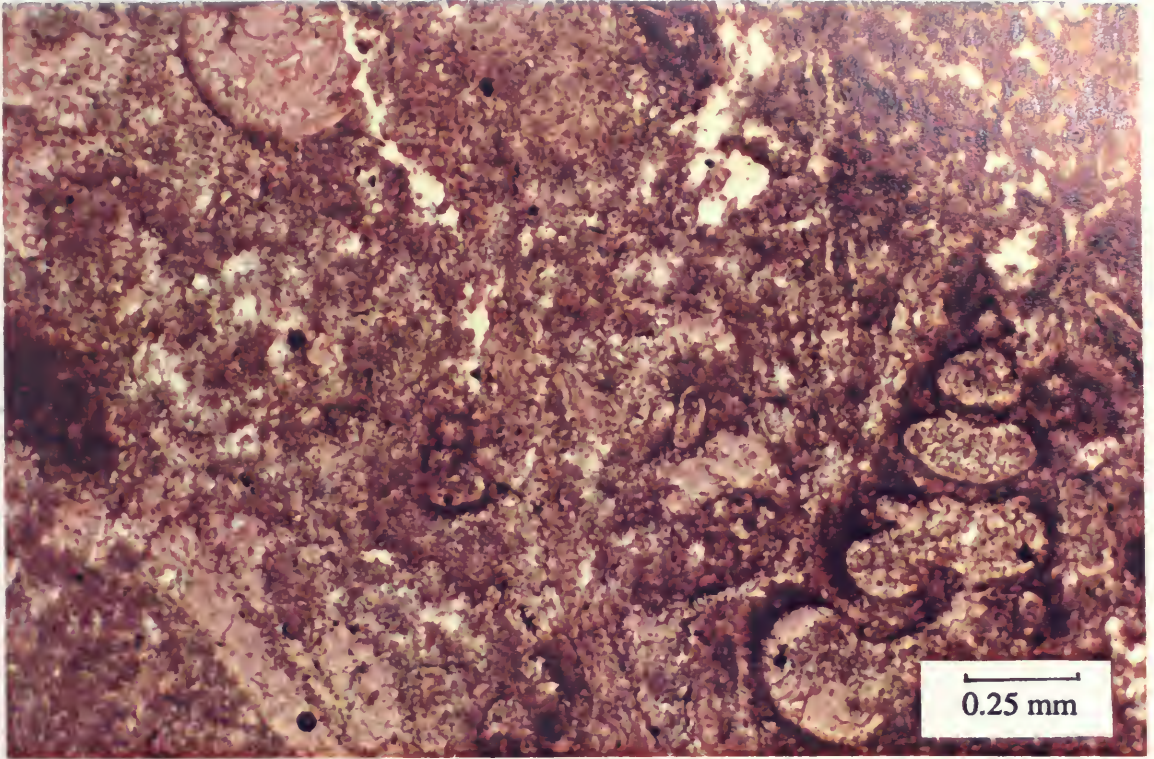


PLATE C

Figures

0b

Thin-section photomicrograph under polarized light showing early replacement and cement crystals of dolomite in a micrite matrix(TMFC1) at a depth of 1472.5m in well 6A1-59. The dolomite crystals represent an early replacement of the micrite matrix and infilling of ostracode shells prior to lithification. The sediment was soft or partially lithified, as evidenced by the microfractures and displacement of crystal edges. Notice the edges of the dolomite crystal in the upper right corner of the photomicrograph. Finally, pyrite cement precipitated within the dolomite crystals and skeletal grains.

1

Thin-section photomicrograph under polarized light showing leached fossils in a limestone from TMFC1 at a depth of 1470.3m in well 6A1-59. The chemically unstable grains were dissolved and some molds were subsequently cemented by anhydrite. Finally, partial leaching of anhydrite cement due to late diagenetic solution leaching process. Note the anhydrite cement along solution enlargement of a stylolite at the bottom of the photomicrograph.

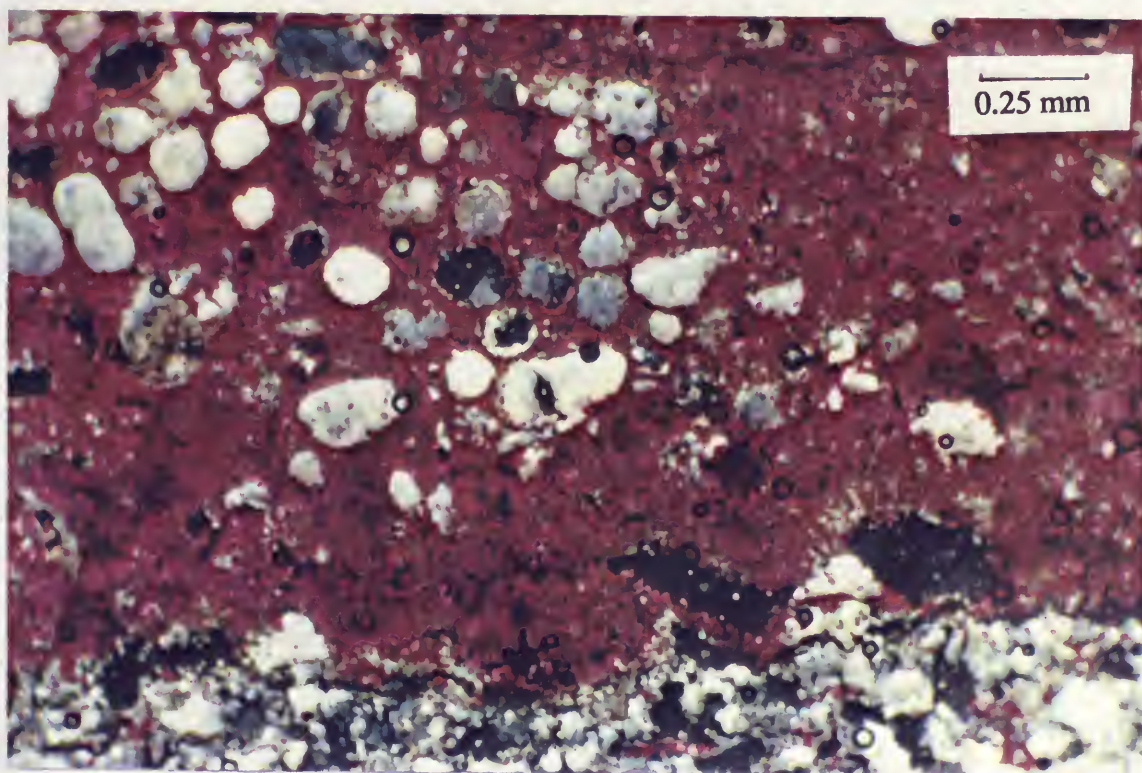
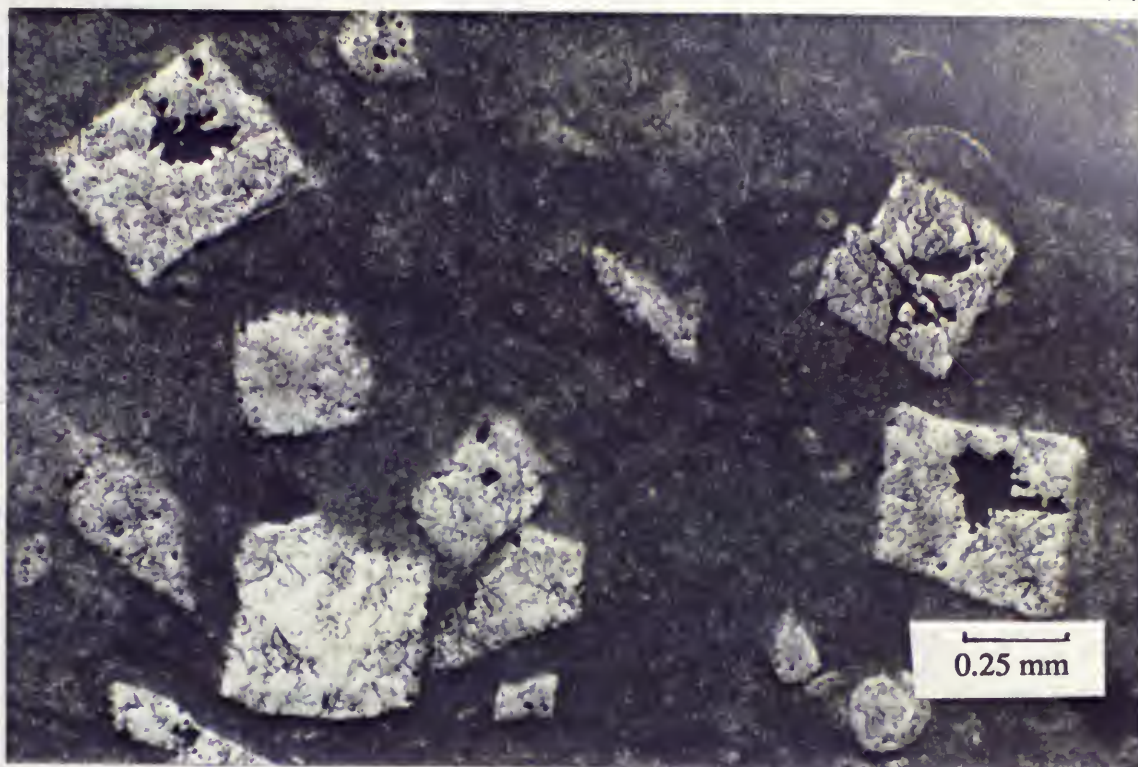


PLATE C

Figure

2

Core slab photomicrograph showing pseudomorphs of discoidal gypsum produced by solution leaching of discoidal gypsum(TMFC1) at a depth of 1473.2m in well 6A1-59.



PLATE C

Figures

3

Thin-section photomicrograph under plane light showing solution leaching and enlargement of molds and fractures(MF5) at a depth of 1585.8m in well Y3-59. Almost all the allochems "fecal pellets" were dissolved except for the recrystallized miliolid in the upper right corner of the photomicrograph.

4a

Thin-section photomicrograph under plane light showing broken and micritized algal plates are an indication of compaction and deformation of the Beda Formation limestone prior to lithification and cementation(MF5) at a depth of 1586.1m in well Y3-59.

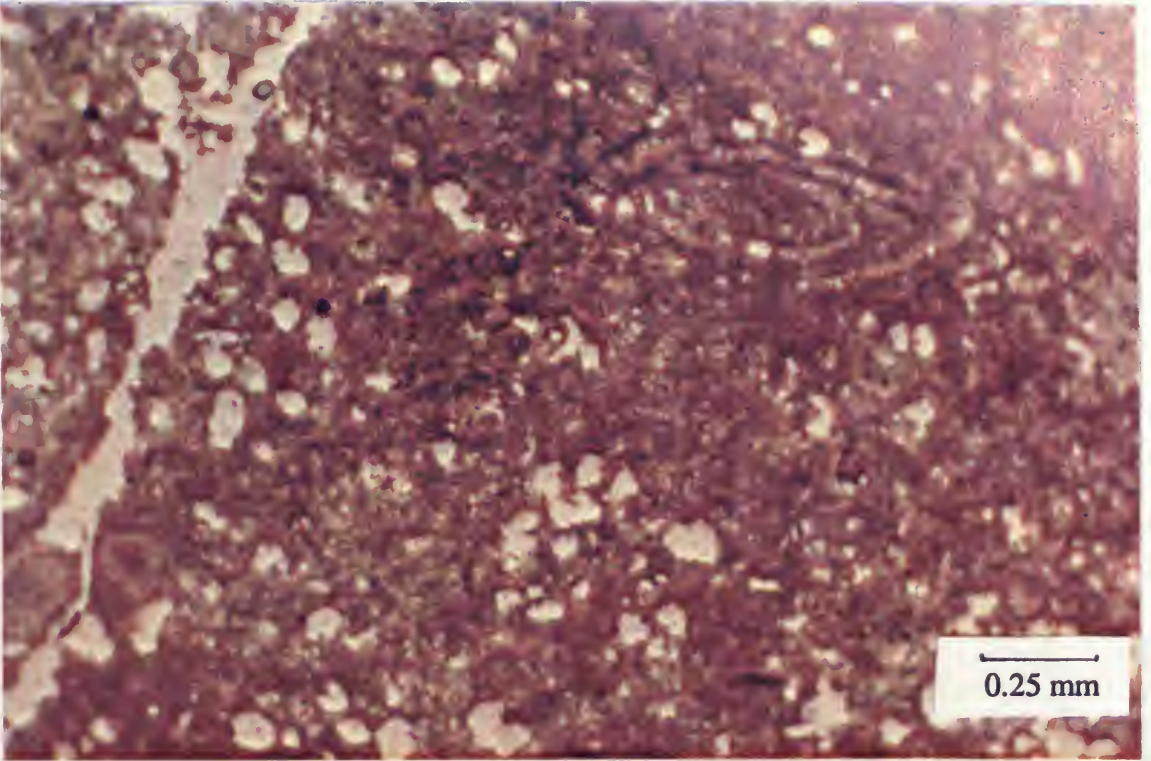


PLATE C

Figures

4b

Thin-section photomicrograph under plane light showing deformed miliolid foraminifera and broken, dislocated molluscan shell fragments. Note how the chamber walls of the miliolid were micritized, deformed, broken and subsequently cemented by a late sparry calcite cement relative to compaction and deformation (MF5) at a depth of 1586.5m in well Y3-59.

5a

Thin-section photomicrograph under plane light showing microstylolite swarms between limestone nodules "light purple" and calcareous shale "dark brown" (MF5) at a depth of 1587m in well Y3-59.

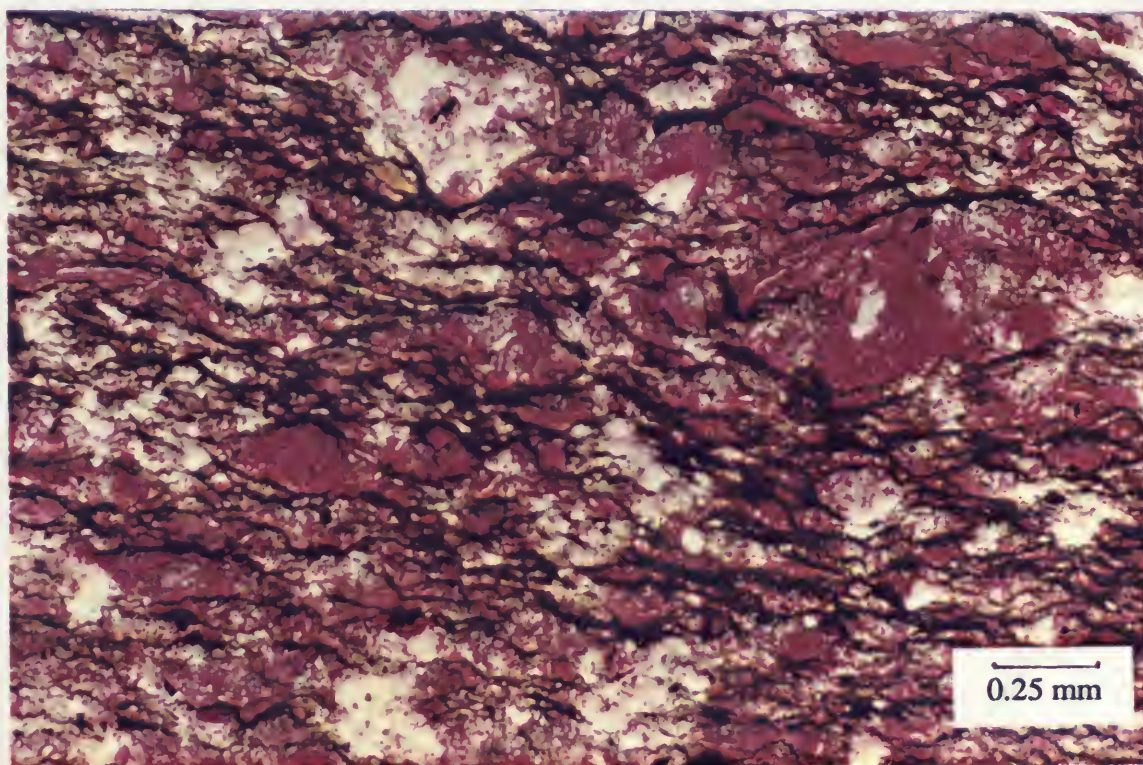
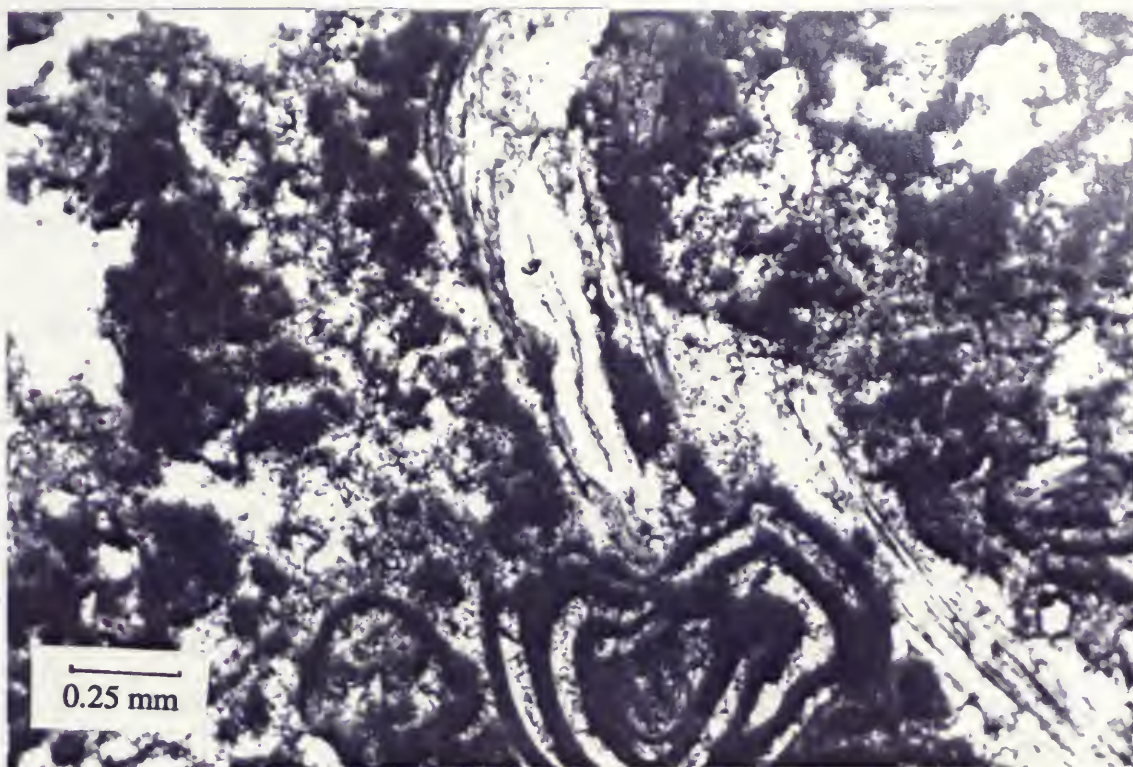


PLATE C

Figures

5b

Core slab showing swarms of microstylolites and non-sutured wispy seams in ostracoda-foraminifera wackestone (MF5) at a depth of 1587.9m in well Y3-59, with lenticular burrow fillings of packstone. Note the intense bioturbation of this rock due to burrowing.

5c

Thin-section photomicrograph under plane light showing stylolite cutting through the micrite matrix of MF3 at a depth of 1564.5m in well Y3-59. Dark brown areas along stylolites are insoluble residue. The rock was compacted as indicated by pressure solution and subsequently fractured. The vertical fracture was cemented by sparry calcite cement.

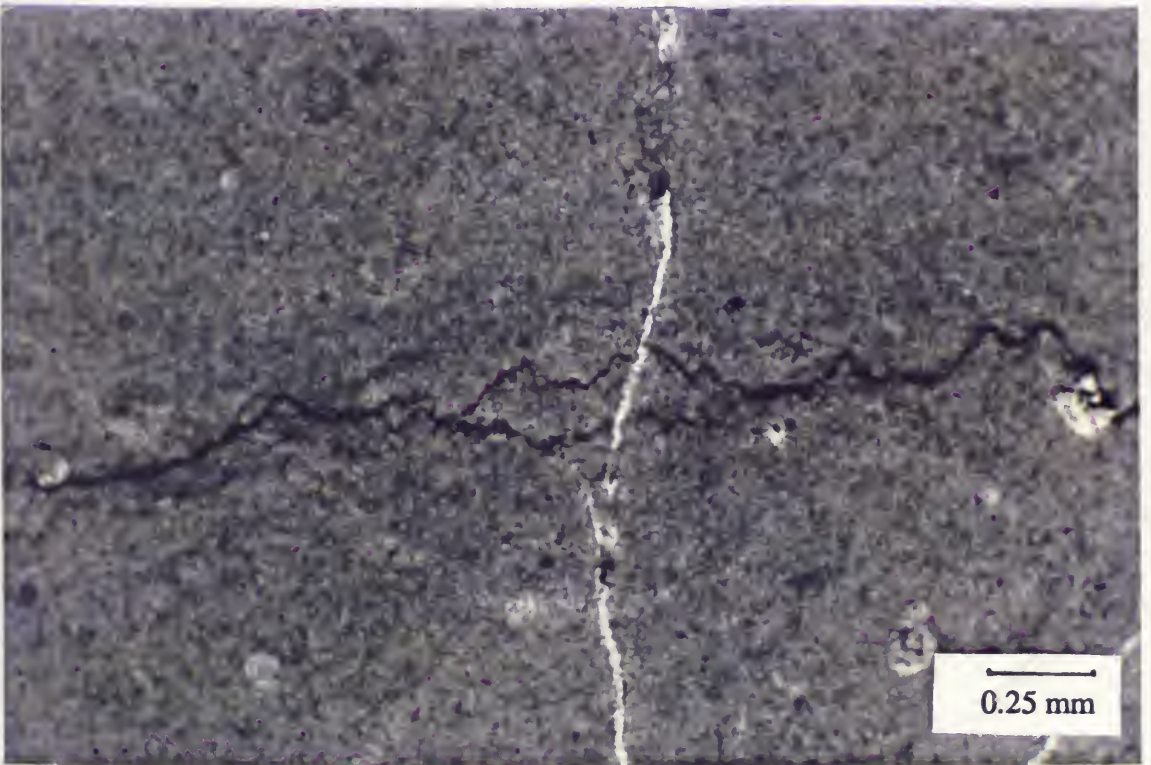


PLATE C

Figures

6a

Thin-section photomicrograph under plane light showing leached grains with micrite envelopes from the dasyclad-foraminiferal packstone (MF4) at a depth of 1570m in well Y3-59. The dasycladacean algae and benthonic foraminifera grains show no internal structures and were survived by dark micritic rims. The grains were completely micritized possibly by endolithic algae and subsequently dissolved and finally cemented by sparry calcite cement.

6b

Thin-section photomicrograph under plane light showing completely dissolved grains and micrite envelopes. Note the deformation of the grain boundaries at the grain contact due to early compaction of the sediment (MF4) at a depth of 1570.5m in well Y3-59.

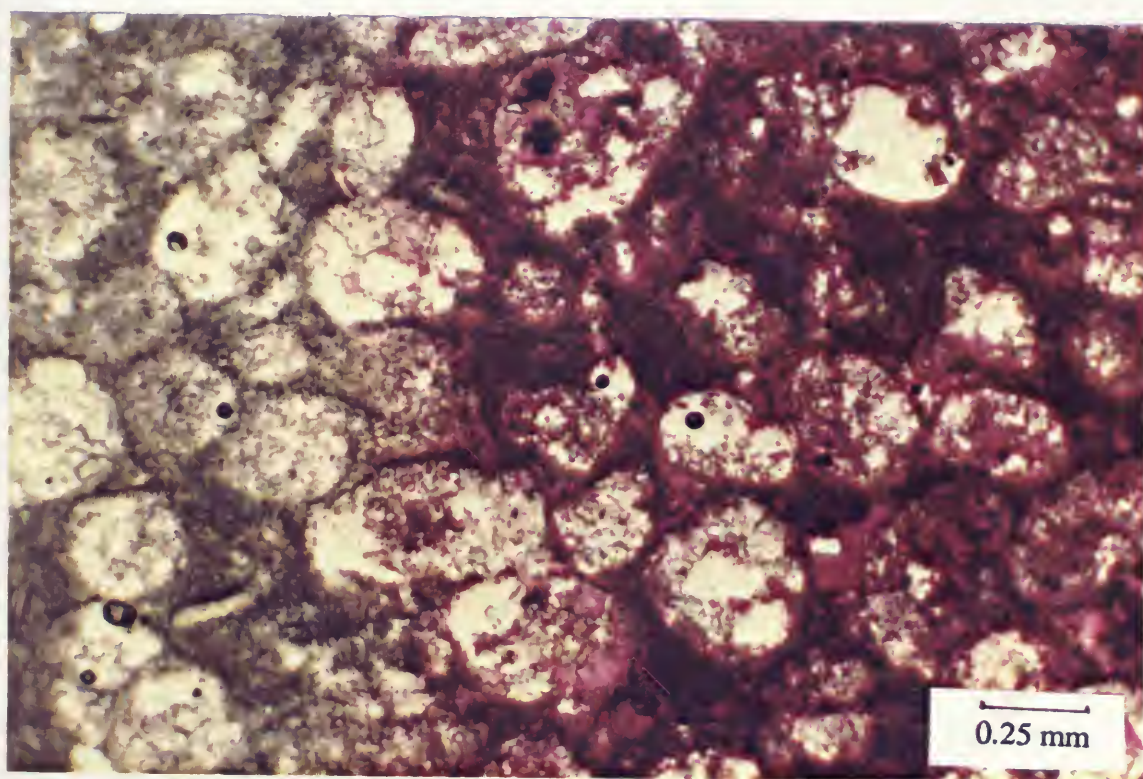
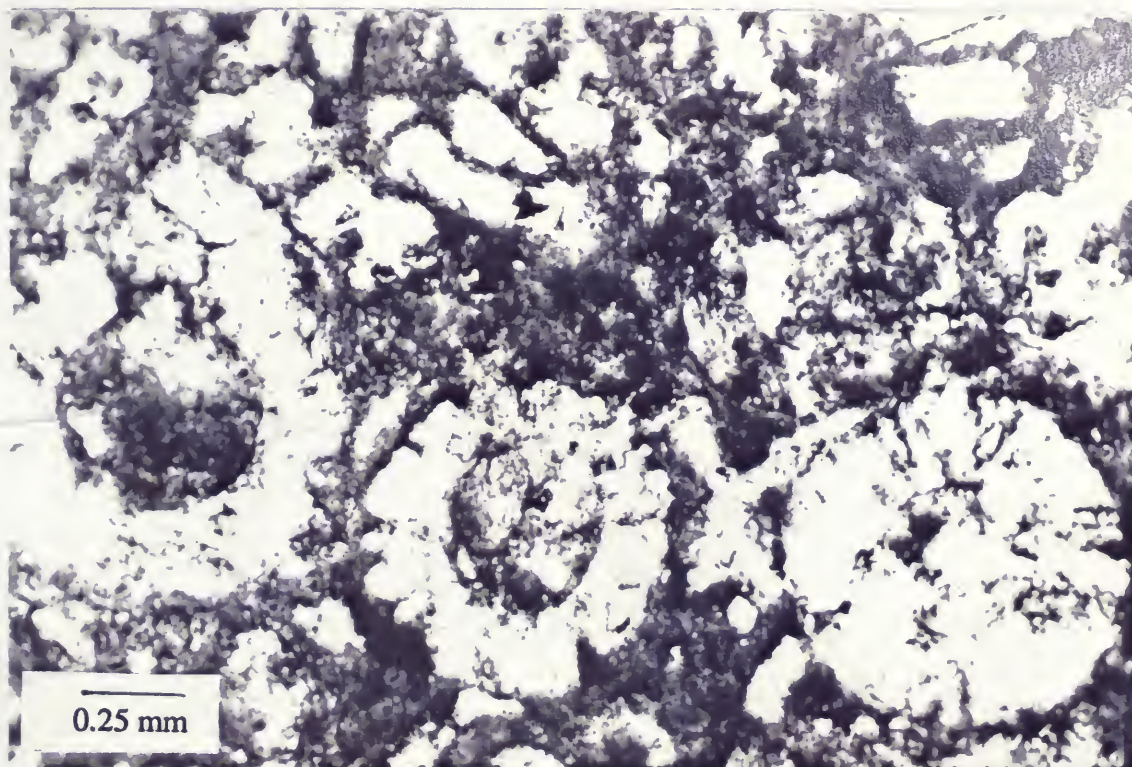


PLATE C

Figures

7a Core slab showing a vertical burrow in the ostracoda-foraminiferal wackestone (MF5) at a depth of 1555.4m in well Y3-59. The burrow was filled with packstone.

7b Core slab showing horizontal burrows from MF5 at a depth of 1555.6m in well Y3-59. Complete homogenization of the sediment was due to bioturbation resulting in the destruction of the primary structures.



PLATE C

Figures

7c

Thin-section photomicrograph under plane light showing mottled skeletal mudstone (MF3) at a depth of 1569m in well Y3-59. Mottling was the result of extensive burrowing of the sediment.

7d

Core slab showing burrowed wackestone (MF5) at a depth of 1556m in well Y3-59. The burrower was a probably pelecypod, as indicated by the pelecypod shell left at "the scene of the crime".

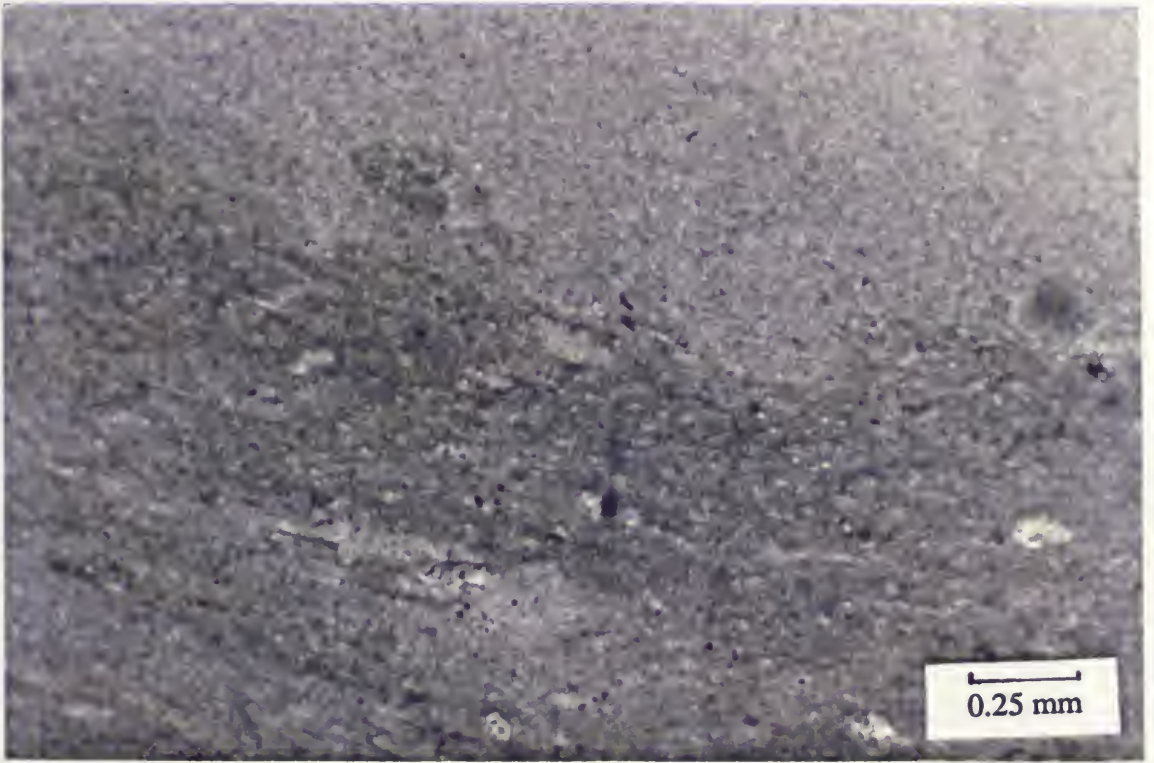


PLATE C

Figures

8a

Thin-section photomicrograph under plane light of foraminiferal dolomitic packstone (MF2) at a depth of 1470m in well 6A1-59 with fecal pellets of unknown origin, but probably fecal. The intergranular space is filled by sparry calcite and dolomite cements. Note the different sizes of fecal pellets and micrite envelopes of a miliolid at the upper left corner.

8b

Thin-section photomicrograph under plane light of MF5 at a depth of 1587.9m in well Y3-59 showing the abundance of fecal pellets throughout the micrite matrix. Note the deformation and solution leaching of several fecal pellets and the miliolid. Sparry calcite cement fills the molds of the dissolved grains and the intraskeletal porosity of the miliolid.

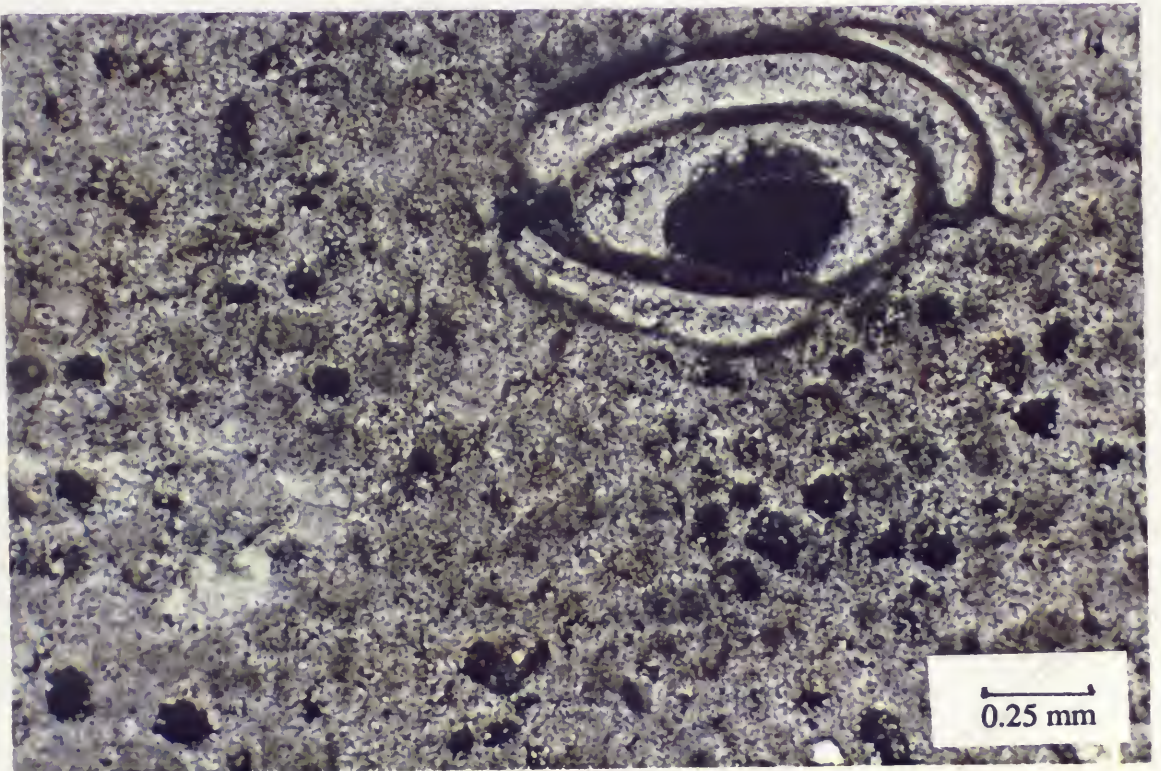
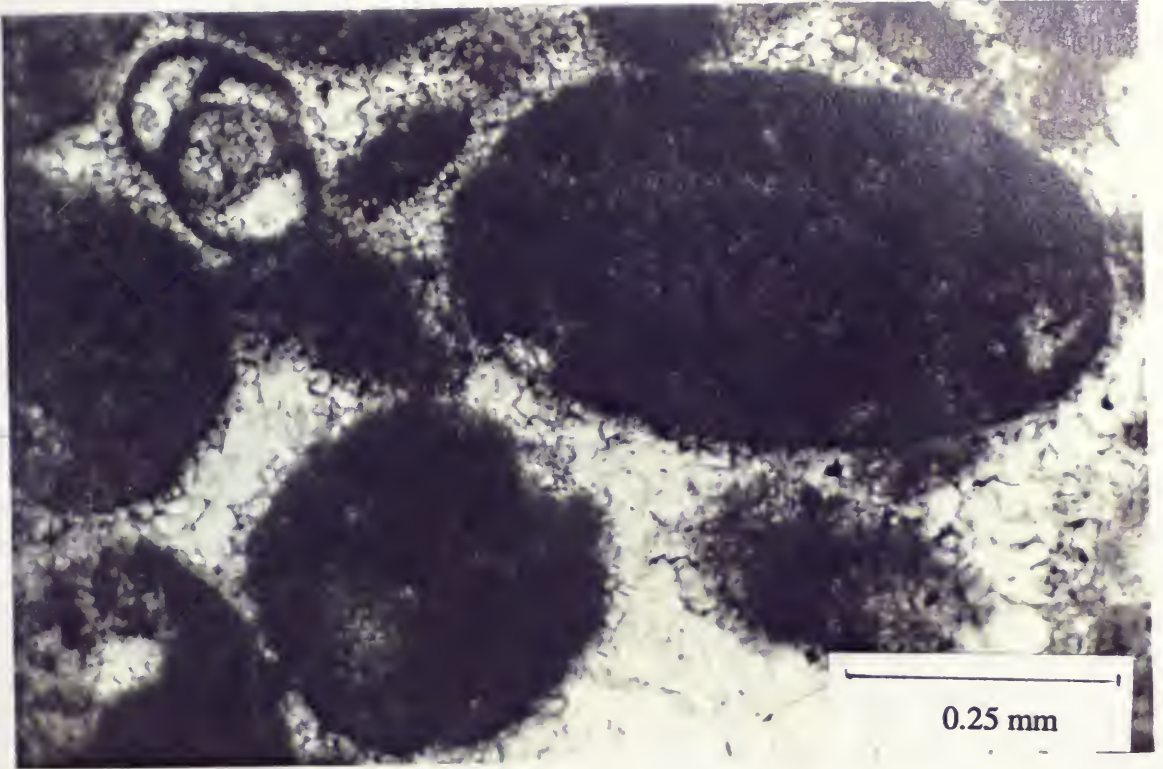


PLATE C

Figure

9

Core slab from the Terminal microfacies complex(TMFC1) at a depth of 1466.2m in well 6A1-59 showing vertical fractures. The fractures were completely cemented by a late diagenetic anhydrite.



PLATE C

Figures

20a

Thin-section photomicrograph under plane light from TMFC1 at a depth of 1537.9m in well Y3-59 showing fenestral porosity. The pores are aligned parallel to an algal mats which were completely dissolved. The pores may be due to the decay of organic matter, air bubbles and escaping gases.

20b

Core slab from the foraminiferal dolomitic packstone (MF2) at a depth of 1466.7m in well 6A1-59, showing the bird's-eye or fenestral fabric of planar nature.

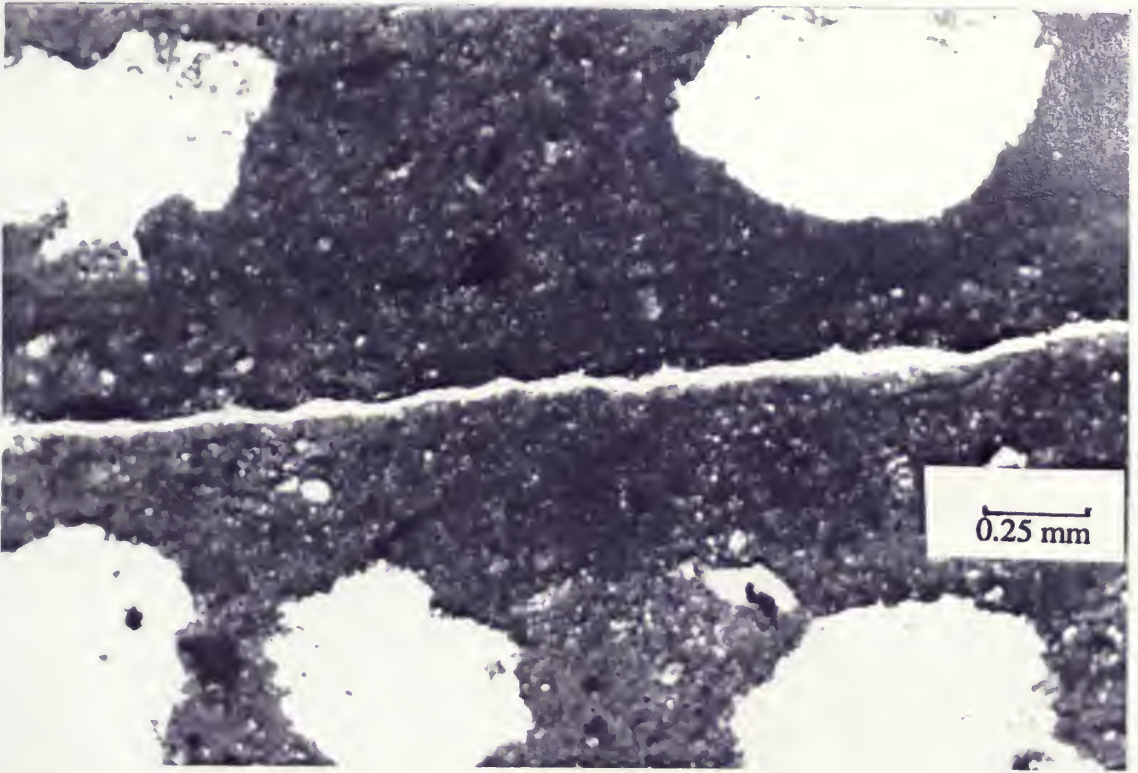


PLATE C

Figure

21

Thin-section photomicrograph under plane light of the ostracoda-foraminiferal wackestone (MF5) at a depth of 1587.2m in well Y3-59. Wackestone with benthonic foraminifera, ostracod, dasycladacean algae, molluscs, echinoderm fragments and fecal pellets. Notice the solution leaching of the lime-mud matrix and sparry calcite cement.

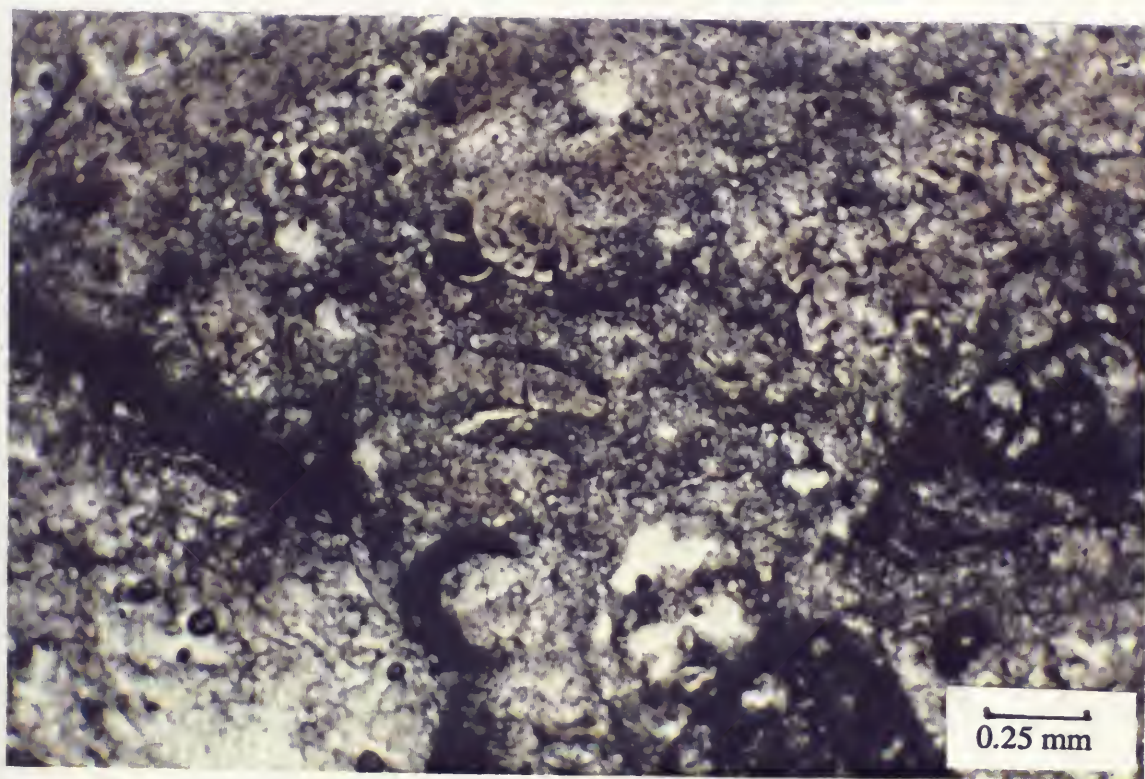


PLATE C

Figures

22

Core slab showing wavy laminations in ostracoda-foraminiferal wackestone (MF5) at a depth of 1587.5m in well Y3-59. These laminations were probably algal in origin or may be formed by compaction and differential cementation of argillaceous limestones.

23

Core slab showing horizontal laminations in MF5 at a depth of 1588m in well Y3-59. They are formed by seasonal storm tides within the tidal flat environment.

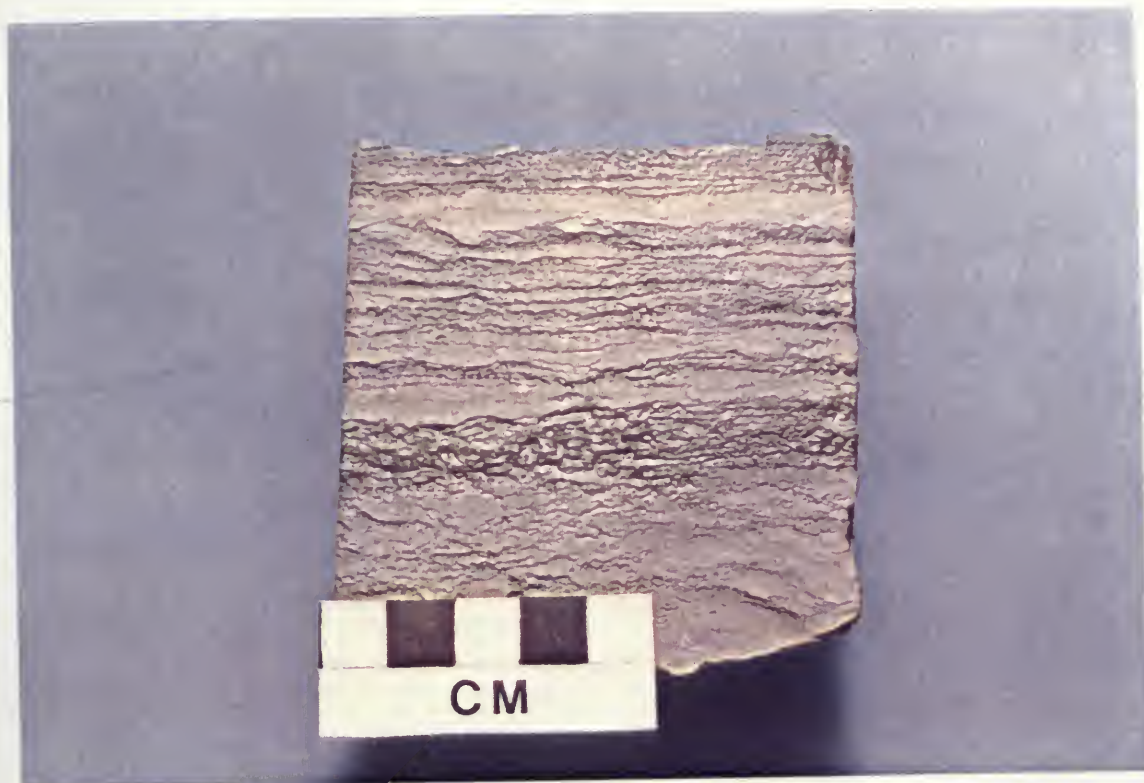


PLATE C

Figures

4a

Core slab from the dasyclad-foraminiferal packstone microfacies (MF4) at a depth of 1573m in well Y3-59 with abundant benthonic foraminifera, echinoderms, dasycladacean algae and fecal pellets. The allochems were later partially dissolved and in some cases filled by sparry calcite and anhydrite cement.

4b

Thin-section photomicrograph under plane light from the dasyclad-foraminiferal packstone microfacies (MF4) at a depth of 1573.5m in well Y3-59. This photomicrograph shows dasycladacean algae, miliolid foraminifera, echinoderms, fecal pellets and undifferentiated skeletal material. Notice the extensive dissolution of allochems, coarse sparry calcite cement and the recrystallization of the dasycladacean algae fragment near the upper right corner of the plate. Porosity includes intergranular, intragranular and solution leaching types. The grains were completely micritized and subsequently leached partially or completely as indicated by micrite envelopes.

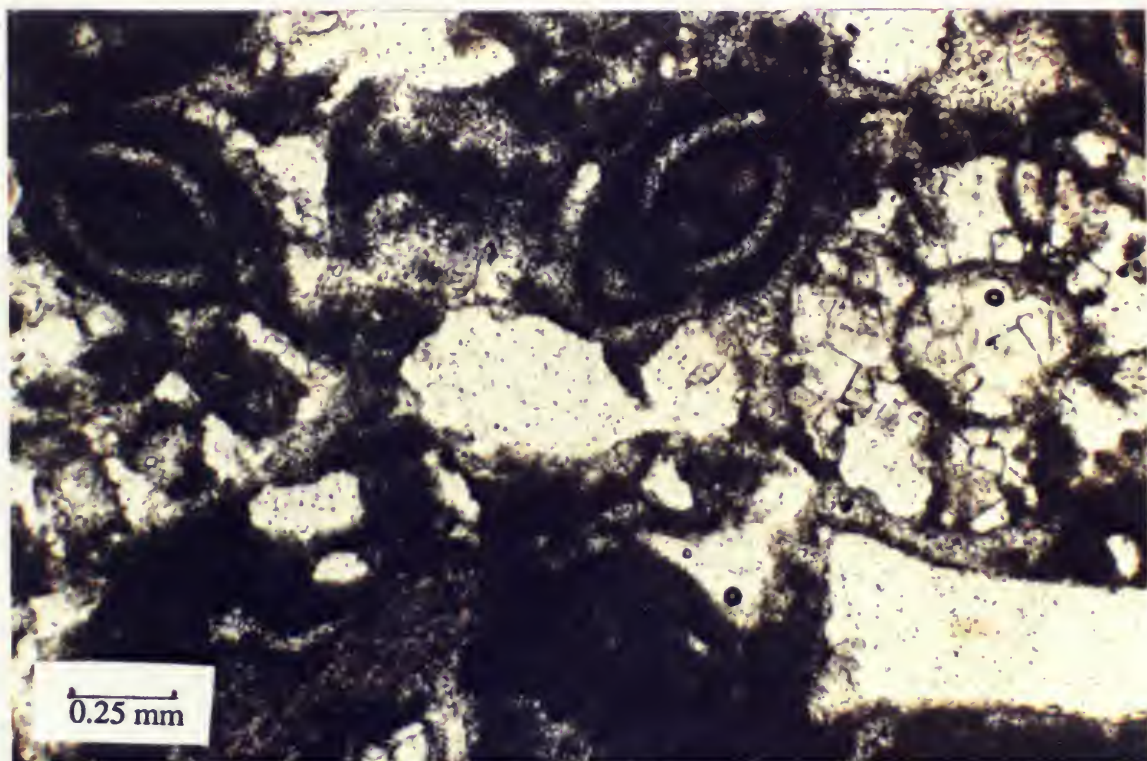


PLATE C

Figures

5 Core slab from the skeletal mudstone microfacies (MF3) at a depth of 1555.5m in well Y3-59 showing extensively burrowed and bioturbated micrite matrix. The matrix contains a high percentage of argillaceous material.

6a Core slab from the foraminiferal dolomitic packstone (MF2) at a depth of 1543.3m in well Y3-59. Notice the abundance of benthonic foraminifera, dasycladacean algae plates and solution porosity. The light brown colour indicates shallow oxidizing conditions. This sample is oil stained and extensively burrowed.



PLATE C

figures

6b

Thin-section photomicrograph under plane light of core samples in PLC26a, showing large miliolids, fecal pellets, pelloids, and algal plates of different sizes. Porosity is predominantly moldic, in addition to intergranular, vuggy and intragranular. The pore system is reduced by sparry calcite cement. The micrite matrix is partly dolomitized in the lower right corner of the plate(MF2).

6c

Scanning electron microscopy photomicrograph showing the partial dolomitization of the micrite matrix, the microcrystalline, intergranular and solution porosities(MF2) at a depth of 1472.7m in well 6A1-59. Magnification 1000X.

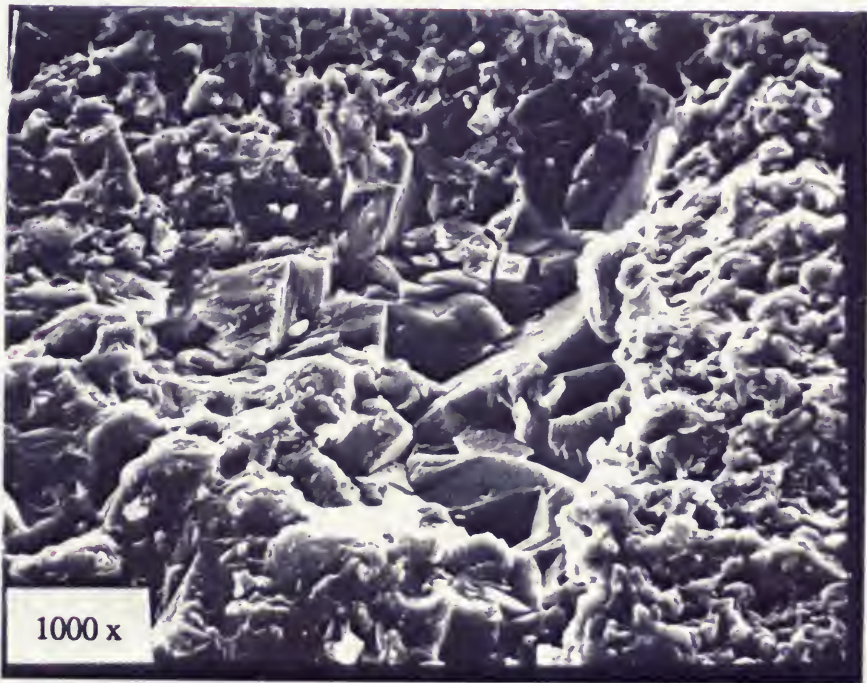
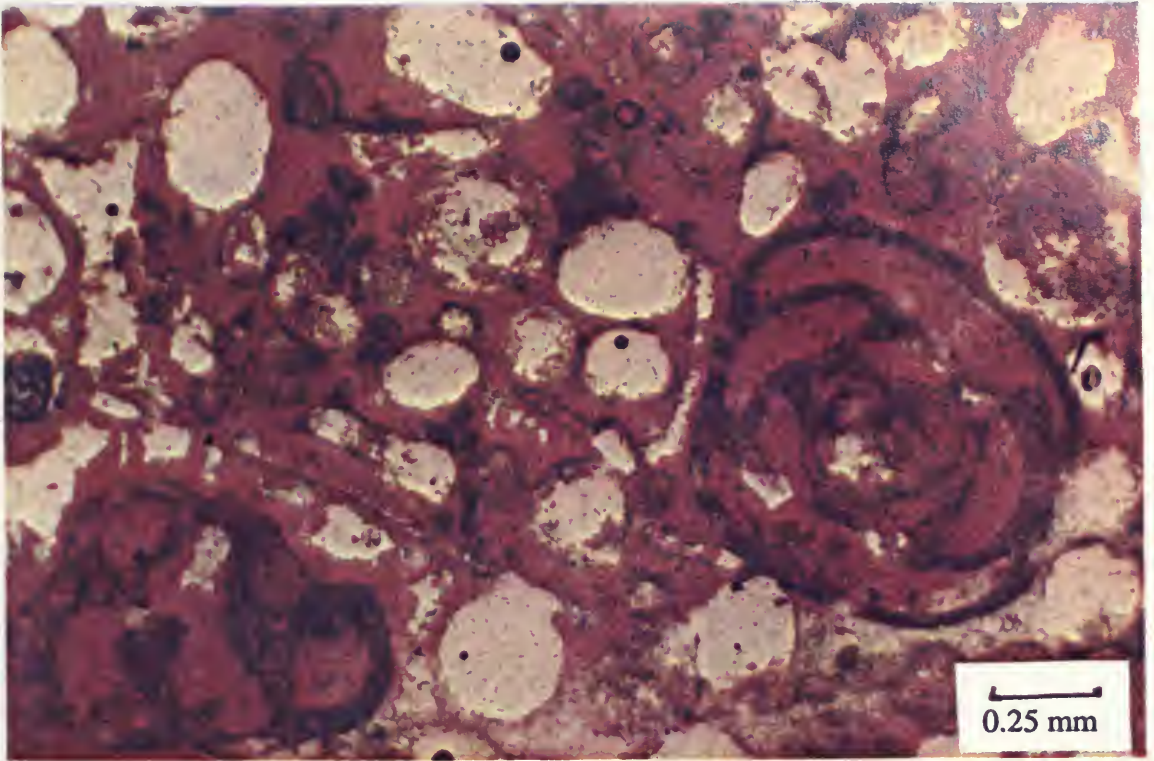


PLATE C

Figure

27

Core slab showing graded layer in MF2 at a depth of 1546.4m in well Y3-59. Note the coarse sediment texture dominated by pelecypod shells towards the bottom which became finer towards the top.

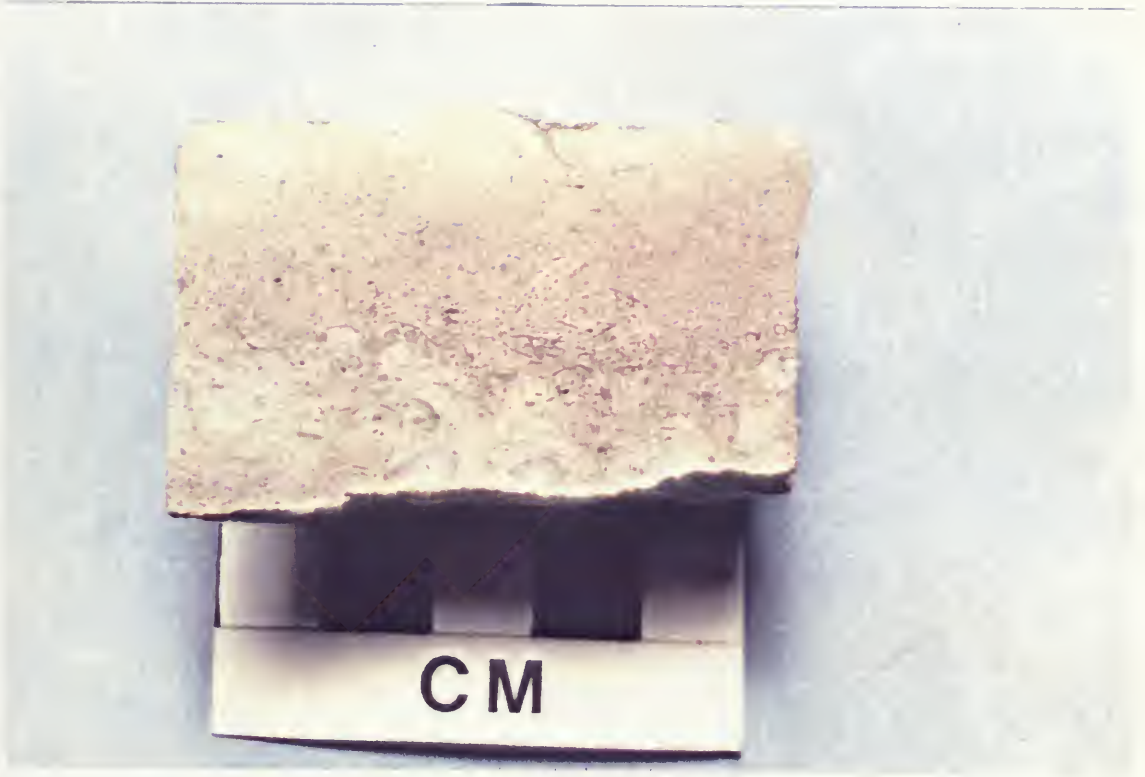


PLATE C

Figures

8

Core slab from the dolomitic mudstone-wackestone microfacies of the Terminal microfacies complex(TMFC1) at a depth of 1469m in well 6A1-59 showing the irregular algal laminae. The rock is partially dolomitized and completely stained with oil due to its microcrystalline porosity.

9

Thin-section photomicrograph under plane light of the above sample showing the microcrystalline dolomite. Note the dissolution pores due to leaching of skeletal grains subsequent to dolomitization of the micrite matrix(TMFC1).

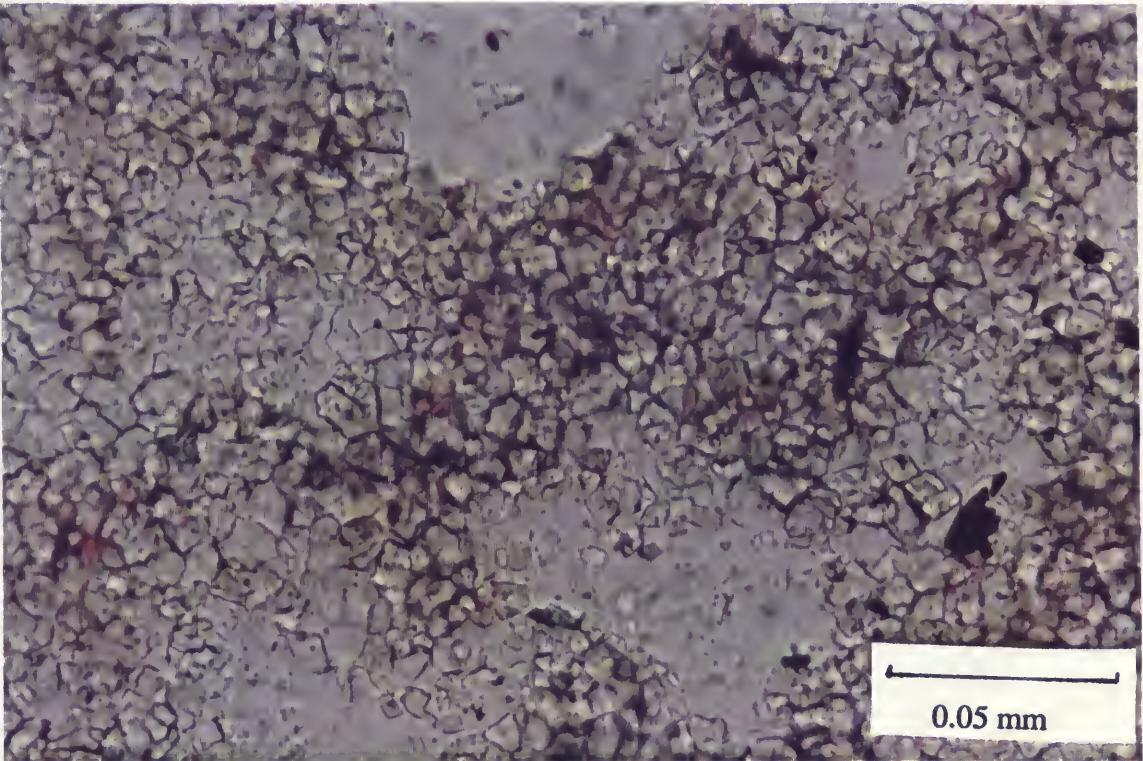


PLATE C

Figures

30

Scanning electron photomicrograph showing microcrystalline dolomite of the core slab in Plate C28. Notice the intercrystalline porosity and corroded surfaces of some dolomite rhombs. A high percentage of micrite matrix was dolomitized(TMFC1) at a depth of 1537.9m in well Y3-59. Magnification 2000X.

31

Core slab showing pseudomorphs of discoidal gypsum developed after dissolution of discoidal gypsum(TMFC1) at a depth of 1473.5m in well 6A1-59.

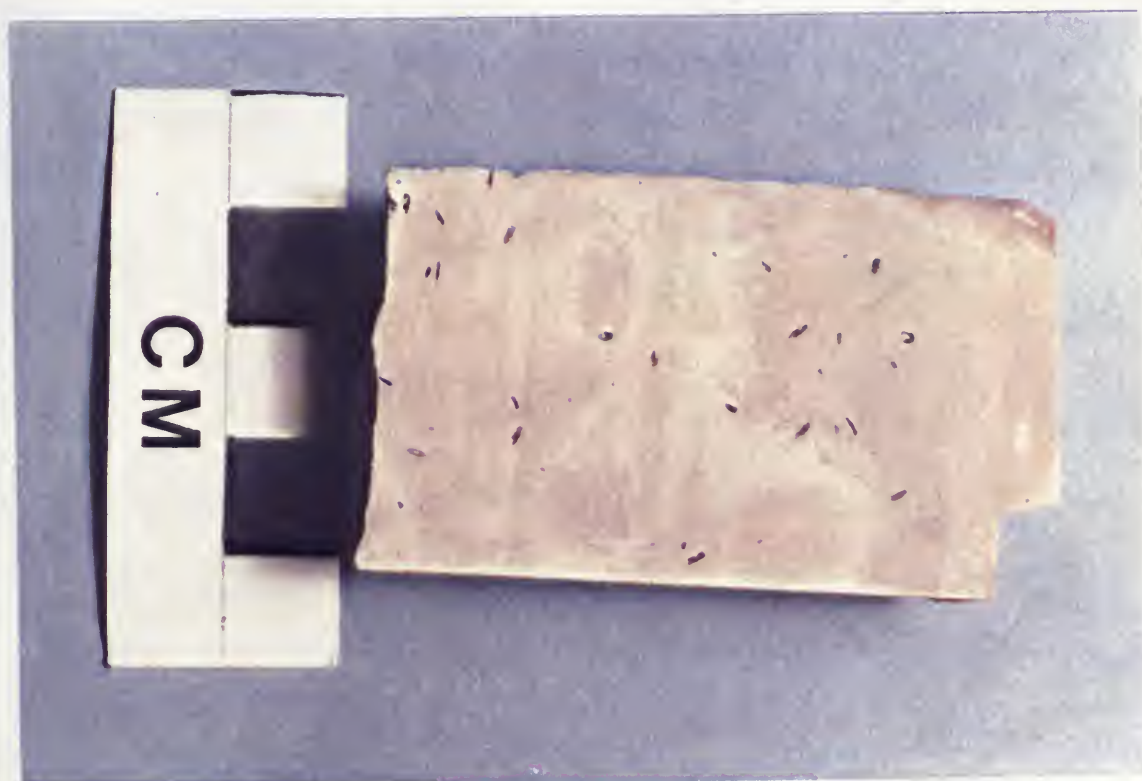


PLATE C

Figure

2

Core slab from the dolomitic mudstone-wackestone with mudcracks (TMFC1) at a depth of 1467.9m in well 6A1-59. The cracks were cemented by anhydrite. Notice the lamination and oil stains in this sample.



PLATE C

Figures

33a Core slab from the Terminal microfacies complex(TMFC1) at a depth of 1539.4m in well Y3-59, showing the nodular anhydrite texture.

33b Thin-section photomicrograph under polarized light showing irregular laminations of anhydrite interbedded with algal mats and marked by stylolites(TMFC1) at a depth of 1540.3m in well Y3-59.

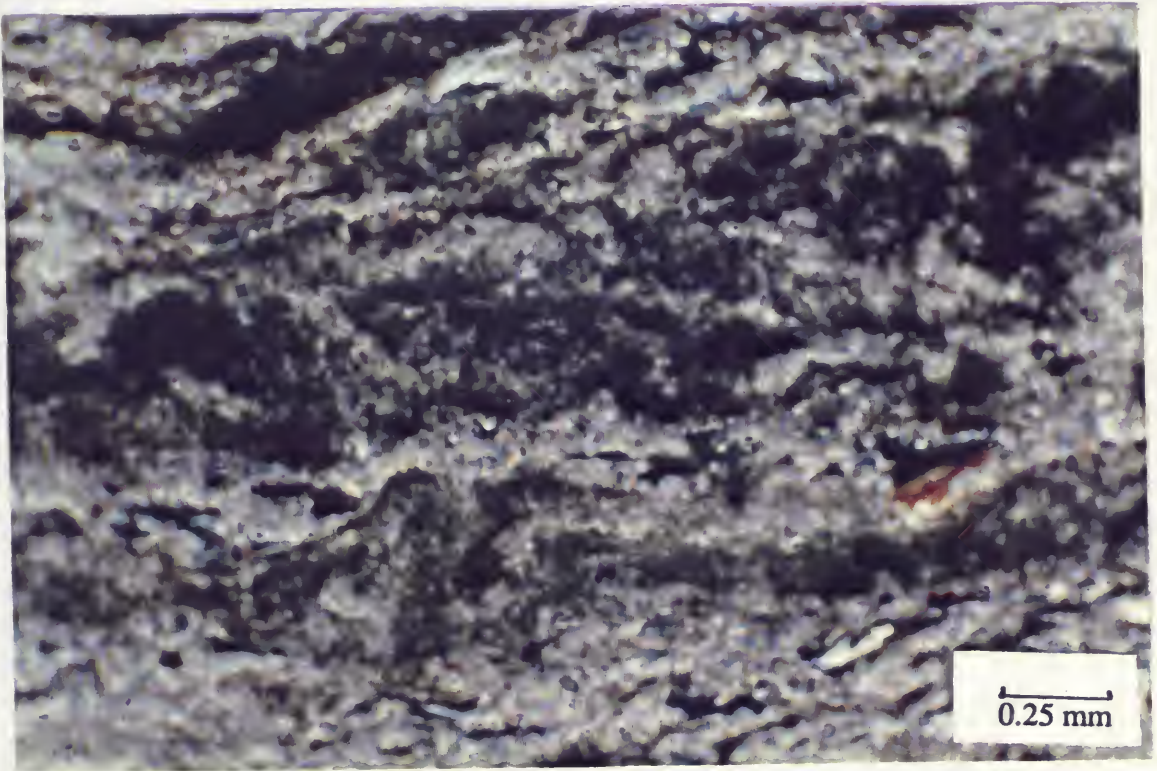


PLATE C

Figure

- 33c Thin-section photomicrograph under plane light showing anhydrite partially replacing a gastropod shell, the sediment filling the shell and cementation of dissolution voids(TMFC1) at a depth of 1537.3m in well Y3-59. Note the extensive dissolution of grains and solution enlargement of molds. Black is porosity.

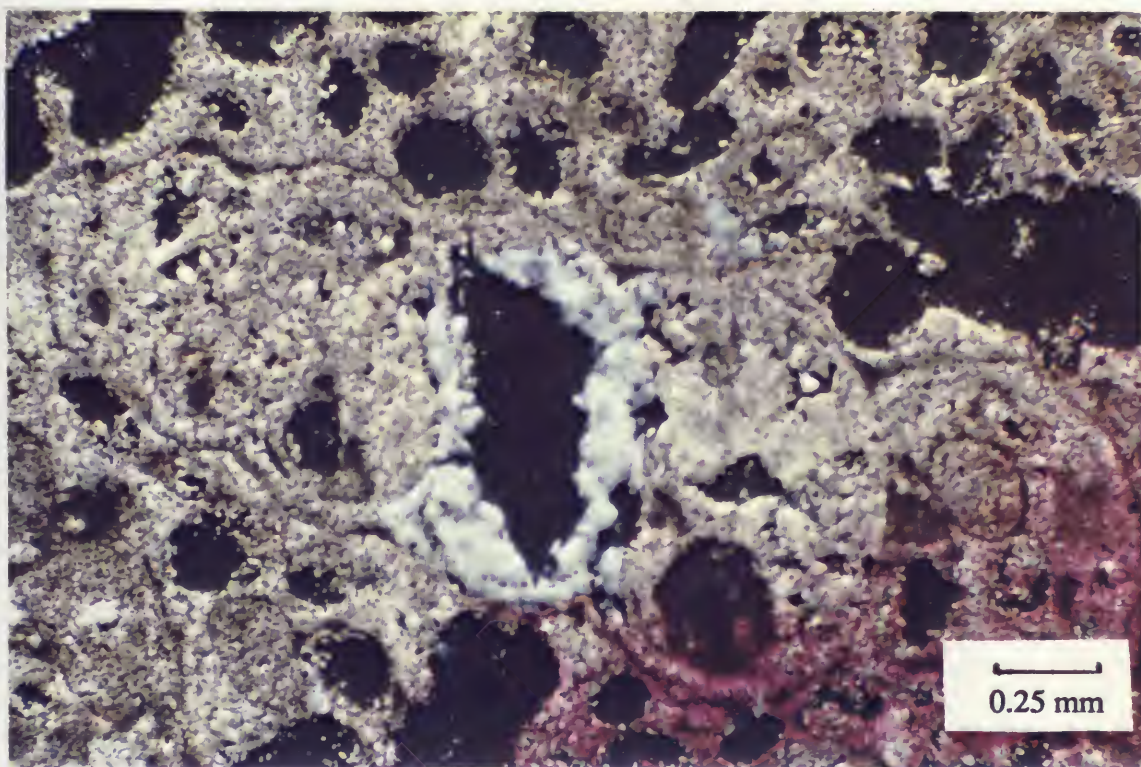


PLATE C

Figures

- 34a Thin-section photomicrograph under plane light showing nodular texture, elongate and rectangular crystal laths of anhydrite(TMFC1) at a depth of 1466.7m in well 6A1-59.
- 34b Core slab showing massive anhydrite of the Terminal microfacies complex(TMFC1) at a depth of 1466.9m in well 6A1-59.

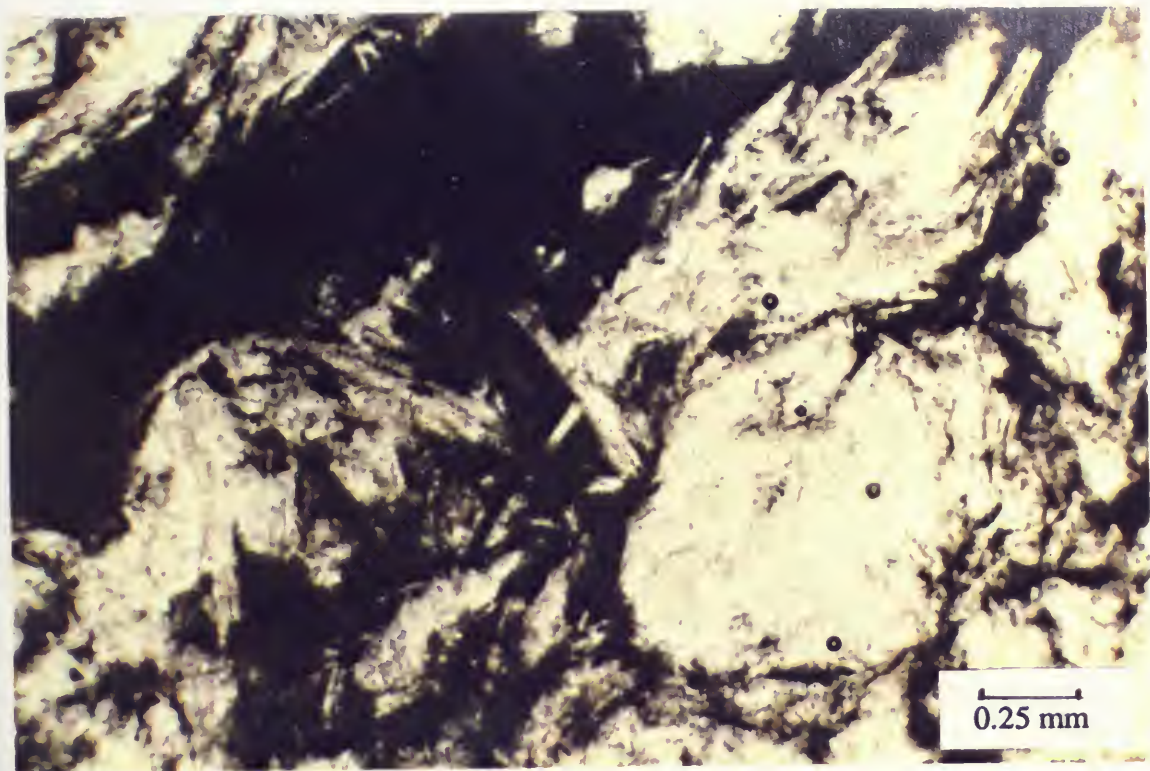


PLATE C

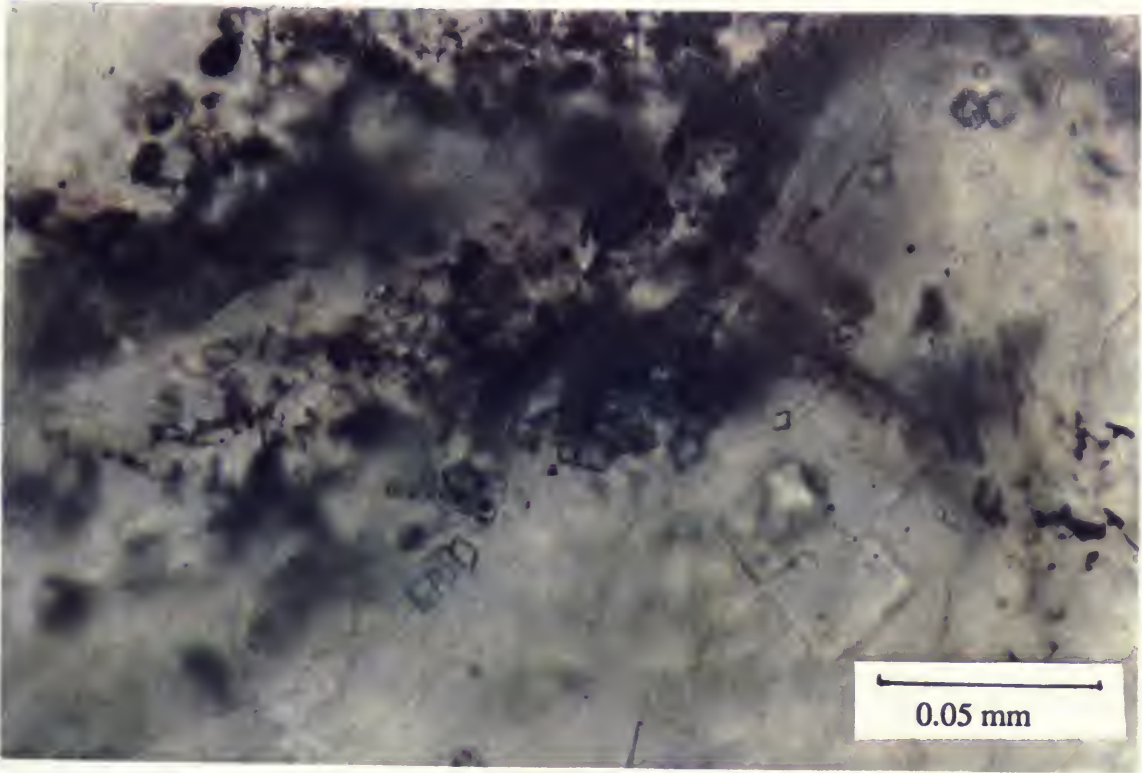
Figures

35

Thin-section photomicrograph under polarized light of anhydrite with pyrite and dolomite crystals lining of the stylolite seams (TMFC1) at a depth of 1466.9m in well 6A1-59.

36

Core slab showing pelecypod shell debris in micrite matrix with extensive anhydrite cement at a depth of 1536.4m in well Y3-59. This bioclastic rock is part of the supratidal facies of the TMFC1 and was probably deposited during a storm event.



APPENDIX II

Lithologic Sample Descriptions of Beda Formation, well Y3-59

APPENDIX II

1,575m (5,081 ft.)	pelecypod shell debris cemented by anhydrite, light brown to gray colour, with pressure solution and dissolution features
1,575.4m (5,082 ft.)	anhydrite nodular to massive smokey white to light gray colours, with remnants of the original gray micrite around the nodules, organic black material and pyrite. Crystal shape varies from rectangular laths randomly arranged as rosettes
1,575.7m (5,083 ft.)	as above
1,576m (5,084 ft.)	micrite with anhydrite nodules. The lime mudstone ranges in colour from light brown to tan in colour with stylolites and pyrite
1,576.4m (5,085 ft.)	massive anhydrite, light gray to tan colours, with stylolites and pyrite. The crystal shape is dominated by rosette and fibrous structures
1,576.7m (5,086 ft.)	as above
1,577m (5,087 ft.)	wackestone-mudstone with ostracods (abundant), small benthonic foraminifera (common), tan to cream colour. The grains were partially leached, leaving molds and vugs that were later filled by anhydrite and/or calcite cement. Some grains were micritized and the matrix was partly dolomitized. This sample is slightly oil stained and porosity is moldic and intercrystalline. Fenestral fabric.
1,577.6m (5,089 ft.)	wackestone with grains, as above, in addition to pelecypods fragments. Oxidation surfaces probably indicate subaerial exposure in sabkha environment. Stylolites are common. Dolomite is more than 50%. The argillaceous content is high
1,578m (5,090 ft.)	mudstone dolomitized with anhydrite inclusions, light brown to tan, microcrystalline dolomite, algal mats inferred with fenestral fabric and wavy laminations, pyrite crystals. Porosity is intercrystalline and seems to be partly reduced by anhydrite cement. This sample is oil stained.
1,578.3m (5,091 ft.)	as above, with discoidal gypsum and ostracods (rare), agglutinated foraminifera (rare), and skeletal material (common)
1,578.5m (5,092 ft.)	lime-mudstone with dedolomitization crystal structures (pseudomorphs of dolomite rhombs), and calcitization of anhydrite, fenestral fabric and ghosts of fossils
1,578.8m (5,093 ft.)	as above, vertical fractures, partial dolomitization of micrite matrix. Ostracods shell fragments are rare, and molds of dissolved grains are common, porosity is moldic and intercrystalline, which is partially cemented by anhydrite

1,579m (5,093.5 ft.)	gray argillaceous micrite with stylolites, algal laminations, dissolution and fenestral fabric. The thin anhydrite laminae are interbedded with micrite
1,579.2m (5,094 ft.)	skeletal wackestone with abundant pelecypod fragments, ostracods (common), foraminifera (rare-common). Dissolution of grains and anhydrite inclusion produced the vuggy porosity. Fecal pellets, and stylolites are common. Dolomite is more than 50% and pyrite crystals were observed in molds and along stylolite surfaces
1,579.5m (5,095 ft.)	as above, with algal laminations, fenestral fabric and fracture porosity
1,579.8m (5,096 ft.)	as above, with discoidal gypsum pseudomorphs
1,580m (5,097 ft.)	as above
1,580.4m (5,098 ft.)	wackestone, nodular textures, dark to light gray, argillaceous, pressure solution structures, burrowed, interbedded with thin anhydrite laminae, and pyrite crystals along stylolite surfaces and in vugs. Skeletal grains are rare to common and dolomitization is less than 50%
1,580.7m (5,099 ft.)	as above, with dolomite and anhydrite crystals filling the molds, and oxidation surfaces
1,581m (5,100 ft.)	mudstone, dark to light gray, with algal laminations, birds-eye fabric and argillaceous. Dolomite is < 50%. Replacement of dolomite and anhydrite by calcite is common, as well as dissolution of skeletal constituents and anhydrite cement
1,581.3m (5,101 ft.)	as above
1,581.6m (5,102 ft.)	wackestone-mudstone, gray to tan, partial to complete dissolution of skeletal grains. The molds and vugs are completely cemented by anhydrite and calcite cement. Dolomite is > 50%. Porosity is moldic and intercrystalline and no oil stains were observed
1,581.9m (5,103 ft.)	as above, with algal mats, fenestral fabric, stylolites and argillaceous seams. Solution enhanced porosity, oxidation surfaces are common
1,582.64m (5,104 ft.)	mudstone with fecal pellets, skeletal material, light gray, stylolitic, bioturbated, dolomite < 10%, algal structures, and pyrite. No oil stains present
1,582.9m (5,106 ft.)	as above
1,583.2m (5,107 ft.)	as above
1,583.5m (5,108 ft.)	as above

1,583.8m (5,109 ft.)	mudstone-wackestone, gray, ostracods (rare-common), small benthonic foraminifera (rare-common), flattening of ostracod shells. Shells indicate physical compaction. Dissolution of fossil grains and anhydrite is common. Red colour indicates oxidation. Stylolite cut through grains and porosity include moldic and fracture but generally low. No oil stains were observed. Dolomitization is partial and calcitization is common, probably due to subaerial exposure and fresh water influx, as indicated by oxidation surfaces and the presence of charophytes
1,584.1m (5,110 ft.)	as above, light gray to tan with vertical fractures filled by anhydrite. Red oxidation surfaces and algal mats are common. Dolomite > 50%. Porosity is moldic, intercrystalline, fenestral and fracture. Oil stains are light
1,584.4m (5,111 ft.)	as above, with algal mats and fenestral structures. Replacement of dolomite and anhydrite by calcite is common
1,584.5m (5,112 ft.)	as above
1,584.7m (5,113 ft.)	wackestone, pelletal with solution structures along algal mat surfaces and stylolites. The colour varies from light gray to tan
1,585.3m (5,114 ft.)	as above
1,585.7m (5,115 ft.)	wackestone, light gray-tan, argillaceous, compacted, nodular texture, stylolitic, fecal pellets (common), ostracods (common), benthonic foraminifera (rare-common), skeletal material (common), solution structures along stylolites. Oil stains are heavy and tan to light brown in colour
1,586m (5,116 ft.)	wackestone-mudstone, as above, with agglutinated and miliolid foraminifera. Dolomite is (< 30%), porosity is moldic and intercrystalline. Molds are filled with anhydrite cement. This sample is slightly oil stained
1,586.3m (5,117 ft.)	as above, with microfacies
1,586.6m (5,118 ft.)	as above, with textularia and miliolid chambers filled by anhydrite. Fecal pellets are common. Porosity is moldic, intercrystalline and fracture. Oil stains are light. Stylolites are common
1,587m (5,119 ft.)	wackestone to packstone, fecal pellets (abundant), miliolids (common), ostracods (rare-common), algal plates (rare-common), bioturbated, solution leaching, stylolites and anhydrite cement are common features. Light to tan colour. Porosity is moldic and intraskeletal. Dolomite < 30%. Oil stains are light

1,587.8m (5,120 ft.)	packstone, light brown to cream, miliolids (abundant), small benthonic foraminifera (c), ostracods (common), fecal pellets (rare-common), pelecypods fragments (common-rare), microcrystalline, partly dolomitized micrite matrix. Sparry calcite and anhydrite cement. Porosity includes intergranular, intragranular, solution and intercrystalline types. Oil stains are common
1,588.1m (5,123 ft.)	as above
1,588.4m (5,124 ft.)	packstone to wackestone. The skeletal allochems include pelloids, benthonic foraminifera, such as miliolids, echinoderms, and other undifferentiated allochems. Porosity is moldic, vuggy and intercrystalline. Dolomite < 50%. Oil stains are common. The pores are partially cemented by sparry calcite and anhydrite. Burrowing is common
1,588.8m (5,125 ft.)	as above
1,589.1m (5,126 ft.)	packstone-grainstone, cream to light brown, the matrix is partly dolomitized and recrystallized. Miliolids and smaller benthonic foraminifera are common. Ostracods (common), molluscs are common, echinoderms and dasycladacean algae (rare), fecal pellets (rare-common) and other unidentified allochems are common. Porosity is moldic, intercrystalline, intergranular and intragranular. Sparry calcite and anhydrite cement were observed in molds and vugs, as well as overgrowths on grain edges and around cavity walls. Oil stains are common
1,589.4m (5,127 ft.)	packstone, as above
1,589.7m (5,128 ft.)	as above, with agglutinated foraminifera, and dasycladacean algae (common) and light oil stain
1,590m (5,129 ft.)	packstone-wackestone, as above, with increasing dasycladacean algae, pelecypods and miliolids. Porosity is moldic and intergranular
1,590.3m (5,130 ft.)	as above, with dissolution porosity as a result of partial dolomitization and solution leaching of micrite matrix and unstable fossil grains
1,591m (5,132 ft.)	packstone-wackestone, miliolids (common), ostracods (common), small benthonic foraminifera (common-abundant), echinoderms (rare), pelloids (common-rare), molluscs (rare-common), dasycladacean algae fragments (rare), agglutinated foraminifera (rare) and fecal pellets (common-rare). Porosity is moldic intergranular and intercrystalline. The matrix is partly dolomitic. Oil stains are light to heavy. Sparry calcite and anhydrite cement are common
1,591.2m (5,133 ft.)	as above
1,591.5m (5,134 ft.)	wackestone with grains, as above. Agglutinated foraminifera (common-abundant), porosity is moldic, intergranular, intercrystalline and partly cemented by sparry calcite and anhydrite. Oil stains are light to heavy

1,591.9m (5,135 ft.)	packstone, light brown-tan, partly dolomitized lime-mud matrix. The grain constituents include miliolids, pelloids, micritized bioclasts, bryozoans and molluscs. Porosity is interparticle, intraparticle, moldic and intercrystalline with heavy oil stains
1,592.2m (5,136 ft.)	as above
1,592.5m (5,137 ft.)	as above
1,592.8m (5,138 ft.)	packstone-wackestone with grains, as above
1,593m (5,139 ft.)	packstone with abundant miliolid foraminifera and other grains, as above. Extensive dissolution and cementation by sparry calcite and anhydrite. Oil stains are light to heavy. Bioturbation is extensive and the primary structures were completely destroyed
1,593.4m (5,140 ft.)	as above
1,593.7m (5,141 ft.)	packstone with grains, as above. the micrite matrix is completely recrystallized, solution leaching of allochems and cementation by sparry calcite and anhydrite. Porosity moldic and intergranular. Dolomite < 50% and oil stains are uniform
1,594m (5,142 ft.)	as above
1,594.3m (5,143 ft.)	packstone. Light brown to tan, partly dolomitized micrite matrix. The skeletal constituents are benthonic foraminifera, such as miliolids, echinoderms, molluscs, ostracods and other undifferentiated skeletal material. Burrowing and bioturbation obliterated the primary sedimentary structures. Sparry calcite was observed within the different pores and around the skeletal grains. Porosity is moldic, interparticle and intraparticle. Brown oil stains are common throughout the sample
1,594.6m (5,144 ft.)	as above, with microfractures and pelloids (possibly fecal pellets). Stylolite and oil stains were observed. Burrowing is extensive, as well as solution leaching of allochems
1,595m (5,145 ft.)	packstone, as above, with reworked allochems, such as miliolids, echinoderms, molluscs, bryozoans and pelloids
1,595.3m (5,146 ft.)	as above, with heavy oil stains and moldic, interparticle and intraparticle porosity
1,595.6m (5,147 ft.)	packstone-wackestone, light brown to tan, recrystallized micrite matrix, partly dolomitized. The grain constituents include miliolids, pelloids of different sizes, echinoderms, dasycladacean algae and pelecypods fragments. The sample is extensively burrowed. Stylolites and fractures are common features. Porosity is moldic, intercrystalline and intraparticle. Sparry calcite and anhydrite cement are common

1,595.9 - 1,596.5m (5,148 - 5,150 ft.)	packstone with grains, as above
1,596.8m (5,151 ft.)	packstone, light brown-tan, recrystallized, partly dolomitic micrite matrix. The skeletal constituents are dominated by benthonic foraminifera, ostracods, pelecypods, echinoderms and dasycladacean algae. Porosity is low, probably due to cementation by sparry calcite and anhydrite. The grains are deformed (ellipsoidal shape), indicating early compaction before lithification and cementation. Porosity is moldic and interparticle
1,597.1m (5,152 ft.)	as above
1,597.4 - 1,599m (5,153 - 5,158 ft.)	packstone. Tan to cream, recrystallized, partially dolomitized micrite matrix with dissolution features, stylolites, burrowing and sparry calcite cement. The allochems are benthonic foraminifera, such as miliolids, Eponides, Cibicides, and agglutinated forms, in addition to pelecypods, echinoderms, dasycladacean algae and pelloids of unknown origin. Porosity is moldic, interparticle and intraparticle
1,599.8 - 1,600.8m (5,159 - 5,164 ft.)	as above, with extensive replacement of skeletal grains by anhydrite. Porosity is moldic and intergranular. Oil stains are common. Ostracods are rare to common
1,601.2 - 1,602.7m (5,165 - 5,170 ft.)	packstone with minor amounts of intergranular micrite. Partially dolomitized (< 30%), completely recrystallized. Tan to light brown colour, sparry calcite cement filled the pore system. The allochems include miliolids and other smaller benthonic foraminifera, in addition to pelecypods, ostracods, echinoderms and fecal pellets. Dissolution is common, as indicated by moldic and vuggy porosity. Burrowing, micritization and compaction are common diagenetic structures. Porosity is moldic, interparticle and intraparticle
1,603 - 1,604.3m (5,171 - 5,175 ft.)	packstone. Tan to cream, recrystallized micrite matrix, partially dolomitic. The allochems include miliolids, molluscs, bryozoans, ostracods, dasycladacean algae fragments, fecal pellets and echinoderms. Stylolite, sparry calcite cement and oil stains are common. The grains were completely micritized and partially dissolved due to solution leaching. Porosity is mainly moldic, intergranular and microfractures
1,604.6 - 1,605.8m (5,176 - 5,180 ft.)	packstone-wackestone with grains, as above. Extensive burrowing and boring was observed. Solution leaching is indicated by moldic and vuggy porosity. Oil stains are common. Minor amounts of calcite spar and anhydrite cement were recorded

1,605.8 - 1,607.4m
(5,180 - 5,185 ft.)

mudstone-wackestone. Light to medium gray, mud supported micrite matrix, completely recrystallized and partially dolomitized (< 25%). The grains are scattered throughout the matrix and consist of small benthonic foraminifera, ostracods, fecal pellets, bryozoans and dasycladacean algae fragments. Compaction structures include deformed allochems, stylolites, and alignment and flattening of ostracods and mollusc shells. Micrite envelopes and burrowing are common diagenetic features. Pyrite crystals are scattered throughout the matrix and within intraskeletal pores. Vertical fractures are rare and mostly cemented by calcite and anhydrite cement. Porosity is low and includes moldic, vuggy and fractures. Oil stains are light and the argillaceous content is high, resulting in permeability reduction

1,607.4 - 1,608.9m
(5,185 - 5,190 ft.)

mudstone with grains and structures, as above

1,608.9 - 1,610.5m
(5,190 - 5,195 ft.)

mudstone. Light gray-tan, microcrystalline micrite matrix, partially dolomitized. Skeletal fragments of benthonic foraminifera, ostracods and molluscs are scattered throughout the matrix. Pyrite is rare. Fractures and burrows are common diagenetic features. Porosity is generally low and includes moldic and fracture types. No oil stains were observed

1,610 - 1,612m
(5,195 - 5,200 ft.)

mudstone, as above, with microfractures and solution enlargement of pores and occasionally they are filled with anhydrite and sparry calcite. Oil stains were recorded. Porosity is low and includes fractures and solution types

1,612 - 1,613m
(5,200 - 5,205 ft.)

mudstone, gray-tan, recrystallized, mud supported texture and partially dolomitized micrite matrix, fenestral fabric, indicative of algal mats were observed. The fenestrate porosity is cemented by calcite and anhydrite cement. Stylolites, burrowing and micritization are common features. Dissolution of skeletal grains resulted in the development of moldic, vuggy and solution enlargement of microfractures. Oil stains are light. Clay seams are present and the argillaceous content is moderate

1,613.6 - 1,615m
(5,205 - 5,210 ft.)

mudstone, as above. Dark brown dead oil stains were recorded. Anhydrite inclusions and sparry calcite cement were observed in pores. Extensively bioturbated resulting in the obliteration of the primary sedimentary structures. Dolomitization is not pervasive. Stylolites and microfractures were also recorded

1,615 - 1,616.7m
(5,210 - 5,215 ft.)

packstone. Light brown-tan colour. Grain-supported textures, the allochems are dominated by dasycladacean algae, benthonic foraminifera, especially miliolids, molluscs, ostracods, fragments of red algae, fecal pellets and echinoderms. The grains are recrystallized, micritized and partially leached. Sparry calcite is common in different types of pores and anhydrite inclusions were observed. The primary sedimentary features were destroyed due to burrowing. Light brown oil stains are common. Porosity varies from interparticle, intraparticle and moldic

1,616.7 - 1,618.2m
(5,215 - 5,220 ft.)

as above

1,618.2 - 1,619.8m
(5,220 - 5,225 ft.)

packstone, as above

1,619.8 - 1,621.3m
(5,225 - 5,230 ft.)

as above

1,621.3 - 1,622.9m
(5,230 - 5,235 ft.)

packstone. Tan, recrystallized, grain supported matrix. The allochems are partially dissolved and micritized. They include dasycladacean algae and benthonic foraminifera in abundance. Echinoderms, molluscs, ostracods are common, in addition to pelloids and unidentified skeletal material. Porosity is intergranular, moldic and intragranular. Oil stains are common. Burrowing, stylolites and micritization are common diagenetic features

1,622.9 - 1,624.4m
(5,235 - 5,240 ft.)

packstone, as above, with minor amounts of anhydrite inclusion. Dasycladacean algal plates are abundant, in addition to nummulites and miliolids. Gastropods and fragments of pelecypods were recorded

1,624.4 - 1,626m
(5,240 - 5,245 ft.)

as above

1,626 - 1,627.5m
(5,245 - 5,250 ft.)

packstone, as above, with agglutinated foraminifera and ostracods. Skeletal shells were deformed due to compaction. Stylolites are common. Porosity is fair and includes moldic, intergranular and intragranular types. Sparry calcite is common, while anhydrite inclusions are rare. Oil stains are heavy

1,627.5 - 1,629m
(5,250 - 5,255 ft.)

as above

1,629 - 1,630.6m
(5,255 - 5,260 ft.)

packstone. Light brown to cream, recrystallized micrite matrix. Grain supported textures. The grain constituents include dasycladacean algae, miliolids, gastropods, ostracods, bryozoans and echinoderms. Fecal pellets are common. Oil stains are abundant. Solution leaching of unstable allochems resulted in the development of moldic porosity. Sparry calcite cement was observed throughout sample

1,630.6 - 1,632.2m (5,260 - 5,265 ft.)	Packstone, as above, grading occasionally into thin stringers of wackestone that is partly argillaceous
1,632.2 - 1,633.7m (5,265 - 5,270 ft.)	as above
1,633.7 - 1,635.3m (5,270 - 5,275 ft.)	packstone. Tan to light brown, completely recrystallized, grain supported texture with dasycladacean algae fragments, benthonic foraminifera and pelecypod fragments. Solution leaching, micrite envelopes and cementation by calcite spar and anhydrite were observed. Oil stains were recorded
1,635.3 - 1,636.8m (5,275 - 5,280 ft.)	as above
1,636.8 - 1,638.4m (5,280 - 5,285 ft.)	packstone, as above, with pelloids, bryozoans and bivalves. Oil stains are common. Porosity is fair and includes moldic, vuggy and interparticle types
1,638.4 - 1,640m (5,285 - 5,290 ft.)	packstone-wackestone. Light brown to light gray colour. Microcrystalline micrite matrix. The allochems are dark in colour due to micritization. They include dasycladacean algae, miliolids, pelecypods and ostracods. Fecal pellets and pelloids are also common. Burrowing, boring, micrite envelopes, solution leaching, and compaction are some of the diagenetic features. Porosity is moldic, interparticle and intraparticle types. Cementation by calcite spar is common
1,640 - 1,641.5m (5,290 - 5,295 ft.)	wackestone. Light brown to light gray, microcrystalline micrite matrix. The allochems are dominated by small benthonic foraminifera, such as cibicides, eponids, anomalinids, miliolids, textularia, gaudryina, and spiroplectamina. Ostracods are the second most abundant organisms while pelecypods, small gastropods and echinoderms are rare. Fecal pellets were recorded. The samples are intensely burrowed, as indicated by mottling of the lime-mud matrix. Horizontal and wavy laminations were observed. The laminations are less than 3mm in thickness. Nodular textures, stylolites, sparry calcite and anhydrite cements are common diagenetic features. Pyrite was recorded as a replacement and with in pores or disseminated in the micrite matrix. Porosity is mostly solution and intraskeletal but generally low. Oil stains were recorded but not uniform
1,641.5 - 1,643m (5,295 - 5,300 ft.)	wackestone, as above, with irregular laminations, possibly crypt-algal. Replacement of fossil fragments by pyrite and anhydrite. Solution leaching and sparry calcite cementation is common
1,643 - 1,644.6m (5,300 - 5,305 ft.)	wackestone, as above

1,644.6 - 1,646.1m (5,305 - 5,310 ft.)	wackestone with grains, as above, nodular texture, stylolitic, argillaceous, microfractures, fecal pellets and micritized grains. Anhydrite and calcite spars are the common cement types. Porosity is low and includes moldic and intraparticle. No oil stains were observed
1,646.1 - 1,649.2m (5,310 - 5,320 ft.)	packstone. Light brown to tan lime-mud matrix. The allochems are partially preserved due to chemical and physical degradation. They are dominated by benthonic foraminifera, such as miliolids, in addition to ostracods, pelecypod fragments and unidentified skeletal fragments of different sizes. The matrix seems to be partially dolomitized and replaced by microcrystalline sparry calcite. No oil stains were recorded. Porosity is interparticle and intragranular
1,649.2 - 1,652.3m (5,320 - 5,330 ft.)	as above. The cuttings appear to be chalky, no visible porosity and no oil stands were recorded. Sparry calcite and anhydrite cements are common
1,652.3 - 1,635.4m (5,330 - 5,340 ft.)	packstone, with grains, as above. Light brown to tan, recrystallized and partially dolomitized matrix (< 20% dolomite). The skeletal constituents are dominated by miliolids, eponids and cibicides. Ostracods, pelloids, echinoderms and pelecypod fragments were observed. Minor amounts of anhydrite were recorded throughout the cutting, in addition to sparry calcite cement. Porosity is moldic, intergranular and intragranular. No visible oil stains
1,635.4 - 1,660m (5,340 - 5,355 ft.)	packstone, as above with dissolution features, leached fossils and cementation by calcite and anhydrite. Pyrite crystals were recorded. Dead oil stains and weak yellow fluorescence appear in some cutting
1,660 - 1,661.6m (5,355 - 5,360 ft.)	wackestone. Tan to light gray, recrystallized lime-mud matrix with scattered skeletal constituents. The allochems consist of small benthonic foraminifera, including eponides, cibicides, miliolids, textularias, lenticulina and gaudryina, in addition to ostracods, molluscan fragments and echinoderms. The micrite matrix is soft and slightly argillaceous. Porosity is low and no oil shows were recorded
1,661.6 - 1,664.2m (5,360 - 5,370 ft.)	wackestone-mudstone with grains, as above. The allochems decreased greatly from the above samples in their percentage. The texture is mud supported. The matrix seems to contain a high percentage of clay and argillaceous material. Pyrite is rare. No visible porosity or oil stains
1,664.7 - 1,667.8m (5,370 - 5,380 ft.)	wackestone-mudstone, as above
1,667.8 - 1,670.9m (5,380 - 5,390 ft.)	as above

1,670.9 - 1,674m (5,390 - 5,400 ft.)	wackestone. Light gray to tan, micrite matrix with scattered allochems. They include benthonic foraminifera, ostracods, and unidentified skeletal fragments. The allochems are poorly preserved due to solution leaching, reworking and micritization. Anhydrite and sparry calcite are common. The micrite matrix contains minor amounts of argillaceous material, clay and pyrite. Dead oil stains were recorded. No visible porosity and no oil shows
1,674 - 1,677m (5,400 - 5,410 ft.)	wackestone-mudstone. Light gray wackestone grading occasionally into mudstone. The sample appears to be mud supported in texture, with scattered skeletal grains of benthonic foraminifera, ostracods, echinoderms, pelecypods and unidentified fossil fragments
1,677 - 1,680.2m (5,410 - 5,420 ft.)	wackestone-mudstone, as above
1,680.2 - 1,683.3m (5,420 - 5,430 ft.)	mudstone with occasional stringers of wackestone, as well as shale interbeds. Recrystallized micrite matrix, sparry calcite cement and reworked skeletal fragments of foraminifera and molluscs were recorded
1,683.3 - 1,686.4m (5,430 - 5,440 ft.)	mudstone-wackestone, light gray with grains and textures, as above. Argillaceous micrite matrix with pyrite and carbonaceous material. No visible porosity and no oil stains were observed
1,686.4 - 1,689.5m (5,440 - 5,450 ft.)	wackestone with an increase in the allochem content. The micrite matrix is recrystallized into microcrystalline calcite spar. Some skeletal grains appear to be deformed due to compaction. Dissolution, micritization and cementation are common diagenetic features
1,683.5 - 1,692.6m (5,450 - 5,460 ft.)	packstone-wackestone. The examination of drill cuttings indicates light brown to tan micrite matrix with abundant fecal pellets, dasycladacean algae fragments, miliolid foraminifera, ostracods and molluscan fragments. The grains appear partially preserved, due to diagenetic alteration, such as dissolution and micritization. Sparry calcite and anhydrite are common in molds and within the intraskeletal pores. Porosity is intergranular, intragranular and solution types. No oil stains were recorded
1,592.6 - 1,698.8m (5,460 - 5,480 ft.)	packstone with grains, as above. Anhydrite and sparry calcite cement in mods and vugs. Carbonaceous dark material is common in some cuttings. Recrystallized skeletal grains and micrite matrix with dissolution and micritization features. No oil stains. Porosity is moldic and intraparticle

1,698.8 - 1,701.9m (5,480 - 5,490 ft.)	packstone, as above. The allochems are dasycladacean algae fragments, fecal pellets, miliolids, smaller benthonic foraminifera, microgastropods, pelecypod debris, echinoderms and ostracods. The grains are partially dissolved and completely recrystallized to a coarse calcite spar. Porosity is intergranular, intragranular and moldic. Scattered pyrite crystals were recorded. No oil stains were observed
1,701.9 - 1,705m (5,490 - 5,500 ft.)	as above
1,705 - 1,708.1m (5,500 - 5,510 ft.)	packstone with grains, as above. The biotic constituents are partly dissolved, completely recrystallized and composed of fecal pellets, miliolids, dasycladacean algae fragments, pelecypods, echinoderms, ostracods and unidentified pelloids
1,708.1 - 1,711.2m (5,510 - 5,520 ft.)	as above
1,711.2 - 1,714.3m (5,520 - 5,530 ft.)	packstone. Tan to light brown colour, recrystallized lime-mud matrix. The skeletal constituents include fragments of dasycladacean algae, benthonic foraminifera and other unidentified fossil debris. Solution leaching and sparry calcite cement are common diagenetic features. Porosity is moldic, interparticle and intraparticle. No oil stains were recorded
1,714.3 - 1,720.5m (5,530 - 5,550 ft.)	as above
1,720.5 - 1,723.6m (5,550 - 5,560 ft.)	packstone. Light brown to tan, chalky in parts, grain-supported textures and recrystallized lime-mud matrix. The allochems are poorly preserved due to recrystallization and solution leaching and consist of algal fragments, miliolid foraminifera, fecal pellets, echinoderms and pelecypods. Porosity is interparticle, intraparticle and moldic. No oil stains were observed
1,723.6 - 1,726.7m (5,560 - 5,570 ft.)	as above
1,726.7 - 1,729.8m (5,570 - 5,580 ft.)	packstone with grains and sedimentary structures and textures, as above. Dissolution, recrystallization and micritization obliterated the microstructures of the allochems and, consequently, are occasionally unidentifiable. Porosity is moldic, interskeletal and intraskeletal
1,729.8 - 1,732.9m (5,580 - 5,590 ft.)	packstone, as above, with sparry calcite around grains and in molds. Recrystallized micrite matrix. Skeletal fragments of dasycladacean algae and benthonic foraminifera

- 1,732.9 - 1,736m
(5,590 - 5,600 ft.)
- packstone. Light brown to tan, recrystallized, micrite matrix. The skeletal constituents include benthonic foraminifera, including miliolids, eponids, cibicids and textularia, in addition to molluscan fragments, ostracods and fecal pellets. The grains were partly dissolved resulting in the development of moldic porosity. No oil stains were recorded
- 1,736 - 1,742.2m
(5,600 - 5,620 ft.)
- wackestone-mudstone, with micritized grains, pelloids, dasycladacean algae fragments and miliolids. Porosity is moldic and vuggy and no oil stains were observed
- 1,742.2 - 1,745.3m
(5,620 - 5,630 ft.)
- wackestone-mudstone. Light gray to tan, recrystallized micrite matrix with scattered skeletal constituents of dasycladacean algae, benthonic foraminifera, ostracods, molluscs and other undifferentiated skeletal material. The matrix contains minor amounts of clay, organic matter and pyrite
- 1,745.3 - 1,748.4m
(5,630 - 5,640 ft.)
- packstone. Light brown to tan recrystallized micrite matrix, grain-supported texture and reworked skeletal fragments. The allochems are extensively micritized due algal microborings. They include pelloids of different sizes, rounded and elliptical shape and probably they're oolitic in origin. Benthonic foraminifera such as miliolids, eponids and agglutinated forms were recorded. The grains were completely recrystallized and partially leached. Sparry calcite cement is common diagenetic feature. Porosity is mainly interparticle, moldic and intraparticle. No oil stains were recorded
- 1,751.5 - 1,755.5m
(5,650 - 5,663 ft.)
- wackestone, as above. The grains were completely recrystallized, micritized and partly leached out. The matrix appears to contain a high percentage of clay and argillaceous material
- 1,763.9 - 1,767m
(5,690 - 5,700 ft.)
- mudstone. Light to dark gray, mud-supported texture, dense, recrystallized argillaceous micrite matrix with scattered skeletal grains. The allochems are rare and consist of small benthonic foraminifera, ostracods and unidentified broken skeletal fragments. The benthonic foraminiferal assemblage is dominated by cibicids, anomalinids, textularia, gaudryina and miliolids
- 1,767 - 1,770.1m
(5,700 - 5,710 ft.)
- mudstone, as above
- 1,770.1 - 1,773.2m
(5,710 - 5,720 ft.)
- mudstone. Dark gray, shaly, dense recrystallized argillaceous lime-mud matrix. The allochems are rare and contain small benthonic foraminifera and ostracods. Pyrite and black carbonaceous material are common. No visible porosity and no oil stains were recorded

1,773.2 - 1,777.9m
(5,720 - 5,735 ft.)

mudstone, as above, with shale stringers and recrystallized dark gray micrite matrix. The allochems are rare and scattered throughout the matrix. They are dominated by small benthonic foraminifera, ostracods and reworked unidentified skeletal material. No visible porosity and no oil stains were recorded.

096440014 - (X)

